409.24 E1.28:PNL-4100/p

PNL-4100 PT4
UC-11

Pacific Northwest Laboratory Annual Report for 1981 to the DOE Office of Energy Research

Part 4 Physical Sciences February 1982

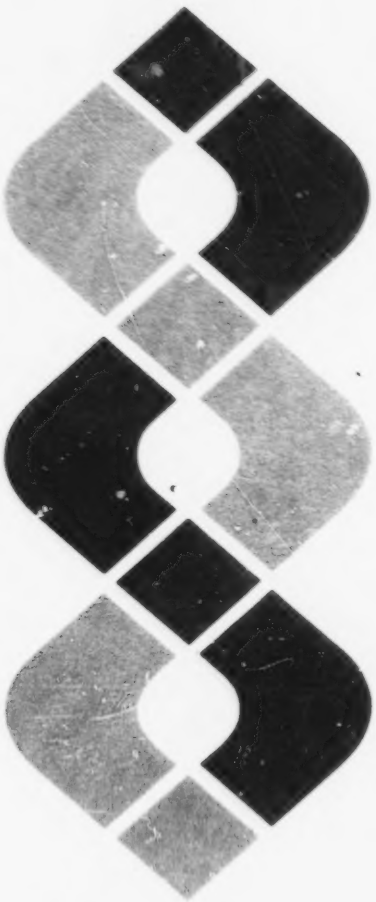

COMPLETED
137

Prepared for the U.S. Department of Energy
under Contract DE-AC06-76RLO 1830

Pacific Northwest Laboratory
Operated for the U.S. Department of Energy
by Battelle Memorial Institute

Battelle

PNL 1981 Environment, Health and Safety Part 4

NOTICE

This report was prepared as an account of work sponsored by the United States Government. Neither the United States nor the Department of Energy, nor any of their employees, nor any of their contractors, subcontractors, or their employees, makes any warranty, express or implied, or assumes any legal liability or responsibility for the accuracy, completeness or usefulness of any information, apparatus, product or process disclosed, or represents that its use would not infringe privately owned rights.

The views, opinions and conclusions contained in this report are those of the contractor and do not necessarily represent those of the United States Government or the United States Department of Energy.

PACIFIC NORTHWEST LABORATORY
operated by
BATTELLE
for the
UNITED STATES DEPARTMENT OF ENERGY
under Contract DE-AC06-76RLO 1830

Printed in the United States of America
Available from
National Technical Information Service
United States Department of Commerce
5285 Port Royal Road
Springfield, Virginia 22151

NTIS Price Codes
Microfiche A01

Printed Copy

Pages	Price Codes
001-025	A02
026-050	A03
051-075	A04
076-100	A05
101-125	A06
126-150	A07
151-175	A08
176-200	A09
201-225	A010
226-250	A011
251-275	A012
276-300	A013

BEST DOCUMENT AVAILABLE

I

PNL-4100 PT4
UC-48

Pacific Northwest Laboratory Annual Report for 1981 to the DOE Office of Energy Research

Part 4 Physical Sciences

J. M. Nielsen and Staff Members
of Pacific Northwest Laboratory

February 1982

Prepared for
the U.S. Department of Energy
under Contract DE-AC06-76RLO 1830

Pacific Northwest Laboratory
Richland, Washington 99352

II

PREFACE

This 1981 annual report from Pacific Northwest Laboratory (PNL) to the Department of Energy (DOE) describes research in environment, health, and safety conducted during fiscal year 1981. The report again consists of five parts, each in a separate volume.

The five parts of the report are oriented to particular segments of our program. Parts 1 to 4 report on research performed for the DOE Office of Health and Environmental Research in the Office of Energy Research. Part 5 reports progress on all research performed for the Office of the Assistant Secretary for Environmental Protection, Safety and Emergency Preparedness. Each part consists of project reports authored by scientists from several PNL research departments, reflecting the interdisciplinary nature of the research effort. Project reports in Parts 1 to 4 are organized primarily by energy technology.

The parts of the 1981 Annual Report are:

Part 1: Biomedical Sciences Program Manager - H. Drucker	D. L. Felton, Editor
Part 2: Ecological Sciences Program Manager - B. E. Vaughan	B. E. Vaughan, Report Coordinator C. M. Novich, Editor
Part 3: Atmospheric Sciences Program Manager - C. E. Elderkin	R. L. Drake, Report Coordinator N. M. Burleigh, Editor
Part 4: Physical Sciences Program Manager - J. M. Nielsen	J. M. Nielsen, Report Coordinator I. D. Hays, Editor
Part 5: Environmental and Occupational Protection, Assessment, and Engineering Program Managers - D. L. Hessel S. Marks W. A. Glass	W. A. Glass, Report Coordinator R. W. Baalman, Editor

Activities of the scientists whose work is described in this annual report are broader in scope than the articles indicate. PNL staff have responded to numerous requests from DOE during the year for planning, for service on various task groups, and for special assistance.

The topic of the 21st Hanford Life Sciences Symposium, which was held this year, was "Biological Availability of Trace Metals: Chemical Estimation, Ecological and Health Implications."

A highlight of the year was completion of the third floor of the office wing of the Life Sciences Laboratory. This opens up substantial laboratory space by allowing investigators to move offices from the laboratory to the new area.

Credit for this annual report goes to many scientists who performed the research and wrote the individual project reports, to the program managers who directed the research and coordinated the technical progress reports, to the editors who edited the individual project reports and assembled the five parts, and to Ray Baalman and Irene D. Hays, editors in chief, who directed the total effort. The size of this year's report has been reduced as the result of an effort to report more fully in the open literature.

W. J. Bair, Manager
S. Marks, Associate Manager
Environment, Health and Safety Research Program

Previous Reports in this series:

Annual Report for

1951	W-25021, HW-25709
1952	HW-27814, HW-28636
1953	HW-30437, HW-30464
1954	HW-30306, HW-33128, HW-35905, HW-35917
1955	HW-39558, HW-41315, HW-41500
1956	HW-47500
1957	HW-53500
1958	HW-59500
1959	HW-63824, HW-65500
1960	HW-69500, HW-70050
1961	HW-72500, HW-73337
1962	HW-76000, HW-77609
1963	HW-80500, HW-81746
1964	BNWL-122
1965	BNWL-280; BNWL-235, Vol. 1-4; BNWL-361
1966	BNWL-480, Vol. 1; BNWL-481, Vol. 2, Pt. 1-4
1967	BNWL-714, Vol. 1; BNWL-715, Vol. 2, Pt. 1-4

1968	BNWL-1050, Vol. 1, Pt. 1-2; BNWL-1051, Vol. 2, Pt. 1-3
1969	BNWL-1306, Vol. 1, Pt. 1-2; BNWL-1307, Vol. 2, Pt. 1-3
1970	BNWL-1550, Vol. 1, Pt. 1-2; BNWL-1551, Vol. 2, Pt. 1-2
1971	BNWL-1650, Vol. 1, Pt. 1-2; BNWL-1651, Vol. 2, Pt. 1-2
1972	BNWL-1750, Vol. 1, Pt. 1-2; BNWL-1751, Vol. 2, Pt. 1-2
1973	BNWL-1850, Pt. 1-4
1974	BNWL-1950, Pt. 1-4
1975	BNWL-2000, Pt. 1-4
1976	BNWL-2100, Pt. 1-5
1977	PNL-2500, Pt. 1-5
1978	PNL-2850, Pt. 1-5
1979	PNL-3300, Pt. 1-5
1980	PNL-3700, Pt. 1-5

BLANK PAGE

FOREWORD

Part 4 of the Pacific Northwest Laboratory Annual Report for 1981 to the Office of Energy Research, DOE, includes those programs funded under the title "Physical and Technological Programs." The Field Task Program Studies reports are grouped under the most directly applicable energy technology heading. Each energy technology section is introduced by a divider page which indicates the Field Task Agreement reported in that section. These reports only briefly indicate progress made during 1981. The reader should contact the principal investigators named or examine the publications cited for more details.

BLANK PAGE

CONTENTS

PREFACE iii

FOREWORD vii

COAL

REACTION KINETICS OF COMBUSTION PRODUCTS 1

KINETICS AND MECHANISMS FOR THE FORMATION OF ORGANIC POLLUTANTS DURING PYROLYSIS COMBUSTION
R. D. Smith and A. L. Johnson 1

FLY ASH ENRICHMENT AND SURFACE SEGREGATION MECHANISMS
R. D. Smith and D. R. Baer 3

DEVELOPMENT OF INSTRUMENTATION FOR SUPERCRITICAL FLUID CHROMATOGRAPHY—TWO DIMENSIONAL MASS SPECTROMETRY
R. D. Smith 4

DEVELOPMENT OF A NEW METHOD OF LIQUID CHROMATOGRAPHY-MASS SPECTROMETRY FOR SYNTHETIC FUELS ANALYSIS
R. D. Smith and A. L. Johnson 5

CHEMICAL CHARACTERIZATION OF MATERIALS FROM COAL LIQUEFACTION PROCESSES
W. C. Weimer and B. W. Wilson 6

MODELING CELLULAR EFFECTS OF COAL POLLUTANTS 11

MODELING THE INFLUENCE OF EXCISION REPAIR ON THE TOXICITY OF COAL POLLUTANTS IN HUMAN CELLS
J. H. Miller and R. H. Heflich 11

EXPERIMENTAL STUDIES OF DAMAGE AND REPAIR IN CHINESE-HAMSTER OVARY (CHO) CELLS EXPOSED TO POLYNUCLEAR AROMATIC HYDROCARBON CARCINOGENS
C. N. Newman 12

PERMEABILITIES OF MODEL LUNG-CELL MEMBRANES TO COAL POLLUTANTS
D. R. Kalkwarf 15

FISSION

RADIATION PHYSICS 19

INITIAL INTERACTION PROCESS 21

DIFFERENTIAL IONIZATION CROSS SECTIONS FOR FAST PROTONS
L. H. Toburen, W. E. Wilson, and S. T. Manson 21

DIFFERENTIAL CROSS SECTIONS AND SCREENING IN IONIZATION BY STRUCTURED IONS
L. H Toburen, S. T. Manson, D. Schneider, N. Stolterfoht, P. Ziem, and M. Prost 23

TOTAL ION AND ELECTRON YIELDS
R. D. DuBois, M. E. Rudd, L. H. Toburen, L. L. Nichols, and C. A. Ratcliffe 24

PARTIAL IONIZATION CROSS SECTIONS FOR PROTON IMPACT
R. D. DuBois, L. H. Toburen and L. L. Nichols 26

ALIGNMENT DUE TO ELECTRON CAPTURE
R. D. DuBois and C. L. Cocke 27

A SIMPLE MODEL FOR THE ENERGY SPECTRUM OF ELECTRONS EJECTED BY HIGH—VELOCITY IONS
J. H. Miller, L. H. Toburen, W. E. Wilson and S. T. Manson 27

TRACK STRUCTURE 31

SYSTEMATICS OF DIFFERENTIAL IONIZATION CROSS SECTIONS
L. H. Toburen and W. E. Wilson 31

IONIZATION DISTRIBUTIONS IN CONDENSED PHASE
W. E. Wilson, L. H. Toburen and H. G. Paretzke 31

ANALYTIC MODEL FOR PRIMARY IONIZATION BY POSITIVE IONS
W. E. Wilson and J. H. Miller 31

ENERGY TRANSPORT 35

STOCHASTIC APPROACH TO TRACK STRUCTURE EFFECTS IN RADIATION CHEMISTRY
J. H. Miller and M. L. West 35

FLUORESCENCE IN BINARY LIQUID SYSTEMS: CONCENTRATION DEPENDENCE
M. L. West and J. H. Miller 37

DEVELOPMENT OF A TEMPERATURE CONTROLLED LIQUID TRANSFER SYSTEM FOR PULSED RADIOLUMINESCENCE STUDIES
M. L. West 38

DOSIMETRY AND BIOPHYSICS 39

MODELING AND CELLULAR STUDIES 41

DOUBLE TWO-EVENT MODELS
W. C. Roesch, L. A. Braby, and J. M. Nelson 41

EXPERIMENTAL EVIDENCE AND SUPPORT OF MULTIPLE TWO-EVENT MODELS
J. M. Nelson, W. C. Roesch, and L. A. Braby 42

TECHNIQUES FOR INVESTIGATING FAST REPAIR PROCESSES IN *CHLAMYDOMONAS REINHARDI*
L. A. Braby, J. M. Nelson, and W. C. Roesch 44

AGE DISTRIBUTIONS IN AGENIC MAMMALIAN CELLS
J. M. Nelson, L. A. Braby and N. F. Metting 46

SLOW REPAIR PROCESSES IN STATIONARY PHASE MAMMALIAN CELLS
J. M. Nelson, L. A. Braby and W. C. Roesch 49

MICRODOSIMETRY 51

MICRODOSIMETRY OF ELECTRON BEAMS
L. A. Braby and W. C. Roesch 51

RADIATION TRANSPORT AND DOSIMETRY CALCULATIONS FOR HIGH-ENERGY ELECTRONS
W. E. Wilson 52

CALCULATION OF DISTRIBUTIONS FOR ENERGY IMPARTED AND IONIZATION BY FAST PROTONS IN NANOMETER SITES
W. E. Wilson and H. G. Paretzke 53

INTERNATIONAL COMMISSION ON RADIATION UNITS AND MEASUREMENTS (ICRU) REPORT ON MICRODOSIMETRY
L. A. Braby 53

MICRODOSIMETRY OF INTERNAL SOURCES 55

MICRODOSIMETRY OF PARTICULATES
W. C. Roesch 55

COMPUTER PROGRAMS
W. C. Roesch 55

COMPUTER PROGRAM MODIFICATIONS FOR APPLIED INTERNAL MICRODOSIMETRY
D. R. Fisher, W. C. Roesch and R. Harty 55

STATISTICAL MODELING OF BEAGLE DOG LUNG FOR MICRODOSIMETRY
D. R. Fisher, R. T. Hadley, and W. C. Roesch 57

DOSIMETRY OF INTERNAL EMITTERS 61

MICRODOSIMETRY—A TOOL FOR INTERPRETING THE DOSE-RESPONSE FROM INTERNAL EMITTERS
D. R. Fisher and R. Harty 61

IN-VITRO ALPHA-PARTICLE MICRODOSIMETRY
R. J. Traub, D. W. Murphy, D. R. Fisher, and R. Harty 62

DEPOSITION OF INHALED ^{239}Pu-NITRATE IN KIDNEYS OF BEAGLE DOGS
R. J. Traub and J. F. Park 63

RADIATION INSTRUMENTATION—RADIOLOGICAL CHEMISTRY 65

APPLICATIONS TO ENVIRONMENTAL MEASUREMENTS OF A LOW-BACKGROUND HIGH-RESOLUTION INTRINSIC GERMANIUM DETECTOR
N. A. Wogman 65

SENSITIVITY COMPARISON OF NaI(Tl) AND GERMANIUM GAMMA-RAY SPECTROMETERS FOR DETECTING RADIONUCLIDES IN ENVIRONMENTAL SAMPLES
N. A. Wogman 68

ALPHA PARTICLE DETECTION USING ALPHA ETCHING TECHNIQUES
C. W. Thomas 69

AN ANALYTICAL METHOD FOR MEASUREMENT OF ^{226}Ra USING ALPHA ENERGY ANALYSIS
C. W. Thomas 70

IN-SITU SUBTERRANEAN DETERMINATION OF ACTINIDES BY HIGH-RESOLUTION GAMMA-RAY SPECTROMETRY
R. L. Brodzinski 71

PROPOSED ULTRASENSITIVE INVESTIGATION OF NEUTRINOLESS AND TWO-NEUTRINO DOUBLE BETA DECAY OF ^{76}GE
N. A. Wogman, R. L. Brodzinski, and F. T. Avigonne, III 72

AN ANTICOINCIDENCE SHIELDED WINDOWLESS GAS-FLOW PROPORTIONAL BETA COUNTER
C. W. Thomas 73

OIL SHALE

OIL SHALE AND TAR SANDS RESEARCH 77

ORGANIC AND MUTAGENIC PROPERTIES OF OIL SHALE RETORT WATERS
A. P. Toste, R. A. Pelroy, R. B. Myers, and D. L. Stewart 77

POLAR ORGANICS IN SHALE OILS
D. S. Sklarew, R. A. Pelroy, A. P. Toste, D. M. Schoengold, R. Pahl, S. P. Downey 79

ISOLATION OF METALLIC COMPLEXES IN SHALE OIL
K. B. Olsen, C. L. Wilkerson, A. P. Toste,
and D. J. Hayes 82

SPECIATION OF SULFUR COMPOUNDS IN OIL SHALE
BY-PRODUCT WATERS
K. H. Abel 83

SULFUR AND NITROGEN GAS ANALYSIS AT RIO BLANCO RETORTS
D. S. Sklarew, D. J. Hayes, and K. B. Olsen 84

PRODUCT AND EFFLUENT CHARACTERIZATION STUDIES
AT RIO BLANCO'S RETORT 0
C. L. Wilkerson, D. S. Sklarew, K. B. Olsen,
K. H. Abel, J. S. Fruchter, and C. L. Nelson 87

FOSSIL FUEL RESEARCH MATERIALS
C. L. Wilkerson and J. S. Fruchter 88

MULTITECHNOLOGY

ENVIRONMENTAL POLLUTANT CHARACTERIZATION
BY DIRECT-INLET MASS SPECTROMETRY 93

CHARACTERIZATION OF ENVIRONMENTAL POLLUTANTS
BY DIRECT-INLET MASS SPECTROMETRY
C. R Lagergren and J. J. Stoffels 93

TRACE ANALYSIS BY LASER EXCITATION 95

DOUBLE RESONANCE IONIZATION SPECTROSCOPY
DETECTION OF HEAVY METALS
B. A. Bushaw 95

PUBLICATIONS 99

PRESENTATIONS 103

AUTHOR INDEX 109

ORGANIZATION CHARTS 113

DISTRIBUTION 115

Coal

• Reaction Kinetics of Combustion Products*

The goal of the Reaction Kinetics of Combustion Products program is to determine the conditions, mechanisms, and chemical reactions that control the identity and concentrations of emissions from coal combustion processes. Presently, the program emphasizes the investigation of the mechanism that forms organic pollutants during combustion. Mass spectrometric techniques have been developed for the study of the high-temperature kinetics relevant to coal combustion, with specific emphasis on techniques that will allow investigation of the mechanisms and rates of formation of toxic and carcinogenic organic compounds. The chemistry of certain model compounds at combustion temperatures is being investigated. Our studies have begun to unravel the complex interactions between organic species in the combustion zone and the kinetic parameters relevant to pollutant release into the environment.

KINETICS AND MECHANISMS FOR THE FORMATION OF ORGANIC POLLUTANTS DURING PYROLYSIS AND COMBUSTION

R. D. Smith and A. L. Johnson

The potential toxicity and mutagenicity of emissions from coal-fired plants continue to be of concern. Of these emissions, the aromatic pollutants probably represent the major source of the mutagenically active constituents. Aromatic compounds, soot and related compounds are known to be produced efficiently under many combustion conditions but their formation mechanisms have not been clearly established.

A fundamental understanding of the kinetics and mechanisms for formation of aromatic pollutants is necessary for a number of reasons. An understanding of the high-temperature chemistry can facilitate the development of effective control strategies based upon manipulation of combustion parameters. Similarly, information from these fundamental studies provides thermochemical data necessary for equilibrium calculations or kinetic data for modeling studies. Measurements of rate constants as a function of temperature also are used to derive both valuable thermochemical information and provide input for modeling calculations. Mechanistic data provide a perhaps even more useful qualitative understanding of pollutant formation. Other practical problems related to soot formation, heat transfer, and combustion efficiency also will benefit from these data.

Studies of the polycyclic organic emissions from flames and various combustion facilities have shown that the emissions are qualitatively similar. Most aromatic compounds (or their precursors) ultimately emitted during coal combustion result from the highly fuel-rich local conditions of coal pyrolysis during the initial stages of combustion. An initial working assumption is that after formation the rates of the various oxidation and destruction pathways govern the emission concentrations. Thus, we first study simple aromatic model compounds which may be formed during coal devolatilization. Our goal is to determine representative primary unimolecular and bimolecular rate data and to identify important reaction pathways for the formation and destruction of representative species.

Modulated molecular beam mass spectrometry and related techniques such as phase angle spectroscopy (Smith 1979a and 1979b) are used to analyze the products from high-temperature reaction cells or flow tubes. In the past year these studies have centered upon the high-temperature chemistry of benzene, naphthalene, anthracene, and pyrene. The research effort has provided significant insight into the formation of both gas phase products and particulate (soot). Figure 1 gives the distribution of carbon introduced as benzene into the Knudsen reaction cell under three different sets of conditions. The figure shows the carbon remaining as benzene, as other gas phase pyrolysis products, and, by contrast, as carbon deposited on the reaction cell walls. The total carbon deposition rates were confirmed by independent measurements of carbon collected on the reactor walls. Thus, these studies are providing data relevant to the mechanisms of the formation of soot and polycyclic aromatic hydrocarbon (PAH). Figures 2, 3, and 4 give the product distributions for the major gas phase species in benzene pyrolysis under conditions similar to those shown in Figure 1. These results are aiding the development of a unified mechanism and model for PAH and soot formation during pyrolysis and combustion.

*Bullets denote Field Task Proposal/Agreement (FTPA) titles.

BEST DOCUMENT AVAILABLE

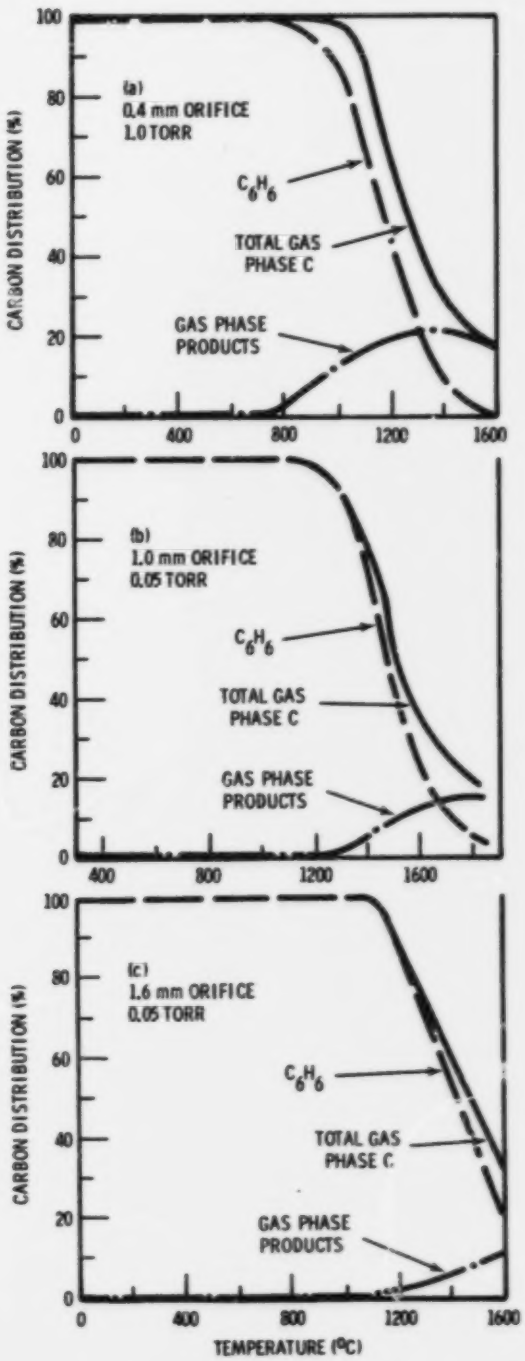

FIGURE 1. Carbon Distributions Observed in the Pyrolysis of Benzene for the Pressures and Reactor Orifice Sizes Noted. The carbon observed as benzene (— —), gas phase pyrolysis products (— • —), and total gas phase carbon (———) are given. Carbon deposition on the reactor walls is assumed to account for the carbon loss.

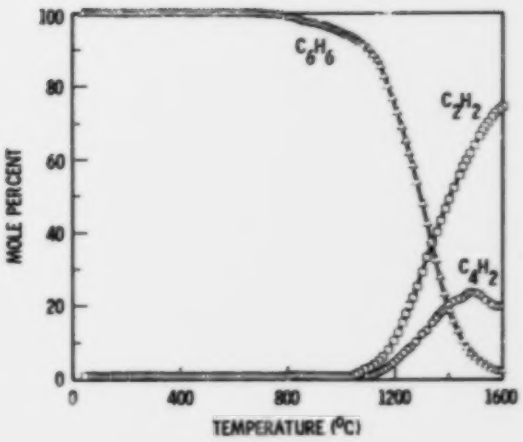

FIGURE 2. Concentration as a Function of Temperature for C_6H_6, C_4H_2, and C_2H_2 for the Pyrolysis of Benzene for a Flow Corresponding to a Pressure of 1 Torr at 1000°C in a Reaction Cell Having a 0.4-mm Diameter Orifice

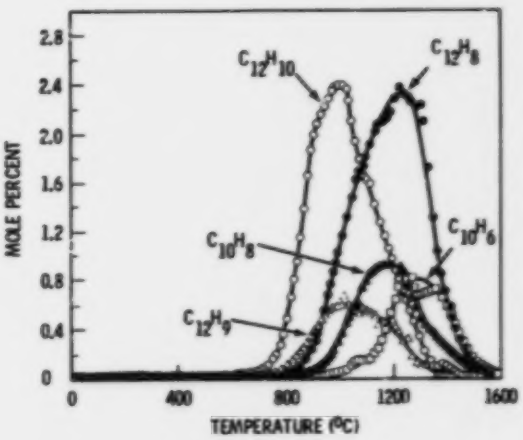

FIGURE 3. Concentration as a Function of Temperature for $C_{10}H_8$, $C_{10}H_6$, $C_{12}H_8$, $C_{12}H_9$, and $C_{12}H_{10}$

BEST DOCUMENT AVAILABLE

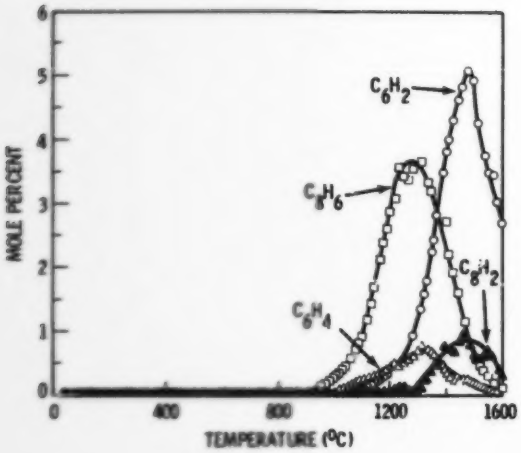

FIGURE 4. Concentration as a Function of Temperature for C_6H_2, C_6H_4, C_8H_2, and C_8H_6

REFERENCES

Smith, R. D. 1979a. "Formation of Radicals and Complex Organic Compounds by High Temperature Pyrolysis: The Pyrolysis of Toluene." Combustion and Flame 35:179.

Smith, R. D. 1979b. "A Direct Mass Spectrometric Study of the Mechanism of Toluene Pyrolysis at High Temperatures." J. Phys. Chem. 83:1553.

FLY ASH ENRICHMENT AND SURFACE SEGREGATION MECHANISMS

R. D. Smith and D. R. Baer

The environmental impact of fly ash resulting from coal combustion depends largely upon the surface composition of the particles (Smith 1980). Extensive study has demonstrated that large enrichments of volatile trace elements occur in the smallest particles as a result of condensation processes during cooling in the post-combustion region (Smith 1980; Campbell et al. 1978; Smith, Campbell and Nielson 1979a, 1979b). One might therefore expect that the surfaces of fly-ash particles would be greatly enriched in these elements. Indeed, surface analyses show that some enrichment does occur (Campbell, Smith and Davis 1978; Campbell et al. 1979); however, the magnitude of the enrichment appears to be much less than predicted by simple condensation models and highly dependent upon the particular element (Smith 1981). Understanding these processes can lead to improved pollution control methods.

The variations in surface enrichment can also reflect contributions from diffusion processes in the condensed phase during heating and cooling. Our studies investigate surface segregation processes in mineral matter representative of that found in coal and in model fly-ash surfaces. We are using modern surface analysis techniques to determine the rates for these processes in several model systems relevant to fly ash. These techniques include Auger electron spectroscopy (AES), X-ray photoelectron spectroscopy (XPS), and secondary ion mass spectrometry (SIMS). For example, studies of two common minerals in coal, feldspar and calcite, show significant variations in surface composition as the material is heated. Quite different enrichment processes are found between samples heated in vacuum and those in air. Studies on fly-ash surfaces prepared from actual melted fly ash are being used to determine surface segregation processes during cooling and diffusion rates into the bulk for species condensing on surfaces. These data ultimately will be incorporated in models that predict environmental impact of coal combustion facilities.

REFERENCES

Campbell, J. A., J. C. Laul, K. K. Nielson and R. D. Smith. 1978. "Separation and Chemical Characterization of Finely-Sized Fly-Ash Particles." Anal. Chem. 50:1032.

Campbell, J. A., R. D. Smith and L. E. Davis. 1978. "Application of X-ray Photoelectron Spectroscopy to the Study of Fly Ash." J. Appl. Spectro. 32:316.

Campbell, J. A., R. D. Smith, L. E. Davis, and K. L. Smith. 1979. "Characterization of Micron-Size Fly-Ash Particles by X-ray Photoelectron Spectroscopy (ESCA)." Sci. Total Environ. 12:75.

Smith, R. D. 1980. "The Trace Element Chemistry of Coal During Combustion and the Emissions from Coal-Fired Plants." Progress in Energy and Combustion Science 6:53.

Smith, R. D., J. A. Campbell and K. K. Nielson. 1979a. "Concentration Dependence Upon Particle Size of Volatilized Elements in Fly Ash." Sci. Technol. 13:553.

Smith R. D., J. A. Campbell and K. K. Nielson. 1979b. "Characterization and Formation of Submicron Particles in Coal-Fired Plants." Atmospheric Environment 13:607.

BEST DOCUMENT AVAILABLE

Smith, R. D. 1981. "Evaluation of Fly-Ash Surface Phenomena and the Application of Surface Analysis Technology." PNL-3842, Pacific Northwest Laboratory, Richland, WA 99352.

DEVELOPMENT OF INSTRUMENTATION FOR SUPERCRITICAL FLUID CHROMATOGRAPHY-TWO DIMENSIONAL MASS SPECTROMETRY

R. D. Smith

A new supercritical fluid chromatograph (SFC) coupled with a tandem quadrupole mass spectrometer has been designed, constructed, and developed to extend greatly the capability for analyzing complex synfuel and environmental samples. The analysis of these complex mixtures is limited by the sensitivity and selectivity of present instrumentation. In comparison to gas chromatography, the SFC potentially can extend chromatographic techniques by increasing the range of molecular weights, volatilities, and polarity of compounds that may be analyzed. In addition, it can improve greatly the chromatographic resolution relative to high-performance liquid chromatography. The technique exploits the high solvating power of supercritical fluids and incorporates new developments that enhance the degree of chromatographic separation. Analysis by SFC includes the use of capillary columns, improved coating techniques, pressure gradient programming, and designs to virtually eliminate dead volumes. The last is particularly important because of the low flow rates (typically 10 to 30 μℓ/min). These rates are also important for allowing direct interfacing to the mass spectrometer.

Figure 1 gives a schematic illustration of the SFC-tandem mass spectrometer. The system includes a new interface design, a dual simultaneous electron impact/chemical ionization ion source, and a tandem quadrupole mass spectrometer to allow collision-induced dissociation studies for two dimensional mass spectrometry (MS/MS). Two dimension mass spectrometry allows any selected ion to be collisionally decomposed to determine its structural makeup, thus enhancing selectivity and sensitivity. The combination of SFC and two dimensional mass spectrometry promises to provide greatly improved performance over existing GC-MS techniques for the analysis of complex-polar and higher-molecular weight compounds.

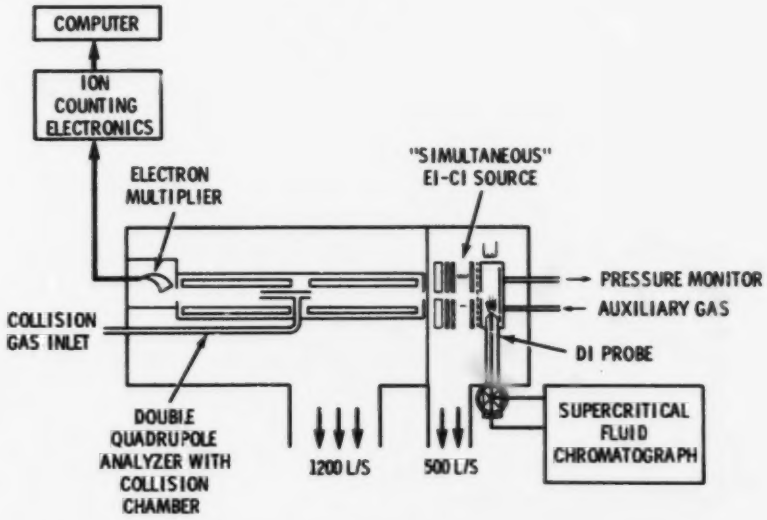

FIGURE 1. Schematic Illustration of the Supercritical Fluid Chromatograph-Tandem Quadrupole Mass Spectrometer Constructed at Pacific Northwest Laboratory

BEST DOCUMENT AVAILABLE

DEVELOPMENT OF A NEW METHOD OF LIQUID CHROMATOGRAPHY-MASS SPECTROMETRY FOR SYNTHETIC FUELS ANALYSIS

R. D. Smith and A. L. Johnson

The liquid chromatograph-mass spectrometer (LC-MS) designed and constructed under this program was described in the last annual report (Smith 1981) and in three scientific publications during FY 1981 (Smith and Johnson 1981a; Smith and Johnson 1981b; Smith et al. 1981). The LC-MS utilizes a moving ribbon interface for evaporation of the mobile phase (from a Spectra Physics 8700 HPLC), sample storage, and transfer to the analysis section. In the secondary ion mass spectrometry (SIMS) analysis mode, the solid residue is bombarded with high-energy ions and emitted secondary ions are energy-selected and analyzed using a quadrupole mass spectrometer. Alternately, the ribbon is heated rapidly and desorbed species are ionized using electron impact. To evaluate these techniques, both simple mixtures and an extremely complex biomass "bottom product" (wood liquefaction residue) have been analyzed.

In the development of a new LC-MS instrument using secondary ion emission, we have attempted to maximize both sensitivity and selectivity. The thermal desorption/electron impact mode of operation was included to allow conventional mass-spectrometric analysis for comparison with the SIMS mode without degrading its performance. The instrument includes a triple quadrupole analyzer to allow the application of collision-induced dissociation (CID) techniques for enhanced selectivity. Novel features of this instrument include aerosol deposition of the LC mobile phase for more efficient evaporation (Smith and Johnson 1981a), ribbon storage (Smith and Johnson 1981b), and improved clean-up techniques (Smith, Burger and Johnson 1981).

The initial analysis of biomass bottom products utilized ternary gradient elution normal-phase (amino 5 μm column) separation using a Spectra Physics Model 8700 HPLC. As expected, the level of separation was insufficient because the samples were extremely complex. Subsequent semi-prep scale separations were made of methylene chloride, methanol chloride, and methanol extracts using a similar ternary gradient elution program. Seventeen fractions were collected in sufficient quantity for multiple analyses. These fractions were then analyzed individually by reverse phase (C-18, 5 μm column) HPLC using a methanol-water gradient program. The normal-phase separation results in a rough division of compounds by chemical class and polarity, while reverse-phase separations are most effective for analysis within compound classes. This combination of analytical techniques, coupled with LC-MS using TD/EI and SIMS, for the ionization of non-volatile or thermally labile compounds is particularly effective for analysis of these and similar complex samples. The triple quadrupole mass spectrometer, with CID capability, should also be effective in separating coeluting compounds with interfering spectra, and in assisting in identification of the various compounds (Smith et al. 1981).

Figure 1 illustrates the application of ribbon storage techniques in the TD/EI mode of operation for a biomass sample. The figure gives the reconstructed total ion chromatogram for a single separation using normal-phase ternary gradient elution (hexane, methylene chloride, and 2-propanol) at three passes of the ribbon at temperatures of 150°C, 254°C, and 350°C, respectively. The results of applying the techniques to a hexane extract of wood liquefaction distillation residue illustrate the effect of the flash heater temperature on the analysis of complex mixtures. The reconstructed ion chromatograms for 150°C, 254°C, and 350°C ribbon passes show significant variations in relative intensity. As demonstrated, compounds are selectively observed at certain flash heater temperatures and discriminated against at higher or lower temperatures. Because this technique provides

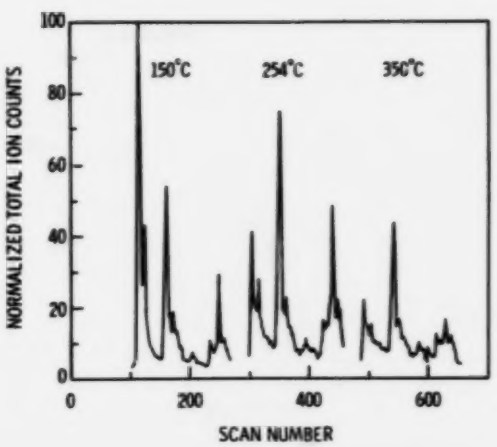

FIGURE 1. Normalized Total Ion Counts as a Function of Scan Number for an LC-MS Analysis of a Hexane Extract of a Wood Liquefaction Distillation Residue. The reconstructed ion chromatographs were obtained in the TD/EI mode (15 eV electrons) and represent three passes of the separated material through the analysis region.

BEST DOCUMENT AVAILABLE

differential information related to compound volatility, it can assist in interpreting complex chromatograms. For experiments where mass spectrometer scan requirements are more demanding, the LC effluent can be deposited on the moving ribbon and the mass spectrometer analysis performed at a different ribbon speed after completion of the liquid deposition, thereby totally decoupling mass spectrometer and HPLC operation.

The use of SIMS ionization in conjunction with the moving ribbon LC-MS interface adds a unique potential to "on-line" mass spectrometric analysis by allowing the analysis of nonvolatile and thermally labile compounds. Our results demonstrate that the most useful information is present in the low-energy secondary ion spectra. The removal of the high-energy ions by the energy filter not only limits loss of mass spectrometer resolution but also reduces contributions to the mass spectra from high-energy processes that contain little useful information. Our results also show that for primary ion currents of ~10^{-6} A/cm^2, a typical ribbon speed of 10 cm/min, and a primary ion beam 1 cm in diameter, the exposure time for a sample is 6 sec and consumption of approximately 6% of a monolayer occurs on each pass. Apparently, the restriction to low primary ion beam currents used for "static-SIMS" is reduced under conditions where the exposure time for a sample is on the order of a few seconds. We suggest that under the present conditions, the larger primary ion currents provide a rapid means for obtaining useful spectra on an essentially real-time basis. An example of a LC-MS analysis of the SIMS mode is illustrated in Figure 2.

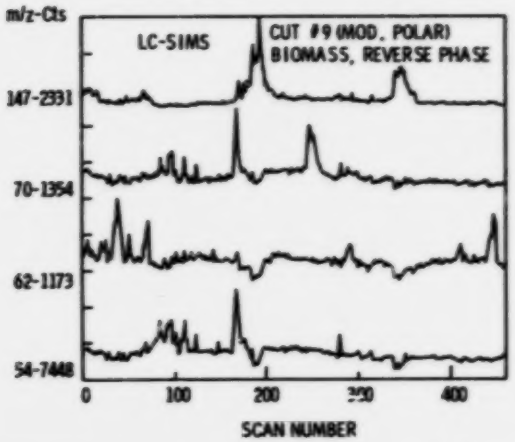

FIGURE 2. Reconstructed Ion Chromatograms for Four Typical Ions in the Reverse Phase LC-SIMS Analysis of a Normal Phase HPLC Semi-Prep Fraction.

This figure shows four reconstructed ion chromatograms for a biomass fraction obtained by semi-prep scale normal-phase HPLC and analyzed by reverse phase.

The characterization of these materials will require more extensive analysis using the triple quadrupole CID capability compared with the more conventional TD/EI spectra. These results clearly demonstrate that the new LC-MS techniques allow the analysis of materials not amenable to other analytical methods.

REFERENCES

Smith, R. D. and A. L. Johnson. 1981a. "Deposition Method for Moving Ribbon Liquid Chromatograph-Mass Spectrometer." Anal. Chem. 53:739.

Smith, R. D. and A. L. Johnson. 1981b. "Ribbon Storage Techniques for Liquid Chromatograph-Mass Spectrometry." Anal. Chem. 53:1120-1122.

Smith, R. D., J. E. Burger and A. L. Johnson. 1981. "Liquid Chromatography-Mass Spectrometry with Electron Impact and Secondary Ion Mass Spectrometry Using a Ribbon Storage Interface." Anal. Chem. 53:1603.

Smith, R. D. 1981. "Development of New Methods and Instrumentation for Liquid Chromatography-Mass Spectrometry." Part 4 of Pacific Northwest Annual Report for 1980 to the DOE Assistant Secretary for Environment. PNL-3700 PT4, Pacific Northwest Laboratory, Richland, Washington.

CHEMICAL CHARACTERIZATION OF MATERIALS FROM COAL LIQUEFACTION PROCESSES

W. C. Weimer and B. W. Wilson

Supporting Staff: C. Willey, R. B. Lucke, D. M. Schoengold, D. R. Kalkwarf, M. R. Petersen, D. S. Sklarew, A. P. Toste and J. R. Morrey

Samples of process streams and possible product materials are being obtained from PDU, pilot-plant, and, where possible, commercial-scale coal liquefaction facilities. The majority of these samples are representative of the solvent refined coal (SRC I and SRC-II). (The SRC-II research is funded by the Office of Health and Environmental Research, while the Office of Fossil Energy funds SRC-I research.) Small-volume samples have been collected during a

BEST DOCUMENT AVAILABLE

variety of operating conditions and documented by the commercial developers. Large-volume samples used principally in programs testing biological and ecological toxicity have been obtained under process conditions which, at the time of sampling, most nearly represented proposed demonstration-scale or commercial-scale operating conditions. Our three objectives in obtaining these samples are: (1) to obtain quantities of representative materials to be stored in a sample repository and subsampled as necessary for chemical, biological, or ecological testing; (2) to obtain general chemical composition data for each material; and (3) to characterize the biologically active components in those samples that demonstrate biological activity.

PNL prepares, on a quarterly basis, status reports covering specific areas of our SRC research. Summaries of two recently prepared status reports dealing with chemical characterization are included at the end of this report. Additional research activities not discussed in these two status reports are presented below.

- Coal Liquefaction Materials Repository

All coal liquefaction research materials are stored in a refrigerated repository. A computerized materials accounting system is used to track the quantity of each material remaining in the repository and to identify the investigators to whom subsamples of these materials have been released. The samples are stored in the dark at a temperature of 4°C, under an N_2 blanket, and are analyzed annually by several techniques to document their stability. Small volumes (<1 liter) of distillates from the SRC-I and SRC-II processes have been collected since 1975 and represent specific sets of operating conditions. Large volumes (>25 liters) of several SRC-I and SRC-II distillate materials have been obtained for biological and ecological testing. Included in these large-volume samples are the following: (1) one SRC-I light oil, (2) one SRC-I wash solvent, (3) two SRC-I process solvents, (4) two SRC-II naphthas, (5) four SRC-II middle distillates, (6) three SRC-II heavy distillates, and (7) four SRC-II fuel oil blends. Additional coal liquefaction samples added to the repository within the last year include the following: (1) a full-boiling-range material and distillate cuts from a two-stage liquefaction process unit, (2) full-boiling-range process solvents and discrete distillate cuts from both SRC-I and SRC-II processes, (3) materials from an indirect liquefaction process, and (4) several petroleum-derived items of commerce representing heavier-end petroleum products.

- Chemical Stability of Coal Liquefaction Materials

The chemical stability of the large-volume samples in the coal liquefaction materials repository is monitored annually by a series of characterization analyses. The purpose of this work is to ascertain the stability of the materials used in long-term biological testing regimes and to document any changes that do occur. In addition to this monitoring effort, an investigation of sample stability has been initiated using an SRC-II fuel oil blend as the test material. In a study for which the intent is to identify the most important parameter(s) in causing sample degradation, we are evaluating the effects of sample dilution, UV irradiation, temperature, and use of air as a cover gas on the sample composition. The samples are analyzed over a 32-week period by high resolution gas chromatography (GC). The GC data are analyzed by a computer-based pattern recognition analysis approach, with all major components referenced to an added internal standard. The observation of any compositional changes occurring under these extreme conditions will allow optimum long-term monitoring protocol for the large-volume samples.

- Chemical Analysis and In Vitro Mutagenicity Testing of Water Soluble Constituents from SRC-I Solid Products

Uncovered stockpiling and shipping of refined solid fuel products are likely to occur through any future use of these materials for stationary power generation. Although no particular environmental problem has been associated with outside storage of raw coal, it cannot be assumed that the same will apply to refined solid products, since there are major differences in the chemical structure of the two types of materials. One problem requiring study is aqueous leaching by rain or other waters that may come in contact with the solid product in an open stockpile. Accordingly, we have carried out a study to assess the comparative aqueous leaching propensities of SRC-I solid product, light de-ashed SRC (an internal process material which is part of the recycle solvent), and a representative feed coal.

BEST DOCUMENT AVAILABLE

The SRC-I solid product, light de-ashed SRC, and representative feed coal were powdered to facilitate aqueous leaching at acidic, neutral, and basic pH values. After leaching, the water was filtered and then forced through a pre-wet C_{18} Sep-Pak column to concentrate the organic compounds. The Sep-Pak was then rinsed with H_2O, methanol, and hexane to obtain fractions of organic compounds which had been retained on the C_{18} Sep-Pak. (The concentration factors ranged from 10^3 to 10^4.)

All fractions were then tested for mutagenicity against Salmonella typhimurium TA98 after metabolic activation with S-9 rat liver homogenate. The powdered feed coal showed no mutagenic activity for any of the H_2O, methanol, or hexane fractions from the acidic, neutral, or basic aqueous leachates. The methanol rinse from the Sep-Pak of the acidic H_2O leachate showed the only mutagenic activity for the SRC-I solid product with a dose response of 3 revertants per microgram. The methanol rinses of the acidic, neutral, and basic water leachates all showed mutagenic activity for the light de-ashed SRC with dose response values of 8, 3, and 6 revertants per microgram, respectively. The majority of activity in the Ames test appears to be in the acidic aqueous leachate of the SRC-I solid product and light SRC.

Detailed chemical analysis of the fractions was accomplished through gas chromatographic separation on high-resolution capillary columns using flame-ionization, nitrogen-phosphorus, and mass spectrometric detection. A one-to-one correspondence of nitrogen-containing species to the mutagenic activity was found. The major species in the aqueous leachates were found to be phenols, alkyl phenols, carbazoles, and aza compounds such as the quinolines. Such studies help to define the interaction of experimental coal refining products with aqueous environments which may be represented by aquatic discharge or longer-term leaching from exposed material stockpiles.

- The Mutagenic and Chemical Properties of SRC-I Materials: A Status Report (PNL-3604)

Process solvent (PS) and solid product (dissolved in organic solvent) produced by the SRC-I process at the Wilsonville pilot plant contain components mutagenically active against the Ames-Salmonella strains, Salmonella typhimurium TA98 and TA100. In relative terms, PS and the organic solvent solubilized product were of approximately the same mutagenic potency as coal-derived jet fuels and SRC-II high-boiling-range distillates. They were somewhat more genetically active in the Ames assay than shale oils and shale oil fractions. Ames-positive mutagens are apparently concentrated in the moderately polar to strongly polar chemical constituents of both materials. However, the dissolved solid product contains a much higher proportion of very strongly polar mutagens, and may be enriched in acidic (i.e., oxygen-containing) mutagens.

- Fractional Distillation as a Strategy for Reducing the Genotoxic Potential of SRC-II Coal Liquids: A Status Report (PNL-3787)

In vitro biological testing and supporting chemical analyses have been performed on two sets of SRC-II distillate fractions. All materials (parent liquids and distillate cuts) were screened for mutagenic activity against Salmonella typhimurium TA98, TA100, TA1537 and TA1535. Prophage induction in Escherichia coli (inductest) was also evaluated for all crude samples from the two sample sets to detect primary DNA damage. Initial chemical characterization, including fractionation and instrumental analysis by gas chromatography and mass spectrometry, was also performed on representative mutagenic and nonmutagenic distillate cuts.

In vitro biological data suggest that nearly all genetically active constituents in wide-boiling-range or full-boiling-range SRC-II liquids were fractionated into the higher-boiling-range (i.e., above 700°F) constituents by distillation. For example, none of the crude liquid under 650°F boiling-point (b.p.) showed genetic activity. The transition from low to high mutagenicity occurred between 730° and 760°F. Above 750°F b.p., the specific mutagenic activity increased two- to four-fold, reaching maximum values above 850°F b.p. DNA damage as detected by prophage induction occurred only in b.p. cuts above 850°F. Mutagenicity data (which appear to be a more sensitive indicator of genetic activity than prophage induction) indicated that constituents boiling below 700°F are genetically very weakly active or inactive. Materials boiling below 700°F comprise about 80% of a wide-boiling-range, demonstration-facility-type SRC-II process distillate product.

Initial chemical analysis of the b.p. cuts showed a general increase in the proportion of polar nitrogen-containing polycyclic compounds and polyaromatic hydrocarbons with

BEST DOCUMENT AVAILABLE

increasing boiling point, while aliphatic hydrocarbon content decreased with increasing temperature. There was a general increase in compound heteroatom content and polarity as well as molecular weight as the boiling point of the cuts increased. High levels of mutagenicity were associated with fractions enriched in high-molecular-weight nitrogen-containing polyaromatic hydrocarbons. Mutagenicity was not associated with fractions enriched in neutral polyaromatic hydrocarbons. Nitrosation of nitrogen-containing fractions substantially reduced their mutagenicity, suggesting that primary aromatic amines were the main determinants of biological activity.

Biological and chemical data suggest that selective distillation of coal liquids during processing may be feasible to produce fuels which have lowered genotoxicity compared to the full-boiling-range material.

BEST DOCUMENT AVAILABLE

BLANK PAGE

• Modeling Cellular Effects of Coal Pollutants

The important role of cellular repair processes in protecting living organisms from damage induced in DNA by ionizing and ultraviolet (UV) irradiation is well established. The goal of this project is to apply concepts of repair developed in radiation biology to obtain a better understanding of the risk associated with exposure to coal-related chemical carcinogens. A model proposed by Haynes (1975) to explain the effect of repair on the survival of bacteria exposed to UV irradiation has been successfully applied to the dose-response of human cells exposed to the aromatic amide carcinogen N-acetoxy-2-acetylaminofluorene. Our experimental program has isolated a mutant of the rodent cell line, CHO-K1, that exhibits a lower mutation frequency than the parent cell line following exposure to benzo[a]pyrene-4,5-oxide. These studies show the importance of repair phenomena in the interpretation of short-term bioassays. Permeability studies with polynuclear aromatic hydrocarbons show that these compounds have a high affinity for the nonpolar, lipid phase of cell membranes. These results are important for understanding the pathway for metabolic activation of these compounds.

MODELING THE INFLUENCE OF EXCISION REPAIR ON THE TOXICITY OF COAL POLLUTANTS IN HUMAN CELLS

J. H. Miller and R. H. Heflich*

Enzymatic repair processes that remove damage from cellular genetic material (DNA) protect higher organisms from naturally occurring carcinogens such as ultraviolet (UV) irradiation. Hence one may expect that these repair processes will have a strong influence on the dose-response for survival of cells exposed to coal-related, chemical carcinogens. We have developed a model that correlates survival of cloning ability of human fibroblasts with the rate at which these cells are able to remove carcinogenic residues that covalently bind to their DNA. A detailed description of this model is given in a manuscript that has been accepted for publication in Chemico-Biological Interactions (Miller and Heflich 1982). This report presents additional data that have been used to test the model.

When normal human fibroblasts are held in a nonproliferating state after treatment with a carcinogen, the fraction of cells that survive the treatment is increased. Our model attributes this recovery phenomenon to the increase in the time available to repair damage to DNA before it is expressed as loss of cloning ability. If this is true then the kinetics of recovery from potentially lethal damage should be the same as the kinetics for removal of carcinogen residues from DNA. Figure 1 shows that this is the case for benzo[a]pyrene

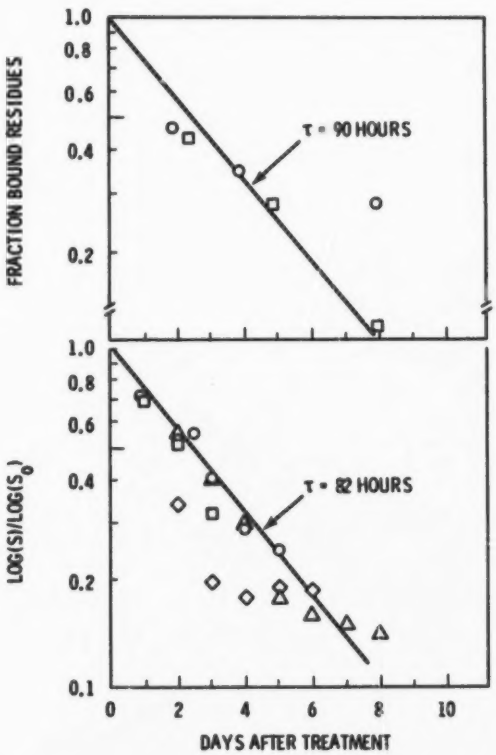

FIGURE 1. Kinetics for Removal of Carcinogen Residues Bound to DNA and for the Recovery From Potentially Lethal Damage by Human Fibroblasts Exposed to Benzo[a]pyrene Diol-epoxide

* Collaborator, National Center for Toxicology Research, Jefferson, Arkansas.

BEST DOCUMENT AVAILABLE

diol-epoxide (Yang et al. 1980), a polynuclear aromatic hydrocarbon carcinogen. The upper graph shows the fraction of carcinogen residues that remain bound to the DNA of nonproliferating human fibroblasts as a function of time after treatment. The lower graph shows the kinetics for removal of potentially lethal damage by plotting the ratio of the logarithms of survival with and without recovery as a function of the recovery time. In both cases we observe first-order kinetics with a characteristic time of about 90 hours.

To further test our model we have investigated the relationship between survival and rate of excision in human cells from xeroderma pigmentosum patients in complementation groups C and E. On the basis of survival data presented in last year's annual report (Miller 1980) we predicted that the rates of excision of DNA adducts produced by the aromatic amide carcinogen N-acetoxy-2-acetylaminofluorene (N-AcO-AAF) in normal, group E and group C cells should be in the ratio 1:0.6:0.4. Measured rates for excision of N-AcO-AAF residues by group E cells were about half as large as for normal cells in reasonable agreement with model predictions, but the rate at which group C cells excise these residues is only about one-tenth the normal rate. This discrepancy between predictions of our model and observed rates of excision in group C cells is probably due to the fact that the survival data on which the predictions are based are influenced by repair during the growth cycle and the excision rates were measured in nonproliferating cells. Techniques for measuring excision rates during the growth cycle and incorporation of these data into our model are currently under investigation.

REFERENCES

Yang, L. L., V. M. Maher and J. J. McCormick. 1980. "Error-Free Excision of the Cytotoxic, Mutagenic N^2-Deoxyguanosine DNA Adduct Formed in Human Fibroblasts by (±)-7β, 8α-Dihydroxy-9α, 10α-Epoxy-7,8,9,10-Tetrahydrobenzo[a]pyrene. In Proceedings of National Academy of Science, USA, 77:5933-5937.

Miller, J. H. 1980. "Modeling the Dose-Response Relationship for Survival of Human Cells Exposed to Chemical Carcinogens." Physical Sciences. Part 4 of Pacific Northwest Laboratory Annual Report for 1980 to the DOE Assistant Secretary for Environment. PNL-3700 PT4, Pacific Northwest Laboratory, Richland, Washington.

Miller, J. H. and R. H. Heflich. 1982. "A Model for the Effect of Excision Repair on the Survival of Human Cells Exposed to Chemical Carcinogens." Chemico-Biological Interaction (in press).

Haynes, R. H. 1975. "The Influence of Repair Processes on Radiobiological Survival Curves." In Cell Survival After Low Doses of Radiation: Theoretical and Clinical Implications., pp. 197-208. The Institute of Physics and John Wiley and Sons, London.

EXPERIMENTAL STUDIES OF DAMAGE AND REPAIR IN CHINESE-HAMSTER OVARY (CHO) CELLS EXPOSED TO POLYNUCLEAR AROMATIC HYDROCARBON CARCINOGENS

C. N. Newman

In this project, separate experimental approaches have been employed to examine the interaction of chemical carcinogens with mammalian cells. A significant effort has been made in the selection of CHO cell repair-mutants and their characterization. These studies have included biochemical measurements of damage to and repair of the target DNA molecule in parent and mutant cells as well as measurements of biological endpoints such as cellular inactivation and mutation induction. Related investigations have been designed to deduce the long-term effects of unrepaired (residual) damage in viable cells since these effects may be cumulative at low doses. For a variety of reasons the CHO cell tissue culture system has been used throughout this work. One reason is that few DNA lesions are excised by these cells. Thus, an opportunity to best study the fate of residual damage is readily available.

The selection of mutagen-resistant CHO cell mutants has proved lucrative. One such cell line, Mut 8-16, has been characterized extensively with respect to its sensitivity to both ultraviolet irradiation (UV) and to the active carcinogen, benzo[a]pyrene-4,5-oxide. Some results are illustrated in Figures 1-3. In Figure 1, inactivations by UV of Mut 8-16 and the parent cell line, CHO-K1, are shown. Clearly, the mutant is more resistant to the killing effects of this treatment judging by the larger shoulder on the survival curve at low UV fluence. As the UV fluence increases, inactivation dose-responses appear similar for both cell lines.

The mutation-induction UV dose dependencies are shown in Figure 2, and are the same for CHO-K1 and Mut 8-16 (Figure 2a). However, when mutation frequencies are plotted as a

BEST DOCUMENT AVAILABLE

function of survival (Figure 2b) an enhanced mutation response in the mutant is observed that manifests most dramatically at the highest survival UV fluences. No differences in post-replication repair ability in the two cell lines was detected judging by the similar molecular weights of radiopulsed-chased cellular DNA in alkaline sucrose gradients. Similarities in both cell lines were also obtained in assays of replication-repair and excision repair (data not shown). Figure 3 shows both survival and mutation induction dose-responses of the two cell lines following treatment with benzo[a]pyrene-4,5-oxide. In contrast to UV, cellular inactivation of mutant and parent were indistinguishable (Figure 3a) while at identical concentrations of carcinogen, mutation frequencies were different (Figure 3b). In contrast to CHO-K1 which yielded an approximately linear dose-dependency, a curvilinear response was observed in Mut 8-16. Closer inspection of Figure 3b shows that at concentrations up to 8 μM, the rate of increase in mutations with increasing dose is smaller in the mutant; however, at higher concentrations, slopes derived from the dose-response of both cells appeared to be the same. An hypothesis to explain these paradoxical results is proposed: Major repair pathways

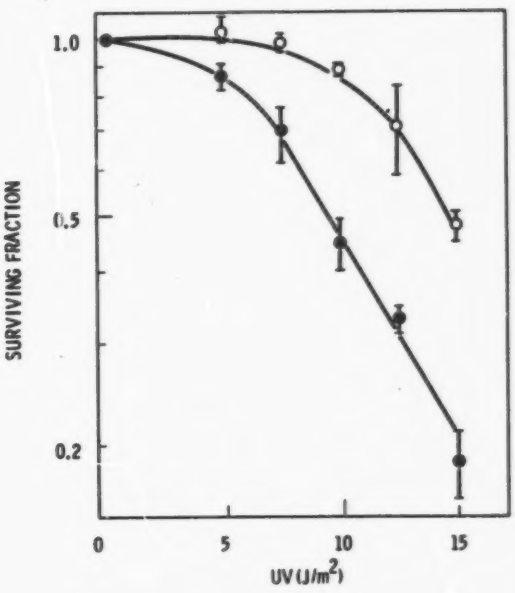

FIGURE 1. Ultraviolet Irradiation Inactivation of CHO-K1 (●) and Mut 8-16 (○)

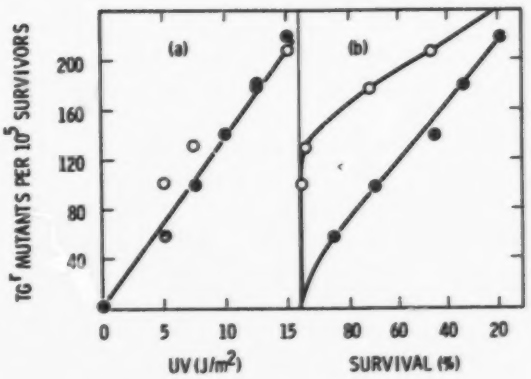

FIGURE 2. 6-Thioguanine Resistance Induced by Ultraviolet Irradiation. CHO-K1(●) and Mut 8-16 (○).

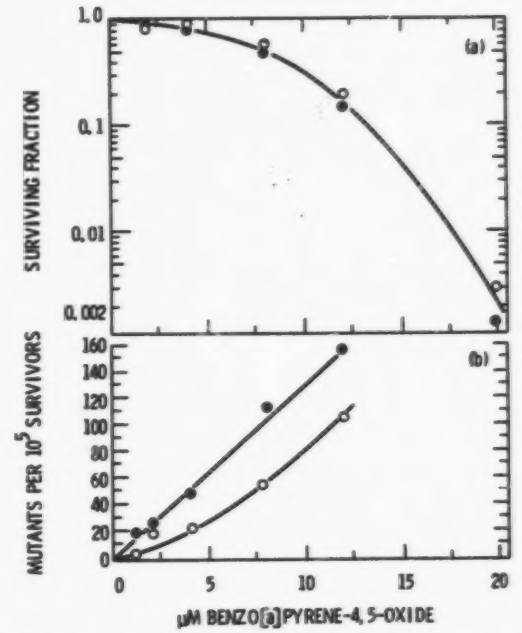

FIGURE 3. Inactivation (a) and 6-Thioguanine Mutation Induction (b) by Benzo[a]pyrene-4,5-oxide. CHO-K1(●) and Mut 8-16 (○)

for the most part are error-free, and only predict parallel changes in the probabilities of survival and mutation by reducing or modifying a portion of all the potentially damaging lesions. These effects of

BEST DOCUMENT AVAILABLE

major pathways on survival and mutation-induction curves are observed most dramatically at higher doses where they predominate. At lower doses, other mechanisms, possibly involving the DNA polymerase α, can be observed better. These act directly to irreversibly "fix" unrepaired (residual) lesions but with entirely independent probabilities for causing either cell death or mutation, depending on the type of lesions. Efforts to model the fate of cells exposed to low doses of carcinogen must account for such cellular processes.

We are attempting to better understand the interrelationship between binding and removal of chemical carcinogen to the target DNA molecule and the biological consequences of these processes. Figure 4 reveals the effects of varying periods of exposure to benzo[a]pyrene-4,5-oxide on population survival of CHO-K1 cells. Note that survival decreases as a clear exponential function with time of exposure both to 6 μM and 12 μM concentrations of this chemical. Interestingly, rates of inactivation for the two concentrations differ by more than the expected factor of two--a phenomenon not yet understood. Corresponding rates of binding and removal of DNA adducts after exposure of cells to 12 μM carcinogen are illustrated in Figure 5. Note that saturation of DNA binding sites is apparent by 3 hrs since binding does not increase even with up to 24 hrs of exposure. The lack of correlation between the number of DNA adducts (Figure 5) and population killing (Figure 3) possibly reflects the presence of non-DNA target molecules in cells, such as proteins and/or RNA. These findings reveal the need to assess genetic effects of chemicals on cells through other biological endpoint measurements such as mutation or transformation, rather than survival of cloning ability.

A strong interest of this laboratory has been to ascertain whether unrepaired damage in viable cells remains potentially hazardous, and thus, whether damage can accumulate from chronic low-level exposure to coal pollutants. Towards this end, we continued a concerted effort to arrest growing populations of cells at specified periods following treatment with carcinogen, as discussed in detail in last year's report (Newman 1980). Previously, methods which appeared to inhibit growth also resulted in nonreproducible or poor cloning efficiency. A major improvement this year has resulted in the ability to retard growth for up to ten days while still maintaining greater than 60% cloning ability of treated cells. Experiments are still needed to further refine this technique to achieve greater resolution and control of the elapsed period of growth and division.

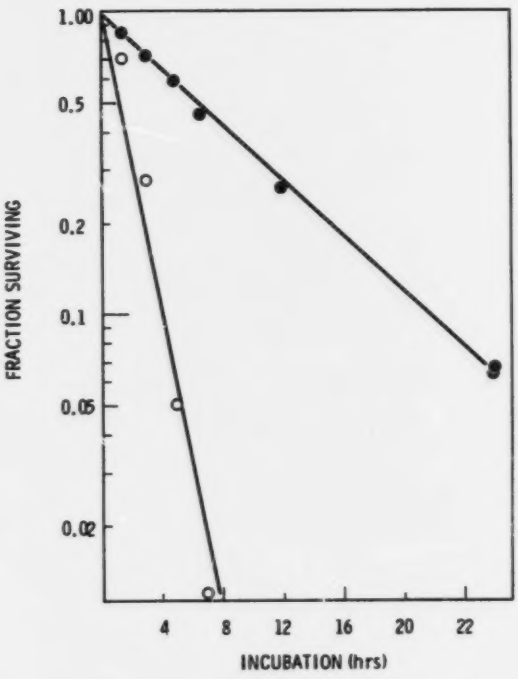

FIGURE 4. Inactivation of CHO-K1 by Incubation With Benzo[a]pyrene-4,5-oxide. 6 μM (•) or 12 μM (o)

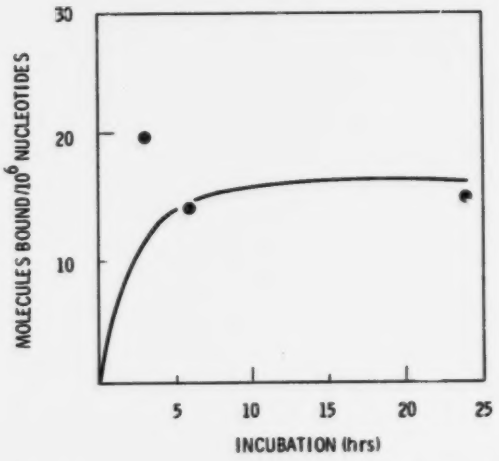

FIGURE 5. Binding of 12 μM Benzo[a]pyrene-4,5-oxide to DNA of CHO-K1 Cells in Culture

BEST DOCUMENT AVAILABLE

REFERENCES

Newman, C. N. 1980. "Biological and Biochemical Experimentation with Coal Related Carcinogens." Physical Sciences. Part 4 of Pacific Northwest Laboratory Annual Report for 1980 to the DOE Assistant Secretary for Environment. PNL-3700 PT4, Pacific Northwest Laboratory, Richland, Washington.

PERMEABILITIES OF MODEL LUNG-CELL MEMBRANES TO COAL POLLUTANTS

D. R. Kalkwarf

To react with the DNA in a mammalian cell, a pollutant must pass through the cell's plasma and nuclear membranes. The objective of this study was to estimate the minimum permeability of cell membranes to several coal pollutants by measuring the permeabilities of model membranes to these substances. The membranes used in this study were phospholipid bilayers prepared in the form of vesicles as described previously (Kalkwarf 1980). Both dipalmitoylphosphatidylcholine and stearoylsphingomyelin were used as these compounds are known to be representative of the phospholipids in mammalian-cell membranes.

Permeability measurements were conducted with three polycylic aromatic pollutants: pyrenedisulfonic acid, benzo[a]pyrene and 1-nitropyrene. The latter two compounds are not very soluble in water, but their solubility increases 100-fold by making the water 0.01 M in caffeine. Thus, the vesicles were prepared with an aqueous solution of 0.01 M caffeine at their interiors to provide a driving force for pollutant diffusion through the model membranes. Each of the pollutants was fluorescent with an intensity that increased with decreasing dielectric constant of the surrounding medium. Thus, addition of an aqueous solution of pollutant to a suspension of vesicles was expected to cause an increase in the fluorescence intensity of the system as the pollutant diffused into the bilayer, followed by a decrease in intensity as the pollutant diffused into the aqueous interior. From the rates of these processes, the permeability of a vesicle's membrane could be calculated.

Fluorescence measurements on the vesicle suspensions following mixing with aqueous solutions of pollutants indicated that the pollutants rapidly diffused into the membranes of the vesicles, but no evidence showed that they diffused through to the aqueous interiors of the vesicles. The fluorescent intensity from each of the three pollutants was at least doubled within 20 seconds after mixing, but this intensity then remained constant for at least 30 minutes. Apparently, the solubilities of these three pollutants in the bilayer were too high for them to diffuse into the aqueous interiors of the vesicles.

The significance of these measurements toward understanding the transport of polycyclic aromatic pollutants into cells is that these compounds can diffuse rapidly in the phospholipid bilayer of cell membranes even though they may have polar substituents such as nitro- and sulfonic acid-groups. Thus, the permeabilities of these compounds should depend more upon the abilities of intracellular-fluid components to extract these compounds from the interior surface of the bilayers than on the composition of the membrane.

REFERENCES

Kalkwarf, D. R. 1980. "Permeabilities of Model Lung-Cell Membranes to Coal Pollutants." Physical Sciences. Part 4 of Pacific Northwest Laboratory Annual Report for 1980 to the DOE Assistant Secretary for Environment. PNL-3700, PT4, Pacific Northwest Laboratory, Richland, Washington.

BEST DOCUMENT AVAILABLE

BLANK PAGE

Fission

BLANK PAGE

• RADIATION PHYSICS

A fundamental knowledge of the mechanisms by which radiation interacts with matter is essential for understanding dose-response relationships in terms of quantifiable chemical and physical processes. The Radiation Physics Program is directed toward investigation of the fundamental processes of energy deposition by fast charged particles and the subsequent transport and degradation of that energy as it leads to the formation of chemically active molecular species. The initial deposition of energy is studied through the measurements of total and differential cross sections for production of ions and electrons in collisions of fast charged particles with atomic and molecular targets. These data, when coupled with theoretical calculations, provide insight into the mechanisms of energy deposition in biologically significant matter. They also provide the necessary data base for energy transport studies. Our effort in energy transport and degradation combines the use of Monte Carlo calculations and theoretical investigation of condensed-phase chemical kinetics. Monte Carlo calculations provide detailed information on the initial structure of the particle track, and the theoretical investigation of energy transport provides the link between initial energy deposition and the final observation of chemically active molecular species. Time-resolved measurements of fluorescence from liquid systems excited by irradiation with pulsed beams of fast charged particles and ultraviolet light provide definitive tests of the theoretical results. Our integrated program of experimental and theoretical investigation results in a unified approach to understanding the mechanisms by which chemically active species are formed as a result of exposure to a radiation field.

This interdisciplinary program in the study of energy deposition, degradation, and transport maintains an active collaboration with scientists at numerous universities and national laboratories. During the past year we have benefited by a close working relationship with research groups, or individuals, at Argonne National Laboratory, GSF-Institut für Strahlenschutz (Neuherberg, GmbH), Kansas State University, University of Nebraska, and Oak Ridge National Laboratory, and by the numerous contacts made at meetings and workshops.

BLANK PAGE

Initial Interaction Process

Our study of the initial interaction processes in the absorption of energy from a radiation field by biologically significant material has concentrated on the measurement and interpretation of total and differential cross sections for the production of electrons and ions in collisions of fast charged particles with atomic and molecular targets. Of particular interest is the determination of cross section systematics and interaction mechanisms which will enable extrapolation of experimental results into regions where experiments are either impractical or unfeasible. A thorough understanding of these processes is particularly important in assessing the reliability of track structure calculations of energy deposition in condensed media based on interaction cross sections obtained from collisions with free atoms and molecules. During the past year, we initiated measurements of total cross sections for ion and electron production resulting from interactions of fast atomic and molecular ions with atomic and molecular targets. This project, in collaboration with Prof. M. E. Rudd (a visiting scientist on sabbatical from the University of Nebraska, in residence at Pacific Northwest Laboratory from January to June 1981), supplies data needed for our track structure calculations and for accuracy tests of our differential cross sections. Measurements were also initiated to provide information on the degree of multiple ionization which occurs in ionizing collisions. Interpretation of collision cross sections in terms of current theory has concentrated on application of Born theory to doubly differential cross sections for ionization of neon by fast protons and to application of Bethe-Born theory to singly differential cross sections measured for H^+ - Ne collisions. The latter is particularily important in devising means of extrapolating and interpolating cross sections into regions where data do not exist. Our work involving structured ions, i.e., He^+, resulted in three publications during the past year which describe effects of screening by projectile electrons. Particularly gratifying is the excellent agreement between Born calculations and our measurements for He^+ - He collisions.

DIFFERENTIAL IONIZATION CROSS SECTIONS FOR FAST PROTONS

L. H. Toburen, W. E. Wilson and
S. T. Manson*

The spatial distribution of primary energy deposition events along a charged particle track has important consequences for the subsequent chemical and biological processes. Calculations of these distributions, using Monte Carlo techniques, require detailed information on the energy and angular distributions of secondary electrons as the primary source term. Although the chemical and biological processes occur in condensed phase, the short range and scattering properties of electrons in condensed media necessitate direct cross section measurements in gas phase targets. To evaluate the applicability of these gas phase data to condensed phase calculations, it is important to know the effects of projectile and target properties on the measured cross sections. Fundamentally, a knowledge of the interaction mechanisms, including the theoretical description, can lend insight into which collision parameters may be most influenced by the target properties including molecular and phase effects. Several years ago we initiated a detailed experimental-theoretical study of doubly differential ionization cross sections (differential in ejected electron energy and emission angle) in collaboration with Dr. S. T. Manson. The initial study involved the simplest experimentally feasible collision system; H^+ + He (Manson et al. 1975). Recently we have extended this work to a detailed study of the ionization of neon by fast protons. During the past year calculations have been carried out for the H^+ - Ne collision system within the framework of the Born approximation using Hartree-Slater wave functions for initial discrete and final continuum states. These calculations include contributions from ionization of the 1s, 2s, and 2p subshells. Results have been compared to our measurements for proton energies of 0.3, 1, 2, 3, 3.67, and 4.2 MeV. For the most part, the experimental and theoretical results agree within experimental uncertainties (± 20%). However, notable differences are observed at large and small emission angles. A comparison of experimental and theoretical results is shown in Figure 1 for selected ejected electron energies and emission angles of 15° and 120° as a function of the incident proton energy.

* Consultant, Georgia State University, Atlanta, Georgia.

BEST DOCUMENT AVAILABLE

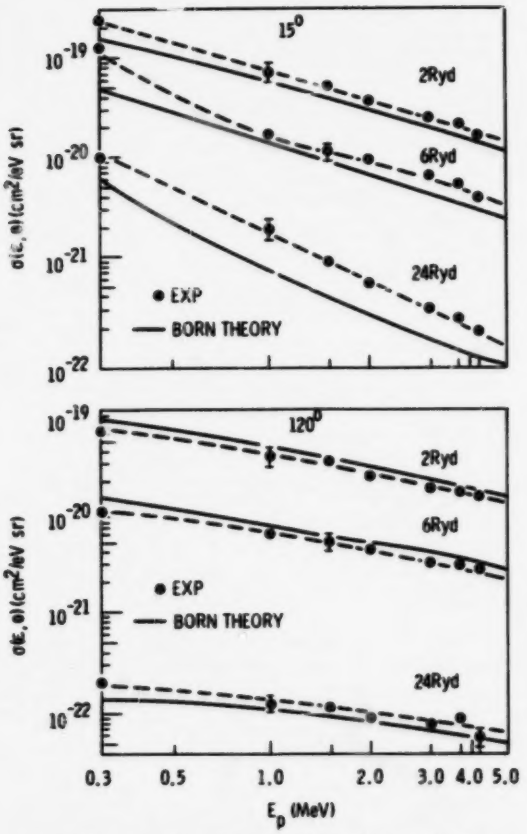

FIGURE 1. Doubly Differential Cross Sections for Ejection of Electrons of Selected Energies at 15° and 120° as a Function of Proton Energy. The Born calculation (solid lines) was performed using Hartree-Slater wave functions for initial discrete and final continuum states.

Representative error bars are shown to illustrate the estimated 20% uncertainty in the experimental results. We note theory tends to underestimate the cross sections for ejection of low-energy electrons into small emission angles and to overestimate them for large emission angles. At higher electron ejection energies, represented by the 24 Ryd data shown in Figure 1, theory is consistently lower than experiment. Although calculations were carried out to still higher ejected electron energies, the theoretical partial wave analysis becomes less reliable at those higher energies. The most curious aspect of the comparison shown in Figure 1 is the lack of proton energy dependence on the observed differences between the calculated and measured cross sections. We had expected to see better agreement for the higher ion energies related to improved validity of the underlying assumptions of the Born theory. We are presently searching for clues in both the experimental and theoretical techniques as to the origin of the observed discrepancies.

The observed differences between experimental and theoretical cross sections shown in Figure 1 do not lend themselves to resolution based on any single experimental renormalization technique. To try to uncover possible experimental uncertainties, we have also studied singly differential and total yields obtained by integration of these differential cross sections. The analysis of singly differential and total ionization cross sections will be discussed in a later section of this report. One can also gain insight into accuracies by comparison of the K-shell ionization cross sections to theoretical results and to previous measurements for other target atoms and molecules.

Auger electron emission following K-shell ionization of neon by protons provides a direct measure of the K-shell ionization cross section. For K-shell ionization of low-Z atoms the fluorescence yield is small and a one-to-one correlation exists between vacancy production and Auger electron emission (Toburen 1973; and references therein). Neon K-shell ionization cross sections were obtained by integration of the K-Auger peak areas and the results are shown in Figure 2 along with previous results for other atomic and molecular targets (Toburen 1973). The data are scaled as predicted by binary encounter theory and the solid line in Figure 2 is a binary encounter theory calculation of Garcia (1970). A representative error bar is shown to indicate the 20% estimated experimental uncertainty. The measured K-shell cross sections for neon are in excellent agreement with the calculated values. The scaled neon cross sections agree well with previous measurements for ionization of oxygen and fluorine and are only slightly smaller than previous work for carbon and nitrogen.

REFERENCES

Garcia, J. D. 1970. "Inner-shell Ionizations by Proton Impact." Phys. Rev. A 1:280-285.

Manson, S. T., L. H. Toburen, D. H. Madison and N. Stolterfoht. 1975. "Energy and Angular Distribution of Electrons Ejected from Helium by Fast Protons and Electrons." Phys. Rev. A 12:60-79.

BEST DOCUMENT AVAILABLE

Toburen, L. H. 1973. "K-Shell Ionization by Fast Protons." In Proceedings of the International Conference on Inner Shell Ionization Phenomena and Future Applications. Atlanta, Georgia, 1972, ed. by R. W. Fink, S. T. Manson, J. M. Palms, and P. V. Rao (CONF-720404, USAEC, Oak Ridge, TN.) pp. 979-992; and references therein.

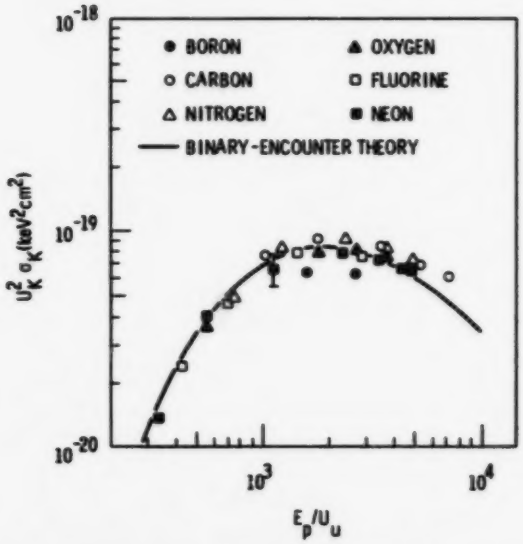

FIGURE 2. Comparison of K-Shell Ionization Cross Sections for Neon to Previously Measured Values for Other Targets (Toburen 1973) and to a Binary Encounter Calculation of Garcia (1970). The cross sections are scaled according to binary encounter theory where U_K is the K-shell binding energy of the target atom.

DIFFERENTIAL CROSS SECTIONS AND SCREENING IN IONIZATION BY STRUCTURED IONS

L. H. Toburen, S. T. Manson,*
D. Schneider,** N. Stolterfoht,** P. Ziem**
and M. Prost**

An understanding of the effects of projectile electrons on ionization cross sections is particularly important in evaluating interaction probabilities for alpha particles and the heavier recoil ions formed in absorption of fast neutrons in tissue. Since these ions pick up and lose electrons as they are stopped, their interaction probabilities will be affected by the nuclear screening ability of the bound electrons. During the past year studies of projectile screening have resulted in several publications. A brief review of the work is presented here.

Our success in application of Born theory to H^+ - He collisions (Manson et al. 1975) has led us to extend this theory to the simplest structured ion collision system amenable to experimental testing. Calculations for the He^+ - He collision system were carried out by S. T. Manson and compared with our measurements for 1.2 and 2.0 MeV He^+ ions. The results of this comparison, published in Physical Review Letters, (1981) show good agreement between calculated and measured cross sections over a broad range of ejected electron energies and emission angles. Some difficulties persist, however, near the forward direction. Additional data will be required to pinpoint the underlying reasons for these discrepancies.

A study of the systematics of differential cross sections for ionization by He^+, He^{2+}, and O^{n+} (n = 4 - 8) conducted in collaboration with the atomic collision group at Hahn Meitner Institut (Berlin) has lead to the development of a model of the effective projectile charge appropriate to energy loss collisions. The utility of such a model is that readily available cross sections from bare charged particles can be scaled to structured ions using the effective charge. In this model, the effective charge of the projectile is estimated as a function of the interaction distance based on the spatial distribution of bound electrons derived from their electronic wave functions. Correlation of the effective interaction distance with collisional energy transfer through the Massey criterion enables comparison of model predictions of effective projectile charge with results obtained from differential ionization cross-section measurements. The model is found to provide a reliable estimate of screening for measurements involving fast helium and oxygen ions. A description of this work has been published in Physical Review A (Toburen et al. 1981b).

The model discussed above, which incorporates the effects of projectile structure as an energy-loss dependent effective charge, is ideally suited for application with binary encounter theory. Such calculations, performed in collaboration with the Hahn Meitner group, were initially discussed in

* Consultant, Georgia State University, Atlanta, Georgia.
** A portion of the work on screening by projectile electrons was performed in collaboration with members of the atomic collisions group at Hahn Meitner Institut, Berlin.

BEST DOCUMENT AVAILABLE

last year's report (Toburen 1980) and published in the proceedings of the Small Accelerator Conference, Denton, Texas, Nov. 1980 (Toburen et al. 1981a). In general, this calculational procedure provides reliable cross sections for target ionization, however, it appears to overestimate the contribution of projectile stripping. Soon these techniques will be investigated further for interpretation of data for ionization by carbon ions.

REFERENCES

Manson, S. T. and L. H. Toburen. 1981. "Energy and Angular Distributions of Electrons from Fast He^+ + He Collisions." Phys. Rev. Letters 46:529-531.

Toburen, L. H. 1980. "Screening in Heavy Ion Collisions." Physical Sciences. Part 4 of Pacific Northwest Laboratory Annual Report for 1980 to the DOE Assistant Secretary for Environment. PNL-3700 PT4, pp. 35-38. Pacific Northwest Laboratory, Richland, Washington.

Toburen, L. H., P. Ziem, N. Stolterfoht, D. Schneider and M. Prost. 1981a. "Dynamic Screening by Projectile Electrons in Heavy Ion Collisions." In Proceedings of the 1980 Conference on the Application of Accelerators in Research and Industry, ed. J. L. Duggan and I. L. Morgan IEEE Transactions on Nuclear Science NS-28, 1131-1145.

Toburen, L. H., N. Stolterfoht, P. Ziem and D. Schneider. 1981b. "Electronic Screening in Heavy-Ion-Atom Collisions." Phys. Rev. A 24:1741-1745.

TOTAL ION AND ELECTRON YIELDS

R. D. DuBois, M. E. Rudd, L. H. Toburen, L. L. Nichols and C. A. Ratcliffe

Absolute doubly differential cross sections (DDCS), traditionally measured under the Radiation Physics project at PNL, provide sensitive detailed information about ion-atom collision processes. Such data, differential in angle of emission and energy of secondary electrons produced during the collision, provide a major contribution to the data base needed for track structure calculations and can be compared directly to theoretical calculations to gain insight into the interaction mechanisms. In principle, these data can also be integrated over angle and energy to provide singly differential and total ionization cross sections. Total ionization cross sections derived in this manner enable an assessment of the experimental accuracy by comparison to independent total yield measurement which are inherently more accurate. In addition, total yields are important in track structure calculations in normalization procedures.

Although numerous measurements of total ionization cross sections have been made in the past, the impact energy range from 5 to 5000 keV is covered sporadically. Also in regions of overlap, particularly for lower impact energies, the agreement among the data is poor. An illustration of the uncertainties and discrepancies between various sets of data in the literature for proton ionization of argon is shown in Figure 1. The previously measured yields differ in some cases by as much as a factor of 3. Because of the importance of accurate ion yields, we initiated a new series of measurements designed to cover the entire energy range from 5 to 5000 keV with a single detection system. These measurements conducted in collaboration with Prof. M. E. Rudd who visited PNL from January to June, 1981, while on sabbatical leave from the University of Nebraska, will emphasize determination of accurate (approximately $\leq$5%) absolute cross sections for light projectiles (H^+, H_2 , H_3 , He^+) impacting on common atomic and molecular gases.

In the present measurement, total ion and electron yields are obtained by passing the ion beam between parallel condenser plates and collecting the beam in a biased Faraday cup. A biased high transmission grid, placed in front of one condenser plate, provides an extraction field for the slow ions and electrons produced during the collision. In addition, any secondary electrons produced at the condenser plates are suppressed. Measurement of the ion and electron currents at the plates, when normalized to collected beam charge and target gas pressure, allows the absolute cross sections (σ_i, σ_e) to be determined. Considerable efforts have been made to determine accurately all experimental parameters and to investigate the effects of unknowns (e.g., the effect of photoelectrons ejected from surfaces).

For unstructured projectiles (e.g., H^+), the electron yield (σ_e) corresponds to the total ionization cross section for the target; whereas the difference of the ion and electron yields ($\sigma_i - \sigma_e$) provides the electron capture cross section. At lower energies the ion yield measures ionization plus electron capture from the target. The electron yield (σ_e) is due to ionization of the target and electrons stripped from the projectile.

BEST DOCUMENT AVAILABLE

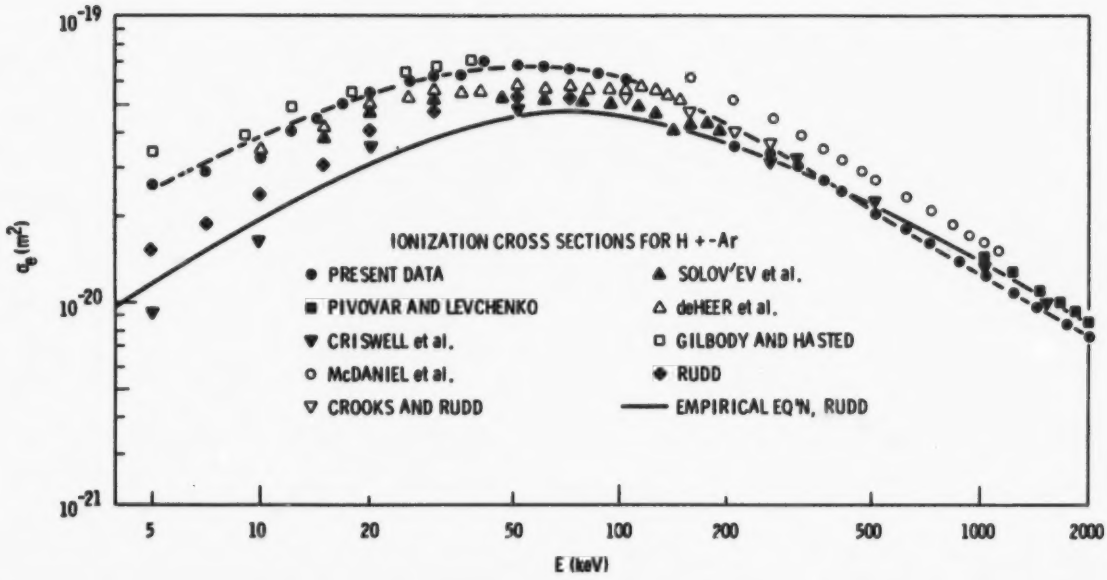

FIGURE 1. Total Cross Sections for Ionization of Argon by Proton Impact. The data are from Pivovar and Levchenko (1967), Criswell et al. (1977), McDaniel et al. (1961), Crooks and Rudd (1971), Solov'ev et al. (1962 and 1963), DeHeer et al. (1966), Gilbody and Hasted (1957), Rudd et al. (1979) and our present work. The empirical equation is from work of Rudd (1979).

An example of the results obtained to date is shown in Figure 2; our data for argon are also shown in Figure 1 and illustrate the degree to which they agree with previous work. A preliminary report of these data was presented at the International Collisions Conference this summer in Gatlinburg, Tennessee (Rudd et al. 1981). Current emphasis is on reducing the errors for H^+- data to a minimal level and on extending the ion energy range minimal level and on extending the ion energy range.

REFERENCES

Criswell, T. L., L. H. Toburen and M. E. Rudd. 1977. "Energy and Angular Distribution of Electrons Ejected from Argon by 5-keV to 1.5 MeV Protons." Phys. Rev. A 16:508-517.

Crooks, J. B. and M. E. Rudd. 1971. "Angular and Energy Distribution of Cross Sections for Electron Production by 50-300-keV Proton Impact on N_2, O_2, Ne and Ar." Phys. Rev. A 3:1628-1634.

DeHeer, F. J., J. Schutten and H. Moustofa. 1966. "Ionization and Electron Capture Cross Sections for Protons Incident on Noble and Diatomic Gases Between 10 and 140 keV." Physica 32:1766-1792.

Gilbody, H. B. and J. B. Hasted. 1957. In Proceedings of Royal Society (London) A240 382.

McDaniel, E. W., J. W. Hooper, D. W. Martin and D. S. Harmer. 1961. "Ionization Cross Sections for Protons on Noble Gases in the Energy Range 0.15 to 1.10 MeV." In Proceedings of the Fifth International Conference on Ionization Phenomena in Gases, Munich. Vol. 1 pp. 60-70. North Holland Publishing Co. Amsterdam, 1962.

Pivovar, L. I. and Yu Z. Levchenko. 1967. "Cross Sections for Ionization of Gases by 1-3-MeV Protons." Sov. Phys. JETP 25:27-30.

Rudd, M. E., R. D. DuBois, L. H. Toburen and C. A. Ratcliffe. 1981. "Ion and Electron Production Cross Sections for H^+, H_2, $^3He^+$, and $^4He^+$ on Ar." In Abstracts of Papers, XII International Conference on the Physics of Electronic and Atomic Collisions, ed., by S. Datz, Gatlinburg, Tennessee, pp. 804-805.

Rudd, M. E., L. H. Toburen and N. Stolterfoht. 1979. "Differential Cross Sections of Ejection of Electrons from Argon by Protons." Atomic Data and Nuclear Data Tables 23:405-442.

BEST DOCUMENT AVAILABLE

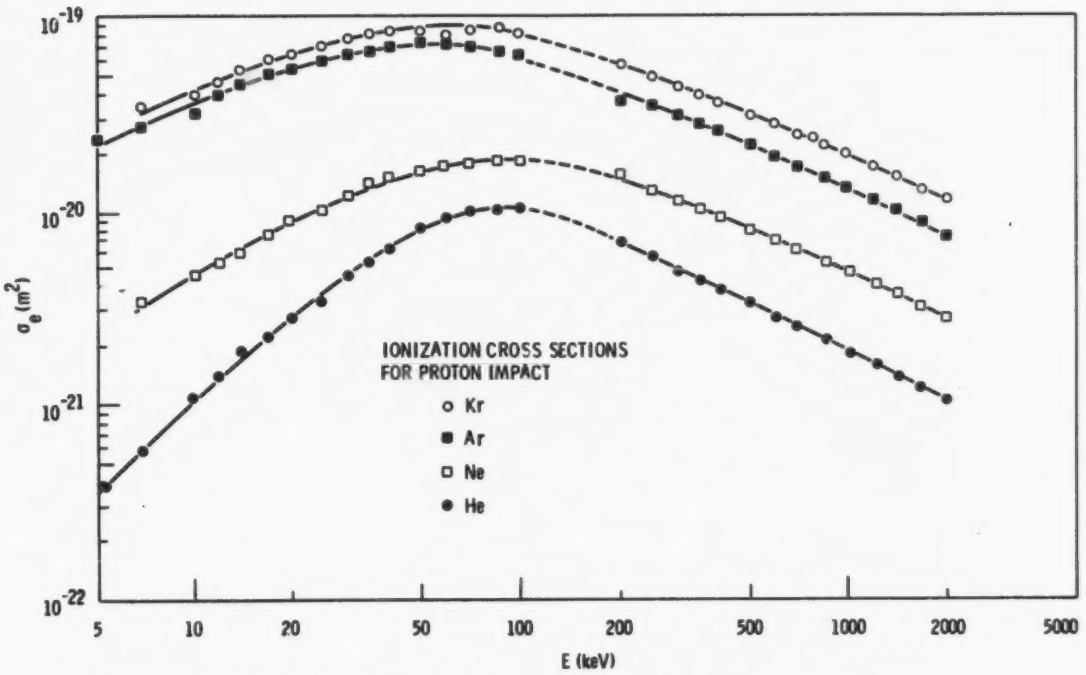

FIGURE 2. Total Ionization Cross Sections Measured for Proton Ionization of Several Gas Targets

Rudd, M. E. 1979. "Energy and Angular Distributions of Secondary Electrons from 5-100 keV Proton Collisions with Hydrogen and Nitrogen Molecules." Phys. Rev. A 20:787-796.

Solov'ev, E. S. et al. Soviet Phys. JETP 42, 659 (63) and JETP 15:459 (62).

PARTIAL IONIZATION CROSS SECTIONS FOR PROTON IMPACT

R. D. DuBois, L. H. Toburen and
L. L. Nichols

The device discussed in the preceding article, "Total Ion and Electron Yields," measures total ion yields but has no energy or charge resolution; therefore, the measured yields include contributions from multiple as well as single ionization events. For example we measure the sum of reaction such as:

$$H^+ + Ne \rightarrow Ne^+ + e^- + H^+$$

$$H^+ + Ne \rightarrow Ne^{2+} + 2e^- + H^+$$

$$\rightarrow \text{etc.}$$

Since neither our total nor differential cross section measurements distinguish the final charge states, an additional experimental technique is required to determine the degree of multiple ionization which occurs during these collisions. This information is particularly important in comparing experimental results to theoretical work that provides only single ionization cross sections. Thus, we have recently added a time-of-flight (TOF) charge state analyzer to the experimental apparatus.

Slow target ions, charge state q, are accelerated to an energy qV and pulsed into a drift tube. They then drift through a field-free region and are detected by a channel electron multiplier. Flight time provides the q/M spectrum. Using this technique ratios of multiple-to-single ionization events have been measured for 10 to 100 keV proton ionization of neon. A ratio of approximately 0.05 ± 0.01 was obtained for Ne^{2+}/Ne^+ for 40 keV proton impact. A preliminary discussion of this work will be presented at the DEAP meeting in December (DuBois 1981) and further investigations to extend the ion energy range and target species are in progress.

BEST DOCUMENT AVAILABLE

REFERENCE

DuBois, R. D., L. H. Toburen and L. L. Nichols. 1981. "Ionization Cross Sections for Ne^+ and Ne^{2+} by Proton Impact." Bul. Am. Phys. Soc. 26:1310.

ALIGNMENT DUE TO ELECTRON CAPTURE

R. D. DuBois and C. L. Cocke*

Detailed information about collision processes can be obtained by studying the angular distributions of Auger electrons produced during the collision. Under certain circumstances (Mehlhorn 1968), the nonisotropic angular distribution of Auger electrons can be directly related to the nonstatistical population of magnetic substates (i.e., alignment). A detailed experimental study of collisional-induced alignment in H^+- Mg collisions (Rodbro et al. 1978) agreed only qualitatively with theory (Berezhko and Kabachnik 1977). Later calculations (Berezhko et al. 1980) attributed this discrepancy to Auger emission following electron capture by the proton as well as to normal direct Coulomb ionization. Thus, in collaboration with C. L. Cocke of Kansas State University, we are attempting to measure the degree of alignment of initial states as a result of electron capture. The experimental apparatus has been assembled and preliminary tests have been made. Currently efforts are being made to reduce background effects.

REFERENCES

Berezhko, E. G. and N. M. Kabachnik. 1977. "Theoretical Study of Inner-Shell Alignment of Atoms in Electron Impact Ionization: Angular Distributions and Polarization of X-rays and Auger Electrons." J. Phys. B: Atom Molec. Phys. 10:2467.

Berezhko, E. G., N. M. Kabachnik and V. V. Sisov. 1980. "On the Role of Electron Capture in the Inner-Shell Alignment of Atoms in Ion-Atom Collisions." Phys. Lett. 77A:231.

Mehlhorn, W. 1968. "On the Polarization of Characteristic X-Radiation." Phys. Lett. 26A:166.

Rodbro, M., R. DuBois and V. Schmidt. 1978. "$L_3 - M_1M_1$ Auger Electron Study of Collisionally Induced Alignment for e^-, H^+, and He^+ Impact Ionization in Atomic Magnesium." J. Phys. B Lett. Atom. Molec. Phys. 11:L1.

* Work performed in collaboration with Prof. C. L. Cocke at Kansas State University.

A SIMPLE MODEL FOR THE ENERGY SPECTRUM OF ELECTRONS EJECTED BY HIGH-VELOCITY IONS

J. H. Miller, L. H. Toburen, W. E. Wilson and S. T. Manson*

Applying cross section data to problems of track structure and dosimetry is facilitated greatly by simple, analytic models. These models require a sound physical basis if they are to be used to predict cross sections where no data presently exist. Our work on the Bethe-Born approximation has continued during this fiscal year with the goal of developing a model of the single differential cross section (SDCS) for ionization that has predictive capability. An informal workshop on mechanisms of ionization by charged particles held at PNL this year was a significant milestone in this project. Round table discussions among PNL staff members (L. H. Toburen, J. H. Miller, R. D. DuBois, and W. E. Wilson), S. T. Manson (Georgia State University), Y. K. Kim (Argonne National Laboratory), and M. E. Rudd (University of Nebraska) helped to clarify the principles underlining the Bethe-Born theory and the binary encounter approximation (BEA).

The open circles in Figure 1 show the ratio of the SDCS for ionization of neon by 4.2 MeV protons to the BEA plotted as a function of the kinetic energy of the ejected electrons in units of Rydbergs (13.6 eV). This ratio is about 20 to 30% greater than unity for ejection of high energy electron and rises to a maximum of nearly 2.5 for electrons ejected with an energy near 10 Rydbergs. Most of the difference between the measured cross sections and the BEA can be attributed to the fact that the BEA neglects the contribution to the cross section from collisions in which the momentum transferred from the projectile to the target electrons is small. Bethe (1930) developed a theory which includes these glancing collisions by expanding the Born approximation in inverse powers of the kinetic energy of the projectile. Based on this theory, Kim (1975) and Gabler (1974) have proposed that the contribution to the SDCS from glancing collisions be approximated by

* Consultant, Georgia State University, Atlanta, Georgia.

BEST DOCUMENT AVAILABLE

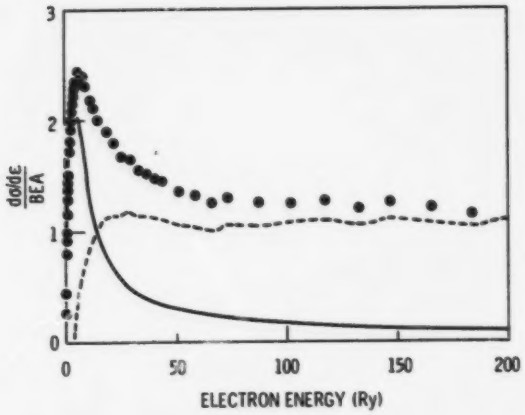

FIGURE 1. Energy Spectrum of Electrons Ejected From Neon by 4.2 MeV Protons. Closed circles show the ratio of measured singly differential cross sections to the same calculated in the binary encounter approximation. Solid and dashed curves show contributions to the spectrum from glancing and hard collisions respectively.

$$\frac{d\sigma}{d\epsilon}\Big|_G = \frac{4\pi a_o^2 Z^2}{T} \frac{R^2}{(\epsilon+B)} \frac{df}{d\epsilon} \ln\left(\frac{4T}{R}\right) \qquad (1)$$

where a_o is the Bohr radius (0.529 Å), Z is the projectile's charge and R is the Rydberg unit of energy. The kinetic energy of the ejected electron that was bound to the target with energy B is denoted by ϵ and T is the kinetic energy of an electron with same velocity as the projectile. The optical oscillator strength $df/d\epsilon$ is proportional to the cross section for photo-absorption and has been measured for many species of radiological interest. The solid curve in Figure 1 is the ratio of $d\sigma/d\epsilon_G$ to the BEA.

We define the contribution to the SDCS from hard collisions by

$$\frac{d\sigma}{d\epsilon}\Big|_H = \frac{d\sigma}{d\epsilon}\Big|_{exp} - \frac{d\sigma}{d\epsilon}\Big|_G \qquad (2)$$

where $d\sigma/d\epsilon$ exp is the measured cross section.

The ratio of $d\sigma/d\epsilon_H$ to the BEA is shown by the dashed curve in Figure 1. The glancing component proposed by Kim (1975) and Gabler (1974) is larger than the experimental cross section when the energy of the ejected electrons is less than about 5 Rydberg. In the Bethe-Born theory the hard collisions component contains a term proportional to the logarithm of the momentum transfer separating hard and soft collisions. This term allows the hard collisions component to be negative at small ejected electron energies. The ratio of the hard collision component to the BEA increases rapidly for electron energies between 10 and 20 Rydbergs and is a constant equal to unity within experimental error for electron energies greater than 30 Rydbergs.

Figure 2 compares the hard collision component of the SDCS for ejecting electrons from neon by protons of several energies. As in Figure 1 we have divided our results by the BEA. The shape of the hard collision component does not vary greatly between 1.0 and 4.2 MeV; however, the asymptotic limit of the ratio of the hard collision component to the BEA increases from a value of about 0.9 for 1 MeV protons to a value of about 1.1 for 4.2 MeV protons. A part of this dependence of the hard collision component on the proton energy can be explained by the Bethe-Born theory, but a part may be caused by experimental error. In our present model we assume that the ratio of the hard collision component to the BEA is independent of the proton energy and approaches unity as the energy of the ejected electron increases. The dashed curve in Figure 2 illustrates this approximation. When this result for the hard collisions component is combined with the glancing component given by Equation 1, we are able to predict the SDCS and the total ionization cross section as a function of proton energy. Figure 3 compares predictions of the model with data on the total ionization cross sections and Figure 4 compares the SDCS for ionization of neon by 10 MeV protons predicted by our model with calculations using the Hartree-Fock, Born approximation. These results show that our semi-empirical model gives differential and total cross section in good agreement with experimental data and ab initio calculations.

BEST DOCUMENT AVAILABLE

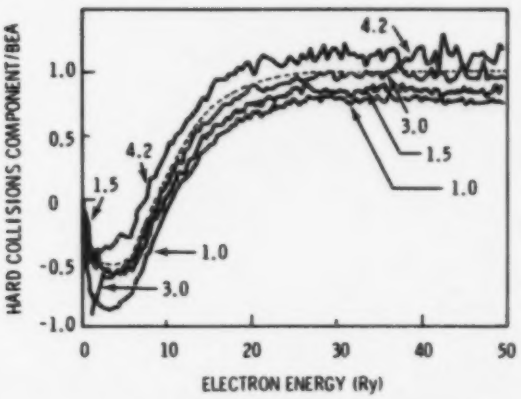

FIGURE 2. Hard Collisions Component of Energy Spectrum of Electrons Ejected From Neon by Protons of Several Energies. Dash curve shows the hard collisions component used in the model discussed in text.

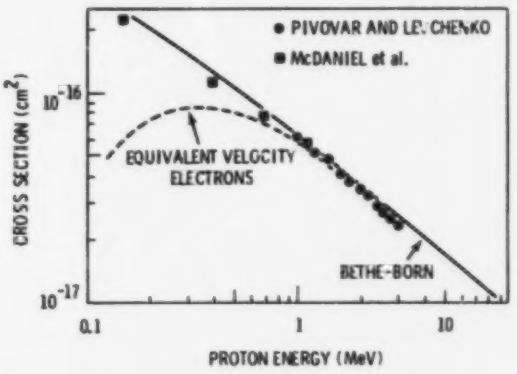

FIGURE 3. Comparison of Model Predictions for the Total Ionization Cross Section with Experimental Data of McDaniel et al. (1961) and Pivovar and Levchenko (1967)

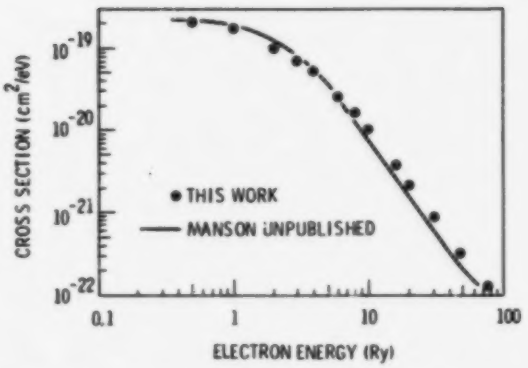

FIGURE 4. Comparison of Model Predictions for the Single Differential Cross Section for Ionization Neon by 10 MeV Protons with Calculations Based on the Hartree-Fock, Born Approximation

REFERENCES

Bethe, Von H. 1930. "Für Theorie des Durchgangs Schneller Korpuskularstrahlen durch Materie." Annelen der Physik. 5:325-400.

Gabler, Hansjorg. 1974. "Emission von Electronen Beim Stross Hochenergetischer Protonen mit Argon." Thesis, Universitat Berlin.

Kim, Yong-K. 1975. "Energy Distribution of Secondary Electrons." Radia. Res. 64:96-105.

McDaniel, E. W., J. W. Hooper, D. W. Martin and D. S. Harmer. 1961. "Ionization Cross Sections for Protons on Noble Gases in the Energy Range 0.15 to 1.10 MeV." In Proceedings of the Fifth International Conference on Ionization Phenomena in Gases, Munich. Vol. 1 pp. 60-70. North Holland Publishing Co. Amsterdam, 1962.

Pivovar, L. I. and Yu Z. Levchenko. 1967. "Cross Sections for Ionization of Gases by 1-3-MeV Protons." Sov. Phys. JETP 25:27-30.

BEST DOCUMENT AVAILABLE

BLANK PAGE

Track Structure

Experimental determination of radiation interactions in small absorber sites is limited to volumes greater than about 0.1 μm. This restriction has encouraged the development of computational methods to obtain the desired information in sites of arbitrary size. We are developing Monte Carlo codes to calculate ionization and energy imparted in submicron sites by energetic charged particles. These codes draw on extensive data for electron production in electron- and ion-molecule collisions as the source term for energy degradation calculations. The systematics of molecular cross sections are studied for information on how molecular structure affects energy deposition calculations. We are assessing the reliability of calculations that use gas-phase cross sections to determine energy transport in the condensed phase. To make this assessment, we are comparing calculated multicollision electron spectra with measurements of the corresponding electron spectra emitted from foil targets on proton impact.

SYSTEMATICS OF DIFFERENTIAL IONIZATION CROSS SECTIONS

L. H. Toburen and W. E. Wilson

A review of the systematics of differential cross sections for charged particle impact was presented in an invited paper at the International Seminar on High Energy Ion-Atom Collision Processes held in Debrecen, Hungary in March 1981. This paper concentrated on applying differential cross sections to understanding the collisional energy transfer process. Illustrations of the effect of target and projectile structure were presented. In reviewing the work on doubly differential ionization cross sections a table was presented which provides a listing of the experimental parameters associated with available data on differential cross sections for ionization by charged particles and which should be useful to the field of Radiological Physics. This paper will appear in the conference proceedings and is presently available by request from the authors at PNL.

IONIZATION DISTRIBUTIONS IN CONDENSED PHASE

W. E. Wilson, L. H. Toburen and H. G. Paretzke*

Real radiological problems in dosimetry most often involve radiation interactions in condensed phase. Because our track structure Monte Carlo code MOCA13 is modeled after gaseous phase data, the validity of our calculations must be carefully and continuously verified for utility in condensed phase. One means of testing is to compare calculated distributions of electrons exiting a foil after the passage of a charged particle to experimentally determined values. During the past year, we completed a study of Auger line shapes observed in H^+ - carbon foil interactions. Auger electrons generated throughout a 3 $\mu g/cm^2$ foil degrade and contribute a low energy component to an otherwise nearly Gaussian line shape. The Auger line shapes calculated by MOCA13 are in excellent agreement with the basic features of the observed spectra. This study also illustrated via the Monte Carlo calculation, a sizeable contribution of degraded Auger and secondary electrons at very low electron energies. These could not be observed directly in the experiment due to the overwhelming contribution of low energy electrons from direct ionization. Information from this study provided confirmation of the applicability of MOCA13 to condensed phase collision processes, at least for amorphous carbon foils, and provided new insight on this background process in beam foil spectroscopy. A paper describing this work is presently accepted and in press for publication in the Physical Review A.

ANALYTIC MODEL FOR PRIMARY IONIZATION BY POSITIVE IONS

W. E. Wilson and J. H. Miller

A variety of applications in computational dosimetry requires an expedient way of getting quantitative secondary electron emission cross sections (delta-ray ejection probability density, differential in angle and energy). This task is an effort to obtain a theoretically sound analytical model for the delta-ray probabilities so interpolation and extrapolation among experimental data sets will not be necessary.

---

* Consultant, Institut für Strahlenschutz, Neuherburg, Fed. Rep. Germany.

BEST DOCUMENT AVAILABLE

Preliminary results were reported under the same title last year (Wilson and Paretzke 1981).

Review of the extensive experimental and theoretical literature (see e.g., Wilson and Toburen 1981, and Kim 1972) indicates that the doubly differential cross section (DDCS) for secondary electrons ejected from atomic and molecular targets by energetic charged particles may be reasonably represented as the sum of three terms, one for each of the commonly observed interactions

$$\sigma = \sigma_{hc} + \sigma_{gc} + \sigma_{cct} \qquad (1)$$

where σ_{hc} represents hard collisons, σ_{gc} glancing, and σ_{cct} continuum-charge-transfer interactions. Each is differential in solid angle of emission and the inelastic energy loss by the incident ion and, also, each is a function of E_I the incident ion energy. The three terms on the right hand side of Equation 1 are discussed individually.

- Hard Collisions

So-called hard collisions are characterized by small impact parameters and large momentum transfer. The single differential cross sections (SDCS) for hard collisions are reasonably described in the binary-encounter-approximation (Rudd and Macek 1972).

Therefore, we let,

$$\sigma_{hc}(\theta,w,E_I) = S_{BEA}(w,E_I) \cdot R(\theta,w) \qquad (2)$$

where S_{BEA} is SDCS for electron ejection of energy w by an ion on energy E_I. S_{BEA} is not a function of θ. The angular dependence is incorporated into the empirical term $R(\theta,w)$, which is taken to be Gaussian in shape,

$$R(\theta,w) = \frac{1}{2\pi^{3/2}\Gamma} \exp\left|\frac{\cos\theta - \overline{\cos\theta}}{\Gamma}\right|^2 \qquad (3)$$

centered about $\cos\theta$ and of width Γ. The normalization is chosen so that $\int R\, d\Omega = 1$, and hence $\int \sigma_{hc} d\Omega = S_{BEA}$.

The value of $\overline{\cos\theta}$ is determined by the kinematics of the collision. If the target electrons were free, then their angular distribution resulting from purely elastic collisions would be a δ-function centered at angle θ_M given by

$$\cos^2\theta_M = \frac{E}{E_M} \qquad (4)$$

where E is the energy transferred to the electron and E_M is the maximum such energy transfer, $E_M = 4T = 4\left(1/2\, m_e V_I^2\right)$. Now, from the actual data, $\cos\theta$ is not exactly equal to $\cos\theta_M$, presumably because the electrons are not free (Drepper and Briggs 1976).

The quantity

$$\delta = \frac{\overline{\cos\theta}}{\sqrt{E/E_M}} - 1 \qquad (5)$$

which by Equation 4 should be zero, is found to be small in magnitude and to vary systematically with w and E_I. The data required to evaluate (5) were obtained by fitting Equation 3 in the least-squares sense to experimental data for H^+ on H_2O. These results were described earlier (Wilson 1977). A phenomenological parameterization of $\delta(\theta, E_I)$ provides a correction for the deviation of $\overline{\cos\theta}$ from $\cos\theta_M$. This parameterization is based on the very limited ion energy range 0.3 to 1.5 MeV and hence has a large uncertainty for extrapolation to higher energy.

The width parameter of the Gaussian in Equation 3 arises out of a combination of binding effects and the velocity distribution of the molecule's orbital (valance) electrons. There is no useful, concise theoretical treatment of the convolution of these two effects. Until such is developed, we are using the following phenomenological representation

$$\Gamma = \frac{\sqrt{W \cdot E_2}}{W + E_2} \qquad (6)$$

which works fairly well over the limited ion energy range of 0.5 to 1.5 MeV. E_2 is probably somehow related to the mean kinetic energy of orbital electrons in the molecule.

- Glancing Collisions

For the distant glancing collisions, Bethe-Born theory gives us

BEST DOCUMENT AVAILABLE

$$\sigma_{gc}(\theta,w,T) = \frac{4\pi a_o^2}{T/R}\left[A(\theta,w)\ln\frac{4T}{R} + B(\theta,w) + O\left(\frac{1}{T}\right)\right] \quad (7)$$

where $a_o = 0.529$ Å, $T = 1/2\, m_e v_I^2$, $R = 13.6$ eV, and within the dipole-approximation,

$$A(\theta,w) = \frac{1}{4\pi}\sum_{nl}\frac{R}{w+I_{nl}}\frac{df_{nl}}{d(w+I_{nl})} \times \left[1 - \frac{\beta_{nl}}{2}P_2(\cos\theta)\right] \quad (8)$$

(see Inokuti 1971, Kim 1972, and Manson et al. 1975). The parameters of Equation 8 are given as follows: I_{nl} is the binding energy of an electron in shell nl, $df_{nl}/d(w+I_{nl})$ is the optical oscillator strength distribution in energy transfer $E = w+I_{nl}$ for shell nl, P_2 is the Legendre polynomial in the second order [1/2 $(3\cos^2\theta-1)$]. β_{nl} is the photoelectron asymmetry parameter for shell nl and in general depends on energy transfer $w+I_{nl}$. According to Born theory, $\beta_{ns} = 2$ but β_{nl} $(l \neq 0)$ is not well known nor are they simple functions of w.

We are currently exploring the applicability of dipole oscillator strengths for water vapor (Zeiss et al. 1977), using the branching ratios of Tan et al. (1978) for fitting the low energy electron emission data. Unfortunately, no data exist for the asymmetry parameters, β_{nl}, for the H_2O molecule. Some data are available, however, on the asymmetry parameters for CH_4 and neon, which are isoelectronic with H_2O (Marr and Holmes 1980). These data indicate that the shapes of angular distribution for photoionization as a function of the energy of the ejected photoelectron are moderately similar for CH_4 and neon. It remains to be seen whether this similarity will be useful for fitting H_2O angular distributions, because CH_4, like neon, is very symmetric in its ground state, whereas H_2O is less so.

- Continuum-Charge-Transfer Collisions

No suitable quantitative theory exists for continuum-charge-transfer process (see Rudd and Macek 1972; and references therein) at MeV energies and angles for which cosine <0.99. Dettmann et al. (1974) have proposed a quantitative theory for the near zero-degree emission of continuum electrons; however, our needs are for larger angles. A priori extension of the Dettmann theory to large angles leads to larger theoretical cross sections than those necessary to account for the difference between experiment (for H^+ on He) and Born approximation calculations using Hartree-Slater wave functions (Manson, et al. 1975). We have temporarily adopted a semi-theoretical phenomenological approach; i.e.,

$$\sigma_{cct}(\theta,W,E_I) = \frac{\sigma_o f(\theta,v_e)}{T^5\,|\,\vec{v}_e - \vec{v}_I\,|} \quad (9)$$

where σ_o is a constant. We expect $f(\theta,v_e)$ to be a relatively simple function of w and θ.

REFERENCES

Dettmann, K., K. G. Harrison and M. W. Lucas. 1974. "Charge Exchange to the Continuum for Light Ions in Solids." J. Phys. B:Atom. Mole. Phys. 7:269-287.

Drepper, F., and J. S. Briggs. 1976. "Doubly Differential Electron-Loss Cross Sections." J. Phys. B:Atom. Mole. Phys. 9:2063-2071.

Inokuti, M. 1971. "Inelastic Collisions of Fast Charged Particles with Atoms and Molecules - The Bethe Theory Revisited." Rev. Mod. Phys. 43:297-347.

Kim, Yong-K. 1972. "Angular Distributions of Secondary Electrons in the Dipole Approximation." Phys. Rev. A 6:666-670.

Manson, S. T., L. H. Toburen, D. H. Madison and N. Stolterfoht. 1975. "Energy and Angular Distribution of Electrons Ejected from Helium by Fast Protons and Electrons." Phys. Rev. A 12:60-79.

Marr, G. V. and R. M. Holmes. 1980. "The Angular Distribution of Photoelectrons from CH_4 as a Function of Photon Energy from Near Threshold to 30 eV." J. Phys. B:Atom. Molec. Phys. 13:939-943.

Rudd, M. E. and J. H. Macek. 1972. "Mechanisms of Electron Production in Ion-Atom Collisions." Case Studies in Atomic Physics 3:47-136.

BEST DOCUMENT AVAILABLE

Tan, K. H., C. E. Brion, Ph.E. Van Der Leeuw and J. J. Van Der Weil. 1978. "Absolute Oscillator Strengths (10-60 eV) for the Photoabsorption, Photoionization and Fragmentation of H_2O." Chemical Physics 29:299-309.

Wilson, W. E. 1977. "Analytical Expression for Cross Section Data." Physical Sciences. Part 4 of Pacific Northwest Laboratory Annual Report for 1976 to the DOE Assistant Secretary for Environment. PNL-2100 PT4, pg. 40, Pacific Northwest Laboratory, Richland, Washington.

Wilson, W. E. and H. G. Paretzke. 1981. Analytic Model for Primary Ionization by Positive Ions." Physical Sciences. Part 4 of Pacific Northwest Laboratory Annual Report for 1980 to the DOE Assistant Secretary for Environment, PNL-3700 PT4, pg. 44-45, Pacific Northwest Laboratory, Richland, Washington.

Wilson, W. E. and L. H. Toburen. 1981. "Delta-Ray Production in Ion-Atom Collisions." Seventh Symposium on Microdosimetry, September 1980, Oxford/UK, (Booz, Ebert and Hartfiel editors) Harwood Academic Publishers, Ltd, New York Commission of the European Communities, ERU-7147 p. 435.

Zeiss, G. D., W. J. Meath, J. C. F. McDonald and D. J. Dawson. 1977. "Dipole Oscillator Strength Distributions, Sums, and Some Related Properties for Li, N, O, H_2, N_2, O_2 NH_3, H_2O, NO and N_2O." Can. J. Phys. 55:2080-2100.

BEST DOCUMENT AVAILABLE

Energy Transport

The measurement of primary interaction cross sections and the incorporation of these data into Monte Carlo calculations provide detailed information about the initial spatial distribution of absorbed dose. Our theoretical energy transport studies have focused on the use of this information to predict the evolution of chemical species formed as a result of the energy deposition. This effort has led to a stochastic approach to diffusion kinetics that can account for the influence of track structure on the yield of free radicals in the radiolysis of water. Fluorescence studies with pulsed alpha particle and proton beams provided the first experimental test of our stochastic model of tract structure effects. Our experimental studies use time-resolved emission spectroscopy to investigate the mechanism of energy transport in nonpolar liquids. These initial experiments showed the need for a new target cell design to avoid the build up of stable radiolyses products that modify the fluorescence decay. Studies of the concentration dependence of time-resolved emission from solutions of benzene in cyclohexane also show the importance of using low benzene concentrations to minimize the influence of benzene dimers on the emission kinetics.

STOCHASTIC APPROACH TO TRACK STRUCTURE EFFECTS IN RADIATION CHEMISTRY

J. H. Miller and M. L. West

Energy deposited by ionizing radiation produces microscopic regions containing a high concentration of reactive species. These "spurs" play a fundamental role in the mechanisms of radiation action in living organisms (Ward 1981). The spatial distribution of spurs produced in a medium by the passage of a fast charged particle is sometimes referred to as the "track structure" of the radiation. This track structure influences the nature and rate of chemical reactions induced in the absorbing medium by ionizing radiation.

We have developed a stochastic model of track structure effects in radiation chemistry that allows us to use detailed information on the pattern of energy deposition events made available by Monte Carlo calculations. Application of this model to track structure effects in the quenching of radioluminescence is described in a manuscript to be published in Radiation Research (J. H. Miller 1982). In this section we will describe how the model can be used to predict the effect of track structure on the yield of radicals in aqueous solutions.

The major difficulty in predicting the effect of track structure on chemical yields is to allow for the effect of overlapping spurs. Since most secondary electrons ejected into a medium by ionizing collisions have low energy, overlapping spurs occur in the track structure of all types of ionizing radiation, even radiation with low linear energy transfer (LET). The most common approach for treating overlapping spurs is to introduce other track entities such as "blobs" and "short track" to approximate the average effect of commonly occurring groups of spurs. The mathematical basis for this type of approximation was demonstrated by Ganguly and Magee (1956) who showed that diffusion kinetic equations normally associated with cylindrical tracks could be derived from overlapping spurs randomly dispersed on a line. We generalized the Ganguly and Magee model to three dimensions and used Monte Carlo methods to calculate the position of spurs in the irradiated medium. This allowed us to calculate the effect of overlapping spurs on chemical yields without making simplifying assumptions about the initial spatial distribution of the reacting species.

From the Monte Carlo simulation of the slowing down of the primary ion and secondary electrons, we calculated the average density of energy deposited near a reactive molecule, A. When this energy density was multiplied by the yield of another reactive species, B, we obtained the mean concentration of molecules B in the neighborhood of molecule A. When this concentration was multiplied by the biomolecular rate constant, we obtained the rate at which species B contributes to the decay of species A. Finally, by solving a system of coupled rate equations, we obtained the time dependent yields of all chemical species produced by the radiation.

Figure 1 compares the mean energy density near a radical produced in water by the energy transferred from ions with equal stopping power but different velocity and charge. The ordinate is the mean energy density

BEST DOCUMENT AVAILABLE

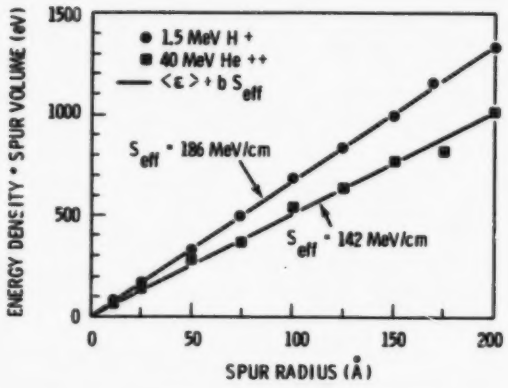

FIGURE 1. Comparison of the Mean Density of Energy Near a Reactive Molecule in the Track Structure of Two Ions with Equal Stopping Power in Water

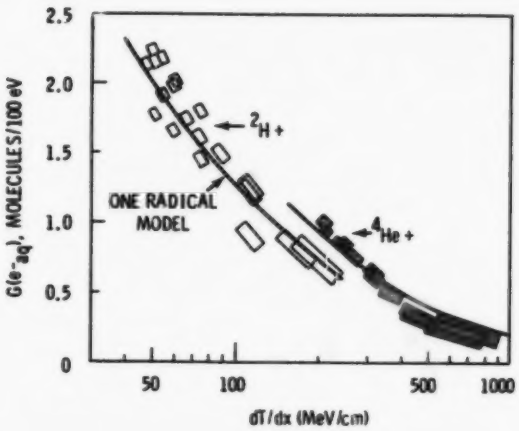

FIGURE 2. Yield of Hydrated Electrons in Segments of Deuteron and Alpha Particle Tracks as a Function of the Ions Stopping Power. Data from Sauer et al. (1977).

multiplied by the volume of the spur containing the radical; the abscissa is the radius of the spur. The spur radius can be related to the time after irradiation because spurs expand continuously as a result of diffusion. At a given time after irradiation, the mean energy density near a radical in the alpha track is less than the mean density of energy near a radical in the proton track. It is less because the initial spatial distribution of energy transferred from the alpha particle to water has a more diffuse radial distribution.

The solid lines in Figure 1 are least squares fits to the Monte Carlo results shown by the open symbols. If the radial displacement of spurs were neglected, the slope of these lines would be equal to the stopping power of the ions. Hence, we refer to the slope of the fit to the Monte Carlo results as the "effective" stopping power. This effective stopping power is nearly equal to true stopping power for the proton track, but is only about 75% of the true stopping power of the alpha particle because of the diffuse radial distribution of energy deposited by the latter ions.

Figure 2 compares the yield of hydrated electrons in water at 10 μsec after irradiation by pulsed alpha particle and deuteron beams (Sauer et al. 1977). The yield is plotted as a function of the stopping power of the ions. The track structure of the deuteron radiation has a compact radial distribution so that the effective stopping power of these ions nearly equals their true stopping power. The solid curve through the deuteron data is a fit obtained by varying the recombination rate constant in a one-radical approximation. The solid curve through the alpha particle data is the result predicted by the one-radical approximation with the same recombination rate constant that gave the best fit to the deuteron data. The model predicts a greater yield of hydrated electrons for alpha particles than for deuterons of the same stopping power because the effective stopping power of the alpha particles is only 75% of their true stopping power. The effect of track structure on the yield of hydrated electrons observed in this experiment is in good agreement with the predictions of our stochastic model.

REFERENCES

Ganguly, A. K. and J. L. Magee. 1956. "Theory of Radiation Chemistry III. Radical Reaction Mechanism in the Tracks of Ionizing Radiation." J. Chem. Phys. 25:129-134.

Miller, J. H. 1982. "Stochastic Model of Radiation Quality Effects in the Quenching of Prompt Radioluminescence." Radiat. Res. 88:280-290 (in press).

Ward, J. F. 1981. "Some Biological Consequences of the Spatial Distribution of Ionizing Radiation-Produced Free Radicals." Radiat. Res. 86:185-195.

Sauer, M. C., Jr., K. H. Schmidt, E. J. Hart, C. A. Naleway, and C. D. Jonah. 1977. "LET Dependence of Transient Yields in the Pulse Radiolysis of Aqueous Systems with Deuteron and α Particles." Radiat. Res. 70:91-106.

BEST DOCUMENT AVAILABLE

FLUORESCENCE IN BINARY LIQUID SYSTEMS: CONCENTRATION DEPENDENCE

M. L. West and J. H. Miller

When dilute solutions of benzene in cyclohexane are irradiated with subnanosecond bursts of protons and with UV radiation there is an observed difference in the fluorescence decay (West 1977). For proton irradiation, nonexponential decay is observed with a rate that is initially much greater than that observed for UV excitation. As time increases, the rate of proton-induced fluorescence decay approaches the UV decay rate. This mode of decay suggests the presence of a radiation-induced quenching species formed in high concentration along the individual proton tracks. The qualitative time dependence of this quenching can be interpreted as a decrease in the quencher concentration as the reacting species diffuse and recombine in the medium. A quenching model based on diffusion kinetics was developed to explain these effects and to explain the dependence of the fluorescence decay on proton beam energy (Miller and West 1979). We do not know the exact nature of these radiation-induced quenching species that are created along the individual proton track. We tentatively assumed that they were products of cyclohexane radiolysis. In particular, the bicyclohexyl radical appeared to be a likely candidate as it is a major product of cyclohexane radiolysis. However, subsequent concentration dependent studies (West and Miller 1980) over the concentration range of 0.01 to 0.4 molar suggested that products of benzene radiolysis were at least partially responsible for the observed quenching. The results of these initial measurements are shown in Figure 1. Our first attempt at explaining these quenching data was to look for products of benzene radiolysis that would give this observed concentration dependence. On the graph of product yield versus benzene concentration in Figure 1, the average triplet yield for a number of aromatic solutes in cyclohexane is also plotted. This type of concentration dependence is typical of ion scavenging reactions where there is an initial square root dependence at low concentrations followed by a limiting value at higher concentrations. These first data suggested that the radiation-induced quenching molecules were totally formed from benzene radiolysis via charge-scavenging ion recombination reactions.

To further test this hypothesis, additional measurements were made at extremely low benzene concentrations (0.0001M) where the

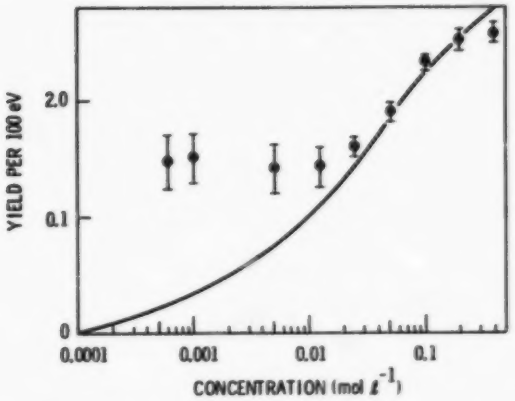

FIGURE 1. Radiation-Induced Quencher Yield as a Function of Benzene Concentration in Cyclohexane

square root dependence is expected to predominate. At these low concentrations, background corrections become a serious problem because of long data accumulation times. A new phototube (Varian Model 162) of extremely low background was incorporated into our detection system. Also, the temperature control and liquid transfer system had to be redesigned to handle requirements for several hours of precise control of uninterrupted data accumulation. In addition, new graphics and data fitting programs were incorporated so that on-line analysis could be made to determine quenching parameters, decay times, and decay shapes.

The results of these new measurements are also shown in Figure 1. The new data do not follow the square root dependence at low concentrations but instead reach a limiting value. At concentrations below about 0.01 molar, the proton-induced quenchers are products of cyclohexane radiolysis. The concentration dependent quenching above 0.01 molar is associated with product yields from benzene. Thus, the fluorescence decay is affected by quenching contributions from both cyclohexane and benzene radiolysis.

The formation of benzene excimers at higher benzene concentrations is presently being investigated as a possible cause of the observed concentration dependence of fluorescence quenching. Previous measurements of UV-induced fluorescence at this laboratory (West and Miller 1980) and as reported in the literature (Gregory and Hellman 1972) have shown that excimer contributions are expected to be negligible at benzene concentrations below 0.1 molar. However, small

BEST DOCUMENT AVAILABLE

contributions at these concentrations may drastically affect the quenching parameters extracted from data analysis. Also, it is possible that excimers may have a different sensitivity to radiation than do the monomers of benzene. If this is true, then excimer contribution may be enhanced under proton irradiation. Excimer kinetics have been studied for the benzene-cyclohexane system for estimated values of the excimer formation and dissociation parameters.

Excimers present a plausible explanation of proton-induced quenching at the higher concentrations.

To test this hypothesis, a least squares fitting program has been developed that will allow us to search for systematic changes in the UV lifetime that are expected under excimer influence. Previously, when extracting quenching parameters, such variations in the UV lifetime were neglected. These analyses should provide definite tests of the role of excimers in the quenching of proton-induced fluorescence.

REFERENCES

Gregory, T. A. and W. P. Helman. 1972. "Temperature Dependence of Specific Rates of Benzene Monomer and Excimer Fluorescence." J. Chem. Phys. 56:377-385.

Miller, J. H. and M. L. West. 1978. "Quenching of Benzene Fluorescence in Pulsed Proton Irradiation: Dependence in Proton Energy." J. Phy. Chem. 81:377-380.

West, M. L. and J. H. Miller. 1980. "Quenching of Benzene Fluorescence in Pulsed Proton Irradiation: Concentration Dependence." Radiat. Res. 82:391.

DEVELOPMENT OF A TEMPERATURE CONTROLLED LIQUID TRANSFER SYSTEM FOR PULSED RADIOLUMINESCENCE STUDIES

M. L. West

The study of radiation-induced fluorescence in binary liquid systems requires a precise control of sample temperature and an adequate adjustment of sample flow-rate to prevent the build up of radiolysis products. Furthermore, samples are sensitive to the oxygen quenching of fluorescence and so must be adequately purged and kept in an inert atmosphere. For our previous experiments, a small reservoir of about 50 cc was precooled to the correct temperature and sample transfer was controlled via gravity flow. This was not a closed system and continuous purging was employed to insure the removal of oxygen.

Such a system was adequate for the small radiation doses and data accumulation times associated with proton irradiation of relatively high concentrations (0.01 m) of benzene in cyclohexane using our 2 MeV Van de Graaff. However, for experiments requiring low concentration of solute with data accumulation taking several hours, and at the University of Washington tandem accelerator where high dose-rate experiments use high-energy proton and alpha particles, a more sophisticated system is required for handling samples.

We have designed and completed a closed sample handling system that will store, cool, purge, and transfer large volumes of liquid sample. With this system, sample flow-rates can be precisely controlled and adequate flow can be obtained for the high dose-rate experiments. The procedure is as follows: the sample is introduced into a 2 liter glass reservoir where it is purged of oxygen by bubbling with nitrogen or helium. The freeze-thaw technique of deaeration can also be used with the vacuum-tight system. The deaerated sample is then transferred from this reservoir through a cooling coil immersed in a precisely controlled temperature bath into the irradiation cell and then into a waste reservoir. Liquid transfer takes place in this closed system under a nitrogen atmosphere. A flow gauge in the transfer line regulates the sample flow-rate. Under normal flow conditions, the reservoir contains enough of the sample for several days of data accumulation. Hence, the experimental condition of sample purity, oxygen content, temperature, solute concentrations, and flow-rate are the same for all experimental runs. Anomalies in some of the previous data, especially at high dose rates, have been attributed to a lack of precise control of these experimental parameters.

BEST DOCUMENT AVAILABLE

• DOSIMETRY AND BIOPHYSICS

The effects of ionizing radiation on living systems begin with basic physical processes and develop through many stages of chemical reactions and biological responses. The goal of the dosimetry and biophysics program is to utilize the best physical data and mathematical techniques available to characterize radiations, in terms of their interactions with biological material, in a way which will help to predict the final biological response. The stochastic nature of energy deposition along particle tracks and in microscopic sites (microdosimetry) is studied by both experimental techniques and computer simulations. These findings are applied to developing an understanding of the linear energy transfer (LET) and time dependence of cellular response. Furthermore, mathematical models of tissues and organs are combined with microdosimetry to provide more relevant data on the dose to cells at risk in cases of ingested radioactivity.

The radiation dosimetry and biophysics program is an interdisciplinary effort requiring input from many specialties within physics and biology. This is achieved through diverse staff at PNL and by various cooperative and consulting agreements with workers at other laboratories and universities.

BLANK PAGE

Modeling and Cellular Studies

Testing the applicability of mathematical models with carefully designed experiments is a powerful tool in the investigation of the effects of ionizing radiation on cells. Such methodology provides both a means of testing fundamental assumptions regarding the mechanisms of damage and repair and extrapolating to low doses and dose rates to predict effects which cannot be measured directly. The modeling and cellular studies complement each other, for modeling provides guidance for designing critical experiments which must provide definitive results, while the experiments themselves provide new input to the model. Based on previous experimental results the model for the accumulation of damage in *Chlamydomonas reinhardi* has been extended to include various multiple two-event combinations. Split dose survival experiments have shown that models tested to date predict most but not all of the observed behavior. Stationary-phase mammalian cells, required for tests of other aspects of the model, have been shown to be at different points in the cell cycle depending on how they were forced to stop proliferating. These cultures also demonstrate different capacities for repair of sublethal radiation damage.

DOUBLE TWO-EVENT MODELS

W. C. Roesch, L. A. Braby and J. M. Nelson

For several years we have been experimenting with the green alga, Chlamydomonas reinhardi, to test models for the effects of protraction and fractionation in the delivery of radiation doses. Initially we found good agreement between experimental data and a simple model; but, as we pushed to higher dose rates, new phenomena appeared that required more complex models. An analysis of last year's data (Roesch, Braby, and Nelson 1981) and data in the literature on LET's effect in C. reinhardi indicated that the main characteristic of a new model had to be inclusion of more than two radiation-induced steps. We reported on one such model, which represented the correct LET behavior. We have now added a number of models to the list we have been studying, and we have explored protraction-fractionation effects in addition to LET effects.

Last year we showed that the data for C. reinhardi required a model that had more than the two charged-particle events which seemed sufficient to explain mammalian cell data. Although we could not be certain just how many more charged-particle events were required, we believe it is likely one or two. We chose first to study models based on two-event processes such as might be involved in mammalian cells, and we called two of them "double two-event" models. We could have called them "four-event" models but chose not to in order to distinguish between double two-event models and models with four (or three) dissimilar processes. (We are studying the latter but do not have enough information to report on them at this time.)

Figure 1 lists the two-event models and the corresponding double two-event models we have studied. A chemical notation was used to describe the models. For example, in the first one, two of product B are produced by the radiation; these products can be repaired (revert to normal) or they can combine to form product C, which is lethal to the cell.

Figure 2 shows typical split-dose curves for a two-event (BC) process and its associated double two-event (BCJ) model. They are plotted in a way we introduced several years ago (Braby 1980) which permits their analysis into components the same way decay curves for mixtures of radioisotopes are analyzed.

The BC model is the one whose kinetics fit our original data. We recognized that to include the LET effect for C. reinhardi required that we assume the B's were the results of another two-event process, but we first neglected its kinetics on the assumption they would be too fast to observe. However, we found this was not true; the present study is aimed at exploring different possibilities for the initial kinetics.

What we are looking for are effects that can form the basis for experiments which can lead us to eliminate inapplicable models. Most recently we have been looking at the split-dose experiment as such a "critical" experiment; and we find it is, at the least, very useful. At present, several of the models give the same general phenomena that

BEST DOCUMENT AVAILABLE

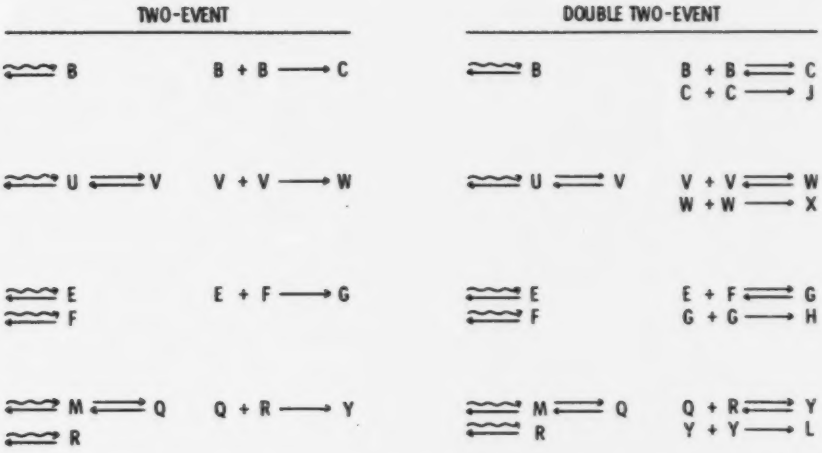

FIGURE 1. The Double Two-Event Models Studied and the Corresponding Two-Event Models

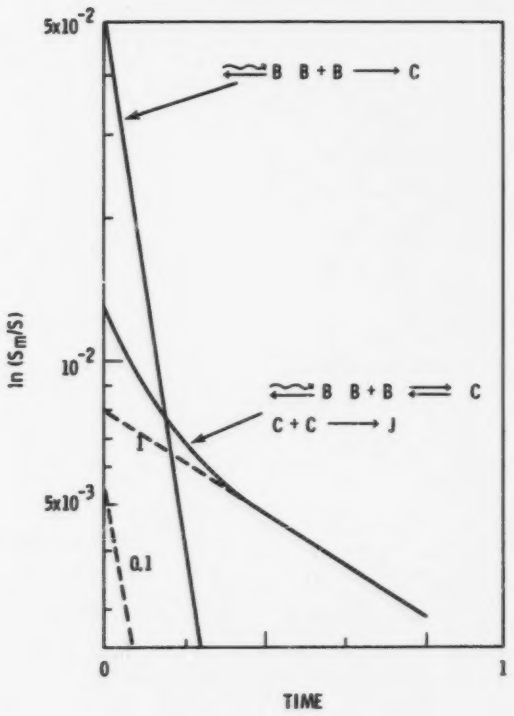

FIGURE 2. Typical Split-Dose Curves for a Two-Event and the Corresponding Double Two-Event Model

we observe for C. reinhardi; but do not seem to give correct details. Thus we think that although we have not found the right kinetic scheme at this time, we are on the right track.

REFERENCES

Roesch, W. C., L. A. Braby and J. M. Nelson. 1981. "Modeling the Radiation Response of Chlamydomonas reinhardi." In Physical Sciences. Part 4 of Pacific Northwest Laboratory Annual Report for 1980 to the DOE Assistant Secretary for Environment, pp. 59-62. PNL-3300 PT4, Pacific Northwest Laboratory, Richland, Washington.

Braby, L. A., J. M. Nelson and W. C. Roesch. 1980. "Comparison of Repair Rates Determined by Split-Dose and Dose-Rate Methods." Radiation Research 82:211-214.

EXPERIMENTAL EVIDENCE AND SUPPORT OF MULTIPLE TWO-EVENT MODELS

J. M. Nelson, W. C. Roesch and L. A. Braby

A primary function of the radiation biophysics program is to test the conclusions of the various models evolving out of the radiation dosimetry program. As mentioned previously in this section (Roesch, Braby and Nelson, this report) the accumulation-of-damage model has recently been modified and extended to include the possibility of multiple events leading to sublethal damage. As a group these modifications are referred to as the multiple two-event models.

Five different double two-event models have been proposed which may apply to the radiation biology of Chlamydomonas reinhardi. Double two-event models as a group can be distinguished from simple two-event models on the basis of the relative influence of fast repair on survival as a function of

BEST DOCUMENT AVAILABLE

dose. This is best illustrated in a plot of ln (S_m/S) versus the interfraction interval in split dose experiments shown in Figure 1. The short interval portion of the curve reflects the contribution of the faster repair processes; in double two-event models its intercept tends to change more with decreasing survival (i.e., with increasing dose) than the intercept extrapolated from the longer intervals which are influenced more by the slower repair processes. This is a characteristic common to all of the multiple two-event models and is illustrated in Figure 1, where several theoretical curves have been normalized with respect to their response in the slow repair region. In addition, the change in ln (S_m/S) as a function of dose within that region where it is not seriously affected by the faster repair processes is different for the various multiple two-event models.

We felt the best way to test the characteristics of the models was to generate complete split-dose survival curves following two greatly differing doses. These curves were then to be compared with expected curves generated from multiple two-event models. No difficulty was experienced with generating the higher dose curves. However, we encountered some technical difficulties associated with generating a survival curve at very high survival levels. The variable S_m represents the hypothetical maximum survival which would occur if two doses were separated by an infinite time interval and complete repair had taken place. According to theory, this value should equal the product of the survival after the first dose times that after the second (S_1S_2), or in the case of two equal doses, should equal the square of the survival after a single fraction. In the past, we have generally determined this value by the latter method, and at lower survival levels (higher doses), this method is still applicable. However, when survival is 90% or above, the product of the individual survivals is a value much lower than expected; it is often lower than that found after two doses separated by 20 minutes or longer. In other words, at low doses we are either observing a decrease in the efficiency of the second fraction when it follows the first by 20 minutes or longer, or we are underestimating survival after very low doses.

This unresolved problem will continue to be investigated. It is particularly puzzling since it has only been observed at survival levels of 50% or more.

To circumvent this problem in determining S_m, we have used an alternate method for the lower doses. If simple survival is plotted as a function of time between doses on a semi-log plot, as seen in Figure 2, the data become asymptotic to S_m. The magnitude of the value for S_m determined in this way is considerably greater than that determined from a single exposure. This value can then be used to compute ln (S_m/S), which is then plotted against time in the normal fashion.

When survival data after each of the different total doses are plotted as illustrated in Figure 3, we find a significant difference between the two curves. In this figure, the line fitted to the slower repair processes has been enclosed by a shaded area representing ±1 standard error of estimation, a value analogous to the point standard deviation. The increasing difference seen here between the short interval data and the intercept of the line with increasing dose supports the multiple two-event damage hypothesis.

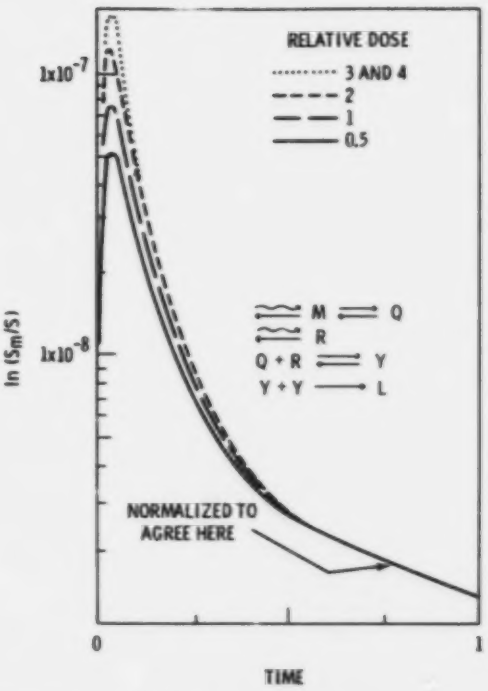

FIGURE 1. A Family of Theoretical Split-Dose Response Curves for *Chlamydomonas reinhardi*, Where *ln* (S_m/S) Has Been Plotted as a Function of Time Between Doses for Several Different Survival Levels. These curves have been normalized throughout the region reflecting slower processes in order to illustrate the relative effects within the region influenced primarily by the faster processes.

BEST DOCUMENT AVAILABLE

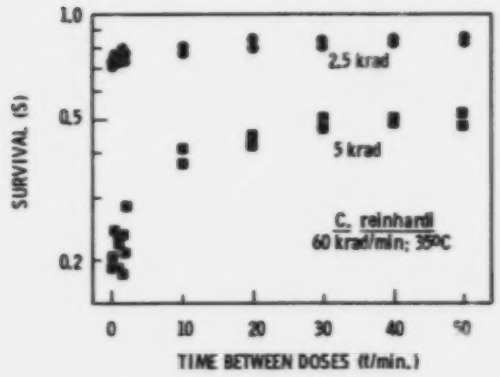

FIGURE 2. Split-Dose Survival Data as a Function of Time Between Doses. When plotted as *ln* S against the interfraction interval, as seen here, these data become asymptotic to the theoretical maximum survival (S_m).

In addition to looking for this change in rapid repair efficiency, the change in survival as a function of dose can also be quantitated by these same experiments. We chose the MQRYL double two-event model to describe the C. reinhardi data, but the model results did not correspond with those calculated from survival data from eight independent experiments (eight pairs of survival curves). For instance, according to this model, the value of ln (S_m/S) should increase with the cube of the dose; instead it was found to change according to the square of the dose. This was determined by experiments designed around a dose ratio of either 2.0 or 2.5, with totals ranging from 4 to 14 krad. When the dose had been doubled, ln (S_m/S) changed by a factor of 4.1 ± 1.5; when it increased by a factor of 2.5, ln (S_m/S) changed by a factor of 7.7 ± 1.5.

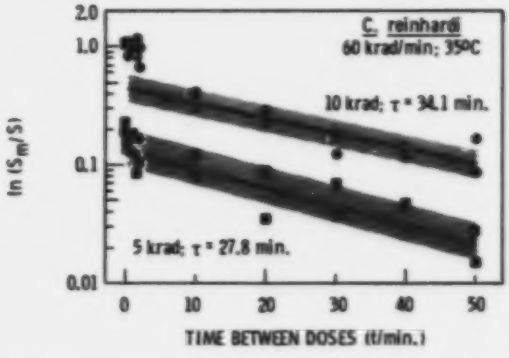

FIGURE 3. Relative Survival of *Chlamydomonas reinhardi* After 5 krad (Lower Curve) and 10 krad (Upper Curve), Given as 2 Equal Fractions. In each case, the longer interval data have been fitted to a straight line, surrounded by ±1 standard error of estimation in order to assess the relative influence of faster repair processes as a function of dose.

We have generally assumed the slower repair found in C. reinhardi to be similar to that identified in the same organism by Jacobson (1957) and in mammalian cells by Elkind and Sutton (1959). Early experiments concerned with the fast repair process and subsequent modeling activity revealed several inconsistencies. We are now aware that although the effect of the slower repair process on survival may change with dose, the effects of the faster repair process will change even more. Even though we believe the action of radiation to be more complex than assumed by the earlier models, we cannot confirm any of the alternate double two-event models developed so far. Since survival does not appear to change according to the cube of the dose, we can rule out the MQRYL model and possibly one other which predicts that survival should increase at a rate somewhere between second and third power of the dose. We will continue our evaluation of the other models.

REFERENCES

Elkind, M. M. and H. Sutton. 1959. "X-Ray Damage and Recovery in Mammalian Cells in Culture." Nature 184:1293–1295.

Jacobson, B. S. 1957. "Evidence for Recovery from X-Ray Damage in Chlamydomonas." Radiat. Res. 7:394–406.

TECHNIQUES FOR INVESTIGATING FAST REPAIR PROCESSES IN CHLAMYDOMONAS REINHARDI

L. A. Braby, J. M. Nelson and W. C. Roesch

As we have reported previously (Braby, Nelson and Roesch 1980; 1981), the reproductive survival of Chlamydomonas reinhardi exhibits reversal of the dose rate effect above 10^4 rad/s. This behavior can be seen both in sets of survival curves at various dose rates and in plots of survival for a fixed dose as a function of dose rate. Mathematical models which include certain types of multiple event interactions (Roesch, Braby and Nelson, this report) result in similar reversals of the dose-rate effect. The theoretical studies indicate that the assumptions of the different models can best be tested by comparing them with the results of fixed dose, variable dose-rate experiments. Unfortunately, at the dose rates

BEST DOCUMENT AVAILABLE

where the effect can be observed it is difficult to achieve the precise exposures needed to make the necessary comparisons. Evaluation of the experiments to date indicates that in order to investigate this effect with confidence a dose rate range of 10^2 to over 10^6 rad/s is required. To irradiate adequate numbers of cells under conditions equivalent to those prevailing in low dose-rate experiments, the usable portion of the radiation beam must be 35 mm in diameter. Since the change in survival with dose rate is not large the dose should be uniform and reproducible to within ±5%. To compare the models with experimental results three major technical problems must be overcome: we must produce a uniform radiation beam over a large area; measure the dose distribution to assess uniformity; and then be able to monitor the dose in each exposure.

Several instruments can measure the dose distribution to assess uniformity. A small ion chamber can be used; however, it is extremely time-consuming and results in resolution too poor to make corrections in beam uniformity. An improvement in resolution to better than 0.1 mm is made with the use of the radiochromic film dosimetry system (see McLaughlin et al. 1977). However, reading the dose by conventional methods and plotting it to determine dose distribution also makes it too time-consuming to be used for routine monitoring of dose uniformity. To improve resolution and reduce time, a microprocessor-controlled scanning densitometer has been developed. This instrument scans films up to 15 x 15 cm, pausing at specified intervals to measure the light transmission using a 1.6 mm diameter light beam. The dose is calculated from the transmission and the film thickness which is determined by interpolation in two dimensions between points where thickness has been measured. The percentage difference between the dose at the point and the dose at a calibration point is then determined. For convenience in visualizing the data, a symbol corresponding to the dose is displayed at the corresponding point on the microcomputer display. The result, shown in Figure 1, can be interpreted as a contour map of the dose distribution. Measuring the thickness of the film and entering it in the computer require only about 15 minutes. Scanning the film and generating a contour map of 660 dose readings require 13 minutes of unattended operation. This provides the resolution needed to check and make corrections in beam uniformity and is quick enough that it can be used in conjunction with each experiment to detect any change in alignment of the accelerator and beam line.

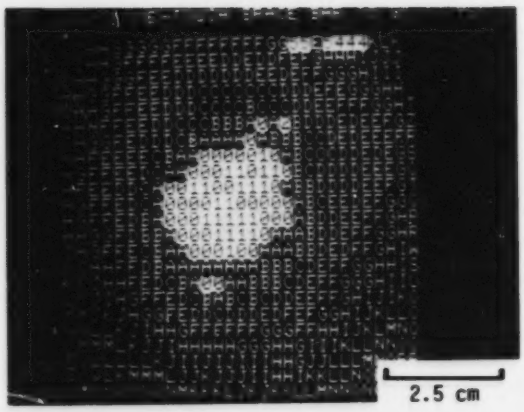

FIGURE 1. Scanning Densitometer Reading of Film Exposed at Output Window of Ring Lens Assembly with Lens Turned Off. Calibration point was at center of film. Symbols represent successive 4% increments in dose. Thus, if calibration point received 100 krad, areas designated "1" received 104 ± 2 krad, and those designated "C" received 88 ± 2 krad.

To spread the beam over a large area and achieve a high dose rate, the natural Gaussian profile of beam intensity must be altered. This can be done with an electrostatic ring lens (Johnson 1975) which is designed to fold the tails of the Gaussian distribution back onto the central peak. Such a lens was originally designed for positive ion beams and had to be scaled up to cover four times the diameter and operate at over ten times the voltage of the original design. This lens is mounted on a portable beam line separate from the Van de Graaff accelerator with its own vacuum system. Tests of this lens assembly indicate that the average dose rate at the exit window can be increased by a factor of three, and that it does concentrate the outer portion of the beam into a ring near the center, as shown in Figure 2. However, beam uniformity is strongly affected by small changes in beam line position, and some method for precisely positioning the beam line may be required.

The dose in each exposure was previously monitored during exposure by measuring the charge on a beam stop surrounding the target. This works well as long as the electric field surrounding the beam stop is low enough that ions formed in the air are not collected. Unfortunately, when the ring lens is used, both the cells to be irradiated and the beam stop must be located within a few cm of the beam exit window. Consequently, a sufficiently low field

BEST DOCUMENT AVAILABLE

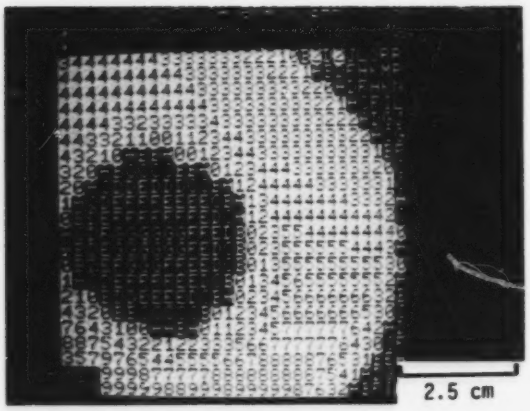

FIGURE 2. Effect of Imperfectly Aligned Ring Lens Assembly. Lens concentrates beam into an annular pattern. When properly aligned the focal length can be adjusted to produce a nearly uniform dose.

cannot be achieved. This problem has been solved by using a thin, three-plate ionization chamber to monitor the beam. This transmission ion chamber is calibrated relative to a small Nuclear Enterprises ion chamber and provides a signal to preset counters which control preprogrammed exposures.

The combination of the scanning densitometer to measure dose distribution and the ring lens with the transmission ion chamber to monitor dose should result in uniform exposures over large areas of cells.

Measurements to determine the maximum dose rate are awaiting final alignment of the accelerator and lens assemblies.

REFERENCES

Braby, L. A., J. M. Nelson and W. C. Roesch. 1980. "Studies of Chlamydomonas reinhardi: Experimental." In Physical Sciences. Part 4 of Pacific Northwest Laboratory Annual Report for 1979 to the DOE Assistant Secretary for Environment, pp. 40-44. PNL-3300 PT4, Pacific Northwest Laboratory, Richland, Washington.

Braby, L. A., J. M. Nelson and W. C. Roesch. 1981. "Fast Processes in Chlamydomonas reinhardi." In Physical Sciences. Part 4 of Pacific Northwest Laboratory Annual Report for 1980 to the DOE Assistant Secretary for Environment, pp. 62-63. PNL-3700 PT4, Pacific Northwest Laboratory, Richland, Washington.

Johnson, C. H. 1975. "A Ring Lens for Focusing Lens Beams to Uniform Densities." Nuclear Inst. and Methods 127:163-171.

McLaughlin, W. L., A. Miller, S. Fidan, P. Petersen and W. B. Pedersen. 1977. "Radiochromic Plastic Films for Accurate Measurement of Radiation Absorbed Dose and Dose Distributions." Radiat. Phys. Chem. 10:119-127.

AGE DISTRIBUTIONS IN AGENIC MAMMALIAN CELLS

J. M. Nelson, L. A. Braby and N. F. Metting

We have already described two techniques by which we can stop exponential growth in Chinese hamster ovary (CHO) cells and establish monolayers of noncycling stationary phase populations (Nelson 1979; Nelson and Braby 1980). One population is induced by growing cells to confluence, at which time proliferative activity ceases because of density-contact inhibition even though the medium has been refreshed at regular intervals; these cells are commonly referred to as "fed" cells. Cultures growing under these conditions are exposed to little or no nutritional stress. Another method is to maintain cell populations for extended periods in their own depleted medium without supplementation or replacement; these cells are referred to as "starved" cells. In this case growth inhibition occurs at a somewhat lower population density due to nutritional deprivation. Both methods have been in general use for some time by other investigators, but cultures were normally not maintained long enough to obtain the degree of growth suppression which we observe in our system.

We have evaluated both of these types of stationary phase populations with respect to a variety of growth parameters. These include cell densities both in terms of cells-per-unit volume and cells-per-unit area, cell viability as defined by erythrosine-B dye exclusion techniques, and DNA synthetic activity by the incorporation of DNA precursors (^{3}H-TdR and ^{125}I-UdR). The labeling studies have provided a means of defining both the mean cellular DNA synthetic activity and the growth fraction (the fraction of cycling cells) in a population at a given time.

BEST DOCUMENT AVAILABLE

Since these two types of stationary phase cells demonstrate different capacities to repair radiation damage, it is important to understand the physiological differences between them. The kinetics of agenic populations is generally restricted to a description of cellular age within the population. We can get at this information in two ways: We can study the kinetics of these populations as they grow into plateau phase; or we can study them as they resume normal exponential growth. Upon release from stationary phase, after an extended period of inactivity, cells will be distributed according to their ages at the time proliferative activity ceased. Studies of age distributions upon release have demonstrated that although these two types of stationary phase populations appear similar in many respects, they are composed of very different distributions of cells. Populations of cells released from nutritionally deprived stationary phase cultures (starved cells) contain a small fraction of cells arrested in G_1 phase, but most of the population are premitotic cells which have completed DNA synthetic activity. As seen in Figure 1, many of these cells will pass through mitosis within the first 3 to 5 hr after release. After this first wave, reduced mitotic activity is observed. The progeny of some cells sometimes divide one more time before becoming strongly synchronized again at 24 to 25 hr after release. At this time, many cells, most of which have divided at least once before, pass through mitosis demonstrating a very high degree of synchrony. In addition, the fraction of synthesizing cells increased from near zero to nearly 100% between the 7th and 15th hour after release, demonstrating a high degree of synchrony persisting for at least 3 generations. This large wave of mitoses at 24 hr has been observed by others (Chapman, Todd and Sturrock 1970); however, it has been assumed that these cells, prior to this time, emerged from a G_0-like stationary phase someplace within G_1 phase, passed through S phase, and into a long and variable G_2 phase.

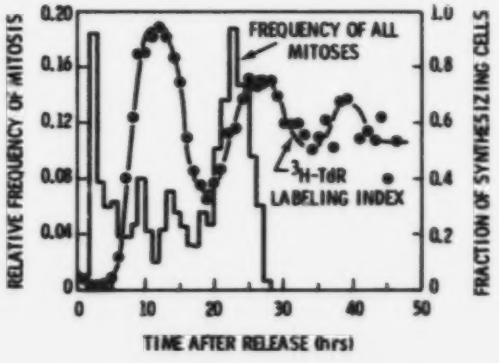

FIGURE 1. Frequency of Mitosis and Fraction of Synthesizing Cells in Populations Derived from Stationary-Phase Cultures Induced by Nutritional Deprivation (Starved Cells) Plotted as a Function of Time After Release. Mitosis was determined by time-lapse video-microscopy. Synthetic fraction was measured by autoradiography after pulse labeling with tritiated thymidine.

On the other hand, populations derived from density-contact inhibited cultures (fed cells) show radically different age distributions. The major fraction of these cells begin synthesizing DNA immediately upon release. Autoradiographic studies, shown in Figure 2, indicate that nearly 50% of the populations are in DNA synthesis at one hour after release and this fraction slowly falls until it reaches its first minimum around the 6th hour. Although some cells may pass through mitosis during the first 3 to 5 hr, indicating that a certain fraction of the cells rest in G_2 phase, the striking wave of division seen in the nutritionally deprived cells is missing in fed cells (see Figure 2). Those passing through mitosis during the first few hours are again synchronized at 24 to 25 hr.

This evidence demonstrates that a predominant fraction of the population ceases proliferative activity someplace during the DNA synthetic phase of the cycle. Note that by definition, cells in DNA synthetic phase are synthesizing DNA. It is obvious, however, that cells which have entered but not yet emerged from this synthetic phase, and have been forced by one mechanism or another to

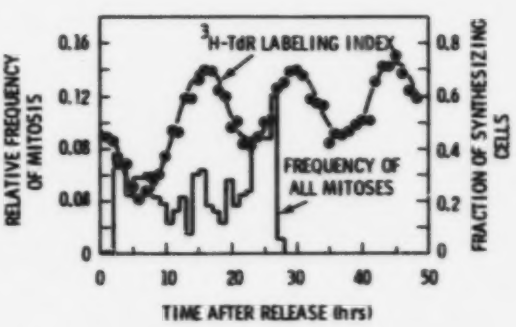

FIGURE 2. Frequency of Mitosis and Fraction of Synthesizing Cells in Populations Derived from Stationary-Phase Cultures Induced by Density-Contact Inhibition (Fed Cells) Plotted as a Function of Time After Release

BEST DOCUMENT AVAILABLE

suspend synthetic activity, will remain at the same physiologic age as they were when they entered the suspended state. This is analogous to the age of cultured cells whose metabolic activity has been arrested by freezing in liquid nitrogen; the age of these populations remains essentially the same throughout the entire period of suspended activity until growth conditions have been restored by thawing and they have been resuspended in an acceptable physiologic growth environment.

Another technique, although somewhat more difficult, is to measure age distributions in these populations as they grow into plateau phase and thus cease proliferative activity. Accumulation of information under these circumstances is hampered by very high cellular densities always associated with contact inhibition and induction of agenesis. Such experiments are further complicated by the fact that nearly any environmental disturbance would immediately alter metabolism and result in a transient restoration of cyclic activity. Such disturbances include changes in nutrient or toxic product concentrations, pH changes, and mechanical shear, which might physically disturb the monolayer and, thus, allow premature cell release.

We have attempted to determine DNA synthetic activity by liquid scintillation counting of ^{3}H-TdR-labeled populations as they grow into plateau phase and enter the agenic state. Although interpretation of these data is somewhat limited because complications are associated with the very high cellular densities, we have been able to verify another distinct difference between density-contact inhibited and nutritionally deprived populations. Other workers studying plateau phase populations have often found large fractions of cells in post mitotic G_1 phase. Generally, these populations are studied at between the 5th and 8th day of the passage, at which time the population density will have reached a relatively high level and stopped increasing (hence the name plateau). As may be noted in Figures 3 or 4 DNA synthetic activity of starved cells is not seriously depressed until about the 10th day. At 5 to 8 days, the majority of cells probably reach some gate in G_1 phase or the G_1-S boundary. Their rate of progress has slowed considerably. At this time, we should observe an abundance of post-mitotic presynthetic cells accumulated near the G_1-S interface. Our results suggest that these cells probably continue to progress very slowly, into, and through S-phase, ultimately ceasing growth activity within either S-phase or G_2-phase.

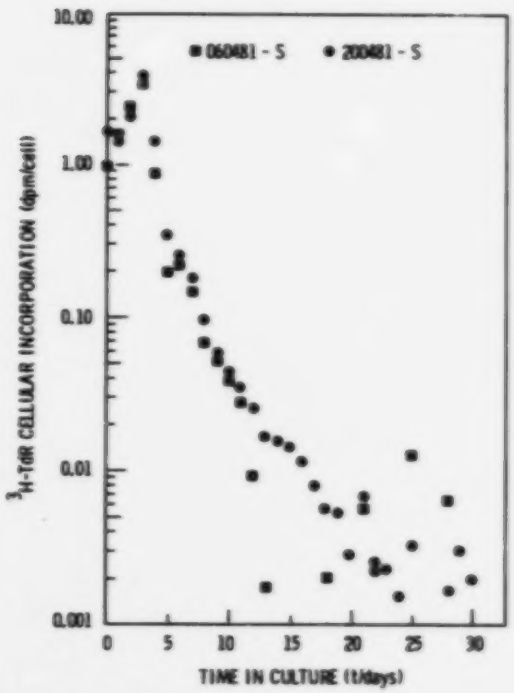

FIGURE 3. Relative DNA Synthetic Activity in Nutritionally Deprived Plateau-Phase Populations (Starved Cells) as a Function of Time After Passage. Cellular incorporation is determined by liquid scintillation counting after pulse labeling with tritiated thymidine.

However, cells within fed cultures are not all alike. Many cells resulting from density-contact inhibition appear to move sporadically through S-phase, perhaps stopping at a variety of different gates. These cells probably retain this resting status only until environmental conditions permit further progress through the cycle. Indeed, complete arrest may not even occur, but rather cyclic activity may merely be slowed down sufficiently to result in the deep suppression seen in Figure 4. Then, whenever physiologically possible (or required), synthetic activity would be allowed to progress. This concept is supported by the fact that these experiments (shown in Figure 4) indicate that DNA synthetic activity in this type of cell does not continue to fall after the first few days but rather reaches a minimum around 10 days and maintains this level thereafter.

BEST DOCUMENT AVAILABLE

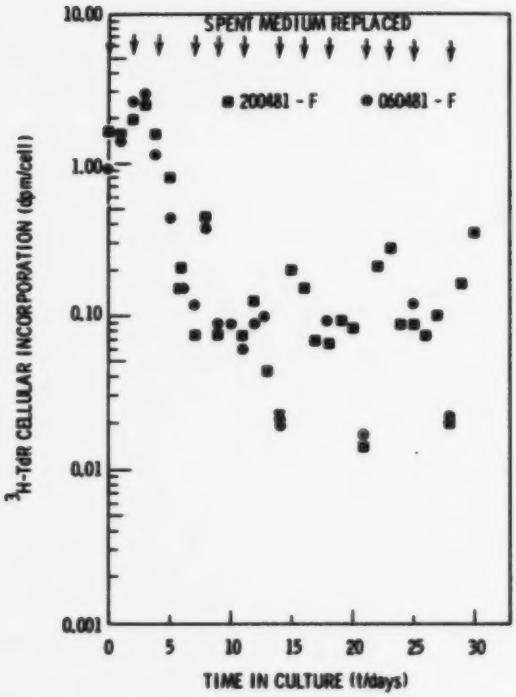

FIGURE 4. Relative DNA-Synthetic Activity in Density-Contact Inhibited Plateau Phase Populations (Fed Cells) as a Function of Time After Passage. Maximum depression occurs around the 10th day, never reaching the very low levels found in starved cells (see Figure 3).

REFERENCES

Chapman, J. D., P. Todd and J. Sturrock. 1970. "X-Ray Survival of Cultured Chinese Hamster Cells Resuming Growth After Plateau Phase." Radiat. Res. 42:590-600.

Nelson, J. M. 1979. "Noncycling Plateau Phase Mammalian Cells." In Part 4 of Pacific Northwest Laboratory Annual Report for 1978 to the DOE Assistant Secretary for Environment, pp. 2.29-2.31. PNL-285C PT4, Pacific Northwest Laboratory, Richland, Washington.

Nelson, J. M. and L. A. Braby. 1980. "Induction and Repair of Radiation Injury in Plateau-Phase Mammalian Cells." In Part 4 of Pacific Northwest Laboratory Annual Report for 1979 to the DOE Assistant Secretary for Environment, pp. 39-42. PNL-3300 PT4, Pacific Northwest Laboratory, Richland, Washington.

SLOW REPAIR PROCESSES IN STATIONARY PHASE MAMMALIAN CELLS

J. M. Nelson, L. A. Braby and W. C. Roesch

In the past, most of our work dealing with repair of sublethal radiation damage has been done using the algal eukaryotic Chlamydomonas reinnardi. This organism was chosen for a variety of reasons. In addition to being easy to handle in the laboratory, it may be easily synchronized by a 12 hr light-12 hr dark illumination cycle. However, most important is that for a period of about 8 hr following initiation of the light cycle, its radiation sensitivity (as measured by reproductive inactivation) changes little as a function of time. This characteristic has permitted extensive investigations of sublethal ionizing radiation damage and repair by both split-dose and dose-rate methods. These studies have led to identification of multiple repair processes which function simultaneously in the same organism. However, extrapolation of these data from a green algae to higher organisms is hazardous because to do so we make a number of questionable assumptions.

As mentioned last year, we are also directing our attention toward mammalian cells and are attempting to identify sublethal damage repair processes similar to those found in C. reinhardi. Most repair processes cannot be quantitated in rapidly proliferating cell systems (excluding ultrafast processes such as observed in mytotic mammalian cells [see Nelson, Braby and Roesch 1980]) because of the cell's rapidly changing radiation sensitivity. Because radiation sensitivity at the end of an experiment does not necessarily correlate with that at the beginning, it is not possible to interpret split-dose experiments in which doses are separated by long intervals or dose-rate experiments where the exposure is protracted over a period of several hours. In addition, the perturbations in cellular kinetics resulting from the first exposure preclude a reasonable estimate of the sensitivity during the second. Experiments such as these are often attempted but the results are not satisfactory and conclusions drawn are generally only quantitative findings. Consequently, efforts were begun to establish a virtually agenic population of mammalian cells. We believe that sublethal damage and its repair can be studied extensively in noncycling stationary phase cells because the radiation sensitivity of these populations is not expected to vary as a function of time.

BEST DOCUMENT AVAILABLE

Two types of stationary phase populations are in current use (see preceding section of this report). The radiation sensitivity of these two noncycling populations has been contrasted with that of exponentially growing cells in terms of reproductive cell survival (Nelson and Braby 1980). The survival curves from the same CHO cell line maintained in these three different states are surprisingly similar. They differ primarily in the D_q value, a parameter reflecting the magnitude of the shoulder, rather than in the D_0 which corresponds to the slope of the survival curve. In these experiments, we observe conventional repair in density-contact inhibited cells (fed cells) which appears similar to that found in exponentially growing populations. However, in this case, not all of the damage produced in these cells is repaired, and that remaining after 4 to 5 hr appears to persist indefinitely. On the other hand, stationary phase cells derived from nutritionally deprived cultures (starved cells) appear to repair much more of their damage but at a much slower rate, i.e, slower than conventional repair. The characteristic time of this slow process appears to be on the order of 15 to 20 hr as compared to about 5 hr for the conventional one. Population densities, cellular viability, average DNA synthetic activity (as determined by ^{125}I-UdR uptakes), morphological appearance, and other characteristics of these cultures appear very similar. However, the differences in the repair capacities of these two groups of cells can be explained by differences in their age distributions in the cell cycle. Precise determinations of repair rate are limited by the precision with which S_m, the theoretical maximum survival, can be determined. We believe the differences observed in repair capacity between these two types of stationary phase cells are real. Only τ (the mean repair time) and the relative amount of repair accomplished at different rates, should depend on the value of S_m. The biphasic nature of repair in density-contact inhibited cells probably would not change.

To further clarify these findings and elaborate on these repair phenomena, it is necessary to improve part of the technical procedure required for determining reproductive survival of cells following treatment. Using conventional equipment for cell transfer, it is not possible to gather a quantity of data sufficient to generate a complete time dependent repair curve in a given experiment. The limiting step is the extensive pipetting required to dilute and prepare the clonogenic cell assay plates. In response to this need, we have designed and constructed an automatic pipetting, diluting, and dispensing apparatus capable of performing a number of these operations, thus permitting a four- to five-fold increase in our capability.

This apparatus consists of a pair of precision peristaltic pumps run by heavy-duty stepping motors: one pump handles displacement medium for the cell suspension, the other handles medium for dilution and washing of the sterile dispensing apparatus. Both motors are controlled by a small desk top computer (COMMADORE 32K PET). Experimental transfer procedures are, of course, performed under sterile conditions and operation is controlled by a special keyboard which may be located next to the dispensing apparatus itself. All pertinent data, requests, and instructions are displayed on the CRT throughout the process.

A highly operator-interactive program has been developed enabling rapid and accurate processing of each assay plate. Computer controlled procedures include all preliminaries such as priming the apparatus and calibrating both pumps, computing required discharge volumes, withdrawing the treated sample containing cells to be assayed, delivering precise volumes of cells to be diluted in predetermined volumes of medium, and final flushing of the sample handling equipment. In addition, the code permits operator initiated changes, deletions, and a variety of modifications as required, by means of the computer keyboard and CRT display. We expect to test this apparatus and begin using it in the near future.

REFERENCES

Nelson, J. M., L. A. Braby and W. C. Roesch. 1980. "Rapid Repair in Mitotic Mammalian Cells." In Part 4 of Pacific Northwest Laboratory Annual Report for 1979 to the DOE Assistant Secretary for Environment, pp. 37-39. PNL-3300 PT4, Pacific Northwest Laboratory, Richland, Washington.

Nelson, J. M. and L. A. Braby. 1980. "Induction and Repair of Radiation Injury in Plateau-Phase Mammalian Cells." In Part 4 of Pacific Northwest Laboratory Annual Report for 1979 to the DOE Assistant Secretary for Environment, pp. 39-42. PNL-3300 PT4, Pacific Northwest Laboratory, Richland, Washington.

BEST DOCUMENT AVAILABLE

Microdosimetry

Projects in microdosimetry and cellular effects are closely integrated and have the joint purpose of exploring the connections between the primary physical events produced by radiation and their biological consequences in cellular systems. The microdosimetry projects include the theoretical description of primary events and their connection with the observable biological effects. This program also is concerned with the design and measurement of physical parameters used in theory or to support biological experiments. Microdosimetric spectra for 2 MeV electron beams in one- and two-micrometer sites have been measured directly. Work on calculating the energy deposition in site sizes and geometries that cannot be measured has led to publication of a paper on proton-induced ionization in nanometer sites. Emphasis in these calculations has now shifted to electron beams.

MICRODOSIMETRY OF ELECTRON BEAMS

L. A. Braby and W. C. Roesch

Many models describing the response of cells to ionizing radiation incorporate the idea of a homogeneous-sensitive site with finite dimensions. Equal amounts of energy deposited in any pattern within such sites are assumed to be equally effective. Microdosimetric quantities such as energy imparted, ε, are expressions of the energy deposited in such a site. Thus, within the limitations of the homogeneous site assumption the dose mean of the single event distribution, ($\bar{y}_D$), can be related to the relative biological effectiveness (RBE) of different radiations. Although all low linear energy transfer (LET) radiations (photons and electrons) have often been considered essentially equal in terms of RBE, we have found (Braby, Nelson and Roesch 1980; Braby and Roesch 1981) significant differences both in the response of Chlamydomonas reinhardi and in $\bar{y}_D$ for different electron beams. Thus, a more thorough investigation of the microdosimetric properties of electron beams is desirable.

To measure ε for electron beams, several problems must be addressed. The major problems include the small size of the events, the wall effect, simulation of the irradiated site and its environment with a detector system, and event coincidence. The wall effect can be effectively dealt with by using a grid walled detector. Since the variance of $f(\varepsilon)$ is due primarily to energy loss straggling rather than the track length distribution, the shape of the detector is relatively unimportant and a cylindrical detector is used. Because the events are small, a significant fraction of them are indistinguishable from the system noise.

Thus, to calculate $\bar{y}_D$, it is necessary to estimate the number of events at the smallest values of ε.

Simulating the radiation environment around the site and reducing the electron fluence to prevent event coincidence are related problems. Last year (Braby and Roesch 1981), we reported two attempts to simulate a typical electron irradiation geometry with a detector configuration that would result in count rates low enough to record single events. The most desirable method of reducing the count rate was found to be collimating the beam. However, a graphite collimator must be a minimum of 10 mm thick to prevent electrons from bypassing the hole; yet the diameter should not be too small relative to the thickness or scattering in the hole will be excessive. We met these requirements by using an additional length of beam line and collimator as illustrated in Figure 1. The results for two simulated site diameters, three accelerator energies and four depths in plastic are presented in Table 1. These values were obtained by exponential extrapolation from the data just above the noise, back to zero energy. When the data for a given site diameter are plotted on semi-log paper the slope from approximately 0.04 to 0.08 keV energy imparted is essentially constant for all electron energies. This slope was used in the extrapolation. Previous experiments (Braby and Roesch 1978) in which specific energy (Z) for pulses of electrons was measured directly indicate that this is an appropriate extrapolation. Interestingly, it results in values of mean linear energy ($\bar{y}$) lower than the minimum stopping power. This is apparently the result of a large number of events consisting of a single ionization. The values of $\bar{y}_D$ in Table 1 extend to 2 MeV the data presented last year for 1 MeV. The increase in $\bar{y}_D$ with depth is expected because of the decrease in electron energy. The ratio of $\bar{y}_D$ at maximum to minimum depth goes from 1.47 for a one-micron diameter site to 1.74 for a two-micron diameter site with 1.5 MeV electrons. It may be possible through the modeling activity described on page 41 of this report ("Double Two-Event

BEST DOCUMENT AVAILABLE

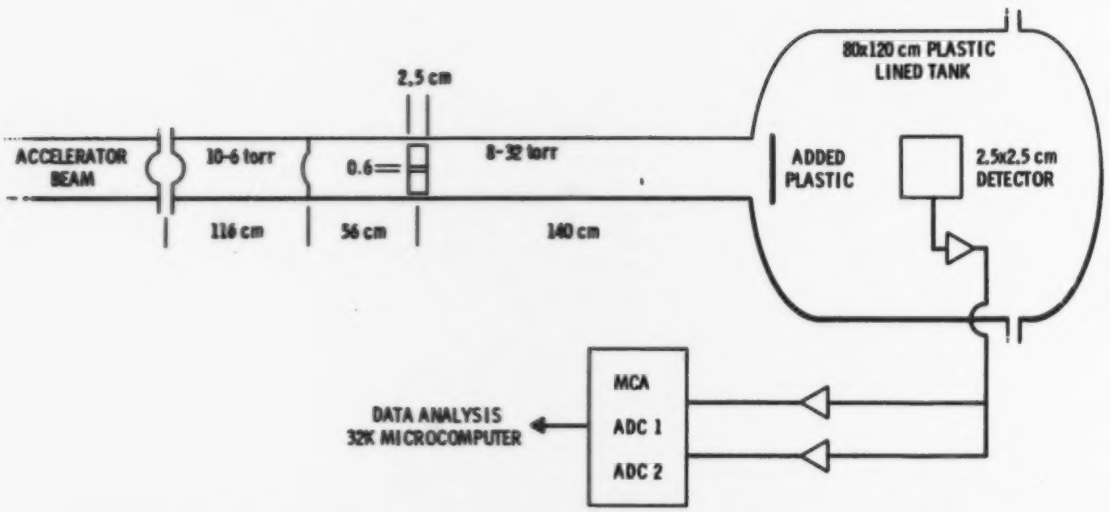

FIGURE 1. Schematic of Detector and Beam Line to Simulate Radiation Environment Used in Cell Irradiations.

TABLE 1. Dose Mean Lineal Energy

$\bar{y}_D$ (keV/μM)

Simulated Site Diameter (μg/mm²)	Accelerator Voltage MV	Depth in plastic (g/cm²) .01	.06	.19	.38
1.0	1.0	1.17	1.54	1.93	2.51
	1.5	1.16	1.21	1.50	1.71
	2.0	1.36	1.18	1.39	1.50
2.0	1.0	.800	1.16	1.79	2.15
	1.5	.747	.923	1.13	1.30
	2.0	.765	.849	1.01	1.12

Models") to relate this ratio to the relative biological effectiveness. The decrease in $\bar{y}_D$ with increasing site size is also expected since the electron beam will contain some low energy particles with high LET. Those particles, which do not cross the detector, produce constant energy imparted (ε), and thus decrease y as the site diameter increases.

REFERENCES

Braby, L. A., J. M. Nelson and W. C. Roesch. 1980. "Studies of Chlamydomonas reinhardi: Experimental." In Part 4 of Pacific Northwest Laboratory Annual Report for 1979 to the DOE Assistant Secretary for Environment, pp. 40-44. PNL-3300 PT4, Pacific Northwest Laboratory, Richland, Washington.

Braby, L. A. and W. C. Roesch. 1981. "Single-Event Distributions for Fast Electrons." In Part 4 of Pacific Northwest Laboratory Annual Report for 1980 to the DOE Assistant Secretary for Environment, pp. 63-67. PNL-3700 PT4, Pacific Northwest Laboratory, Richland, Washington.

Braby, L. A. and W. C. Roesch. 1978. "Direct Measurements of f(z) for Fast Electrons." In Sixth Symposium on Microdosimetry, eds. J. Booz and H. B. Ebert, pp. 251-260. Harwood Academic Publishers, London.

RADIATION TRANSPORT AND DOSIMETRY CALCULATIONS FOR HIGH-ENERGY ELECTRONS

W. E. Wilson

Direct measurement of microdosimetry spectra for electron beams is limited with respect to site size and irradiation geometry. To thoroughly investigate the relationship between microdosimetric parameters and cellular response, we will have to obtain additional data by calculation. Monte Carlo methods will be used to determine the energy deposition in small sites, and the energy of the electrons at the site will be calculated by electron transport.

Several existing computer codes for electron transport were investigated; three were obtained from the Radiation Shielding Information Center at ORNL and one, ETRAN by M. Berger, was adapted to run on the UNIVAC 1100/44. Two versions of the code, differing only in geometry, were converted: one

BEST DOCUMENT AVAILABLE

calculates semi-infinitive slabs; the other calculates transport in cylinders. We are now preparing the input data for the window materials of interest.

CALCULATION OF DISTRIBUTIONS FOR ENERGY IMPARTED AND IONIZATION BY FAST PROTONS IN NANOMETER SITES

W. E. Wilson and H. G. Paretzke

A paper by this title was published in Radiation Research (Wilson and Paretzke 1981); the abstract follows:

Results are presented for a Monte Carlo calculation of energy imparted and ionization in nanometer volumes by individual proton tracks. Representative frequency distributions for ionization are presented for 0.25- to 3-MeV protons passing through and near spherical sites of 1- to 200-nm diameter unit density water in specified geometry. In addition, the radial dependencies of the mean energy imparted and of the relative variance of the distributions are obtained as functions of the site diameter and of the ion energy.

REFERENCE

Wilson, W. E. and H. G. Paretzke. 1981. "Calculation of Distributions for Energy Imparted and Ionization by Fast Protons in Nanometer Sites." Radiat. Res. 87:521-537.

INTERNATIONAL COMMISSION ON RADIATION UNITS AND MEASUREMENTS (ICRU) REPORT ON MICRODOSIMETRY

L. A. Braby

One of the major goals of the dosimetry program has been to develop microdosimetry as a tool for understanding the stochastic nature of the deposition of energy by ionizing radiation. Over the past several years this field has grown rapidly and has contributed to many models of radiation damage and linear energy transfer (LET) effects. As the diversity of work on microdosimetry has increased, the need for a summary of the principles and techniques of microdosimetry and a uniform system of nomenclature has become evident. For this reason, we have participated extensively in the International Commission on Radiation Units and Measurements (ICRU) committee on microdosimetry. We expect our efforts to help clarify this important aspect of dosimetry and at the same time point out the importance of the underlying charged particle track structure. We hope to contribute to more general application of microdosimetry in fields ranging from cellular radiation biology to health physics.

BEST DOCUMENT AVAILABLE

BLANK PAGE

• Microdosimetry of Internal Sources

The purpose of this study is to develop practical methods for calculating microdosimetric distributions of plutonium or other alpha-emitting elements that are deposited, especially as particulates, in soft tissue and lung tissue. This study will aid the correlation and extrapolation of radiation effects measured at different levels of exposure and in different species. Computational methods will be developed and tested in the Radiological Physics Section. Concurrently, the Dosimetry Technology Section will develop cell and tissue models in which those methods will be applied.

MICRODOSIMETRY OF PARTICULATES

W. C. Roesch

In their theory of Dual Radiation Action, Kellerer and Rossi (1972) made use of a quantity, ζ, defined as the quotient of the mean square specific energy to the mean specific energy, both for single events. I have found a similar, but more complicated quantity, ζ', for use in the microdosimetry of particulates:

$$\zeta' = \frac{\int qaw\langle z_r^2\rangle dV}{\int qaw\langle z_r\rangle dV} + a\,\frac{\int qaw^2\langle z_r\rangle^2 dV}{\int qaw\langle z_r\rangle dV} \qquad (1)$$

where

a = average number of particles emitted by each particulate

q = probability of finding a particulate in dV

w = probability that a particle emitted in dV will deposit energy in the site

z^r = specific energy in the site from a particle emitted in dV

$\langle\rangle$ = average over the spectrum of z of the quantity within the $\langle\rangle$

dV = volume element at a distance r from the site. The new quantity obeys the equation

$$\langle z^2\rangle = \zeta' D + D^2 \qquad (2)$$

where z is the specific energy in the site, i.e., due to all particulates depositing energy in the site, and D is the absorbed dose. It was this relation, with ζ instead of ζ', that Kellerer and Rossi found so useful.

The Kellerer-Rossi ζ corresponds to my ζ' in the limit of very small particulate size (i.e., small a) and q uniform in the vicinity of the site. Thus ζ is the first term in Equation (1) (Kellerer and Rossi 1972). The first term represents the effects of individual particles; the second, the effects of the multiple emissions from a particulate. ζ' is never smaller than ζ and it increases linearly with particulate size.

REFERENCES

Kellerer, A. M. and H. H. Rossi. 1972. "The Theory of Dual Radiation Action." Current Topics in Radiation Research Quarterly 8:85-158.

COMPUTER PROGRAMS

W. C. Roesch

The computer codes developed last year for microdosimetry of particulates in the lung are distinct from the ones developed several years ago for homogeneous tissue. Switching from one set of codes to the other became a nuisance; an investigator almost always wants to compare lung microdosimetry with similar conditions in ordinary tissue. Consequently, we have begun adapting the homogeneous-tissue codes to the method of calculation used for lung microdosimetry and consolidating all the codes into a single system.

COMPUTER PROGRAM MODIFICATIONS FOR APPLIED INTERNAL MICRODOSIMETRY

D. R. Fisher, W. C. Roesch and R. Harty

- A Method for Computing the Microdosimetry of Energy-Absorbing Particulates.

The energy of each alpha particle from a radionuclide is a well-defined quantity. Computer programs developed at this laboratory for calculating the microdosimetry of

BEST DOCUMENT AVAILABLE

internal alpha emitters were written for monoenergetic emissions. Often the nuclide of interest emits alpha particles with two or more distinct (but similar) energies. For such cases, the mean energy or abundance-weighted average may be used for the energy input variable in microdosimetry calculations.

Self-absorption of alpha energy results in a spectrum of alpha exit energies from the source material. Self-absorption occurs when the size or density of the matter in which the radioactive atoms are located causes a significant portion of the energy to be deposited in the source material itself. The effect of self-absorption is usually neglected for very small particulates. Recently, however, use has been made of ceramic microspheres containing plutonium to study the effects of "hot particles" in mammalian lungs (Holland et al. 1976). The radioactive microspheres consist of high density (ρ = 4.2 - 5.6 g/cm^3), 10 µm diameter zirconium oxide labeled with different specific activities of plutonium alpha emitter (Anderson and Perrings 1978). The energy spectrum of alpha particles emitted from the microspheres indicates a considerable degree of self-absorption and energy degradation. This factor can produce errors in the microdosimetry calculation if a correction for it is not made.

Having previously measured or calculated the spectrum of exit energies from a microsphere, the spectrum is subdivided into n number of energy divisions (Figure 1). Higher numbers of n result in better overall definition of the spectrum and greater precision, but also increased computing time and cost; 10 or 12 subdivisions may be a reasonably good choice. For each division, the frequency f(E) must be multiplied by the activity of the source to give the fraction of activity represented by that energy subdivision. The mean energy of each subdivision and its activity are used to calculate a probability density in specific energy.

This process results in n different probability density distributions, which must then be combined.

A method for combining probability densities using the convolution integral was described in detail in an earlier report (Roesch 1979). If $f_1(z)$ and $f_2(z)$ are the specific energy densities of any two of the subdivisions, then the convolution of the two is

$$f(z) = {}_d\int^z f_1(z - x)\, f_2(x)\, dx \qquad (1)$$

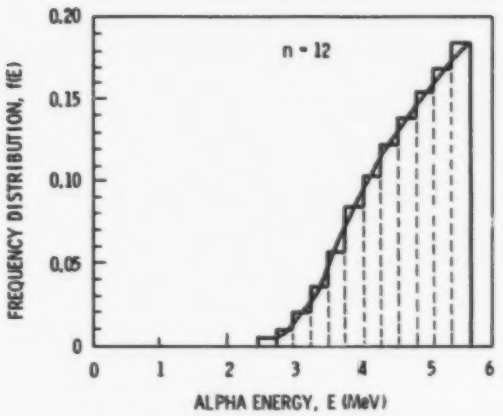

FIGURE 1. A Typical Alpha Exit Energy Spectrum of Microspheres Subdivided into 12 Steps

That result is then convoluted with the third probability density. The new result is then convoluted with the fourth, etc., until the probability densities of each subdivision have been combined. The densities must be combined in proportion to the activity frequency represented by each energy subdivision.

- A Method for Incorporating Consideration of Exponential Retention Functions for Internally Deposited Radionuclides.

The convolution integral (Equation 1) can also be used to calculate the microdosimetry of a radionuclide deposited in an organ of the body, where the organ retention function of the radionuclide has the form:

$$R = a_1 \exp(-b_1 t) + a_2 \exp(-b_2 t) + \ldots a_n \exp(-b_n t) \qquad (2)$$

where a_1, a_2, ... a_n are retention y-coordinate intercepts, and b_1, b_2 ... b_n are the first-order rate constants. The values of b are obtained from the formula:

$$b = 0.693/T_b \qquad (3)$$

where T_b is the biological half-time of the retention function component.

A typical retention curve is illustrated in Figure 2. The curve is subdivided into 10 or 12 steps (equal time divisions), as with the previous example, and the mean value on the curve for each subdivision is determined.

BEST DOCUMENT AVAILABLE

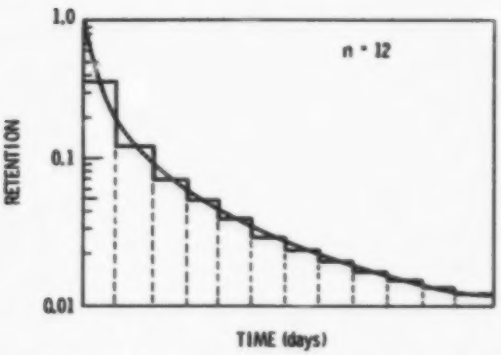

FIGURE 2. A Typical Organ Retention Function for an Internally Deposited Radionuclide. The function has been subdivided into 12 steps.

The microdosimetry calculation is executed separately for each individual time period. The activity of the initial deposition is multiplied by the mean value of the retention function for each subdivision. This process results in n different probability densities in specific energy. The probability densities are then combined using the convolution integral (Equation 1).

REFERENCES

Anderson, E. C. and J. D. Perrings. 1978. "Production and Properties of Radioactive Microspheres for Localized Irradiation of Lung Tissue." Health Phys. 34:225-236.

Holland, L. M., J. R. Prine, D. M. Smith and E. C. Anderson. 1976. "Irradiation of the Lung with Static Plutonium Microemboli." In The Health Effects of Plutonium and Radium, pp. 127-138, ed. W. S. S. Jee. The J. W. Press, Salt Lake City.

Roesch, W. C. 1979. "Microdosimetry for Radiation Nonequilibrium." PNL-SA-7417. Pacific Northwest Laboratory, Richland, Washington.

STATISTICAL MODELING OF BEAGLE DOG LUNG FOR MICRODOSIMETRY

D. R. Fisher, R. T. Hadley and W. C. Roesch

The objective of internal microdosimetry is to develop a more precise understanding of the complex relationship between the initial deposition of radiation energy in microscopic volumes, and early or late biological effects. The present study is concerned with constructing a reliable model of the intricate tissue structure of pulmonary lung to calculate energy depositions and probabilities of radiation interactions with microscopic targets--such as epithelial cell nuclei. This capability is important for determining the specific energy distribution in the lung from an internal deposition of radioactive materials.

Last year we reported preliminary results from the construction of histograms which described the most probable chord lengths through air space and tissue segments of an alpha particle emitted from a radioactive particulate resting on the wall of an alveolus. We also described the distribution of distances taken by the alpha particle as it traversed from air/tissue interfaces to cell nuclei within tissue segments. This information permits the investigator to simulate alpha particle tracks in the lung, determine lengths of random alpha particle tracks, and calculate the alpha energy deposited in tissue or cell nuclei along the alpha particle paths.

The microscopic chord length measurements on lung tissue samples were made using an image analyzer system described in earlier reports (Fisher et al. 1980; 1981). The video display on the image analyzer consists of a rectangular matrix of 5×10^5 individual picture elements (pixels). One pixel represents the limit of resolution of the system. At the magnification selected, the width of one pixel was determined by calibration to be 1.016 μm, or approximately one micron. As an image is displayed on the analyzer, each pixel is assigned a number corresponding to its gray level. Sixty-four shades of gray are recognized by the analyzer in the black to white spectrum. The measurement of microscopic features, therefore, depends upon contrast and gray-level consistency. True color image analyzers are not yet available. To compensate for loss of color contrast in the video display, a color filter was used on the microscope, and great care was taken to optimize tissue staining and microscope light intensity. A continuously variable gray-level discriminator was used to select the desired contrast level or range necessary to encompass and define the structures present in the displayed image.

One of the difficulties encountered during the analysis of lung tissue samples was the preponderance of tissue segments of one and two pixels, possibly attributable to electronic "noise." To identify and separate noise from measurements on actual tissue

BEST DOCUMENT AVAILABLE

segments in the image, a simplex minimization routine was used. A geometric distribution represented the true noise component, and a Johnson s_b distribution provided a good fit to the tissue chord length data. We estimate that 10% to 30% of all one-pixel segments were caused by electronic noise. The analyzer line scan measurements were then adjusted to account for the noise component, and the distributions of air-space chord length, tissue-segment chord lengths, and distances from tissue wall to cell nucleus were reanalyzed. From the distribution histograms, probability density functions (pdf's) were proposed. Parameters for the functions were then estimated by the method of maximum likelihood. The observed cumulative frequency distributions arising from the data were plotted against the proposed theoretical cumulative distribution functions using a QQ-plotting routine that demonstrated goodness of fit.

The frequency distribution of observed air-chamber chord lengths is shown in Figure 1. This distribution closely resembles the gamma probability density function, g(x). The distribution of observed tissue wall thicknesses was best approximated by the Johnson s_b probability density function, j(x), shown in Figure 2. The distribution of distances from tissue wall to cell nucleus was fit to the Weibull probability density function, w(x), shown in Figure 3. Revised estimates of the alpha and beta parameters for each of these distributions are given in Table 1.

The pdf's were found to be consistent for each dog lung and for individual lobes within the lung--regardless of the rotational orientation of tissue specimens.

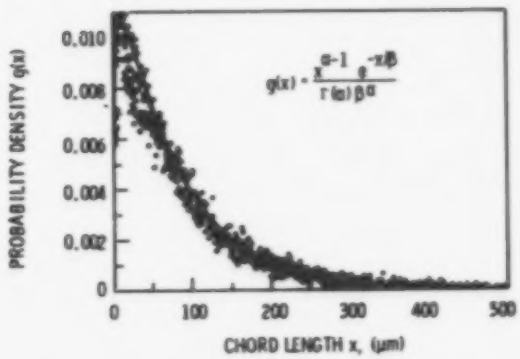

FIGURE 1. Distribution of Air Chamber Chords

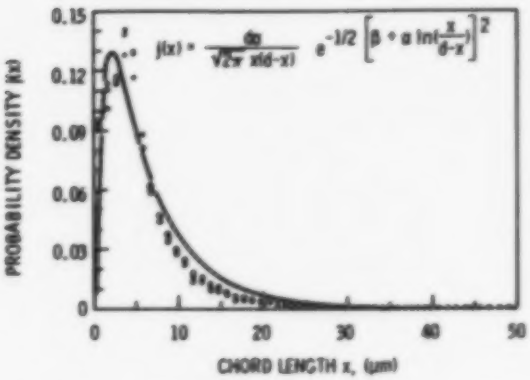

FIGURE 2. Distribution of Tissue Wall Thicknesses

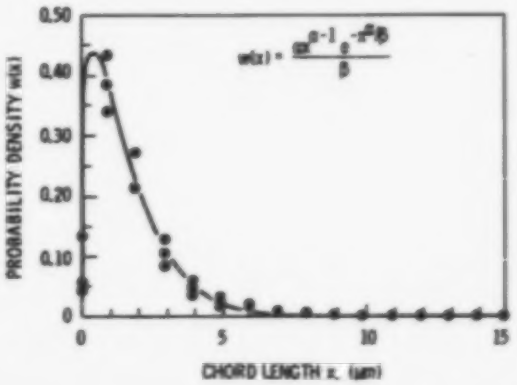

FIGURE 3. Distribution of Distances From Tissue Wall to Epithelial Cell Nuclei

TABLE 1. Estimated Probability Density Function (pdf) Parameters for Lung Model Distributions

Feature	pdf	α	β
Air chords	gamma	1.12	70.0
Tissue chords	Johnson s_b	1.23	1.90
Wall-nucleus distance	Weibull	1.16	2.94

In summary, the above three distributions (Figures 1-3) and their best-fit parameters constitute a pulmonary lung model that can be used in microdosimetry to describe the paths of random alpha-particle tracks and the probability that these tracks will traverse biologically sensitive sites.

BEST DOCUMENT AVAILABLE

This lung model may be used in conjunction with established deposition and retention models for determining the microdosimetry of a variety of inhaled radioactive materials.

REFERENCES

Fisher, D. R., J. L. Daniel and G. F. Piepel. 1980. "Lung Tissue Modeling for Microdosimetry Application." In Part 4 of Pacific Northwest Laboratory Annual Report for 1979 to the DOE Assistant Secretary for Environment, p. 57. PNL-3300 PT4, Pacific Northwest Laboratory, Richland, Washington.

Fisher, D. R., W. C. Roesch, G. F. Piepel, J. L. Daniel and W. M. Bowen. 1981. "Microdosimetry of Plutonium in Beagle Dog Lung." In Part 4 of Pacific Northwest Laboratory Annual Report for 1980 to the DOE Assistant Secretary for Environment, p. 73. PNL-3700 PT4, Pacific Northwest Laboratory, Richland, Washington.

BEST DOCUMENT AVAILABLE

BLANK PAGE

• Dosimetry of Internal Emitters

The Dosimetry of Internal Emitters Program endeavors to refine the correlation between radiation dose and observed biological effects. The program is presently engaged in the development of studies that will demonstrate the applicability of microdosimetry models developed under the Microdosimetry of Internal Sources Program. The program also provides guidance and assistance to Pacific Northwest Laboratory's Biology Department in the dosimetric analysis of internally deposited radionuclides. The investigators work closely with the Biology Department staff and collaborate on the Microdosimetry of Internal Sources Program.

MICRODOSIMETRY--A TOOL FOR INTERPRETING THE DOSE-RESPONSE FROM INTERNAL EMITTERS

D. R. Fisher and R. Harty

Although the concept of absorbed dose is commonly used in radiation biology as a parameter for comparing the toxic effect of different levels of radiation on a system, situations exist where absorbed dose by itself is inadequate, and additional dose distribution information is needed to explain the observed biological effect. An example of such a situation is the irradiation of cells by alpha particles from internal emitters. This report describes a case where microdosimetry methods were used to reinvestigate the dosimetry of two very similar experiments with apparently contradictory dose-response results.

Figure 1 shows a plot of dicentric chromosome aberration yields induced in human blood lymphocytes following in vitro exposure to dissolved americium or plutonium. The experiments were performed at two separate research laboratories (DuFrain et al. 1979; Purrott et al. 1980). Although each irradiation produced linear dose-response functions, the slopes of the best-fit lines (Figure 1) are different by a factor of about 12. This disparity was totally unexpected. The relative biological effectiveness (RBE) of alpha particles compared to ^{60}Co gamma radiation for a dicentric yield of 0.1 per cell reported by Purrott et al. was approximately 10 times lower than the value obtained by DuFrain et al. for the same cell type and mode of irradiation.

We re-evaluated the dosimetry of the two studies using an internal microdosimetry computer code (Roesch 1977). For each experiment, we assumed that the lymphocytes were randomly distributed in a unit-density solution of americium or plutonium, and that the activity was well dissolved and uniformly mixed in. We also assumed that the cells were completely separated from the

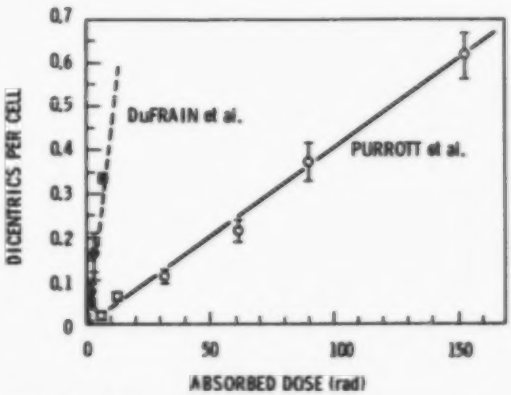

FIGURE 1. Frequency of Dicentric Chromosomes as a Function of Absorbed Dose from Alpha Particle Irradiation *In Vitro*

solution of alpha emitter at the end of the exposure period.

During such an irradiation, only a certain percentage of the cells are hit by alpha particles. The alpha particle energy imparted to individual cells is highly variable. Both the probability that a cell was hit, and the probability that a specific amount of energy was deposited, were calculated using the computer code for internal microdosimetry. In Table 1 the predicted fraction of irradiated cells is compared to the fraction of damaged cells observed in each of the two cell irradiation studies.

We are not yet able to correlate specific energy with discrete biological effects, but we can, as a first approximation, assume that the early effects will occur in that fraction of cells that are irradiated. Table 1 shows that a higher fraction of cells were damaged than were calculated to have been irradiated. It would not be possible, therefore, for the activity in the study of DuFrain et al. to have been uniformly distributed in the solution, as was earlier assumed.

BEST DOCUMENT AVAILABLE

TABLE 1. Summary of Predicted Fraction of Cells Irradiated and Frequency of Observed Cytogenetic Damage in Two Experiments

Experiment	Absorbed Dose (rad)	Irradiated Cells (predicted)	Damaged Cells (observed)
DuFrain *et. al.*	0.85	0.016	0.10
	1.71	0.031	0.13
	3.42	0.061	0.23
	6.84	0.118	0.32
Purrott *et. al.*	6.50	0.105	0.016
	13.0	0.198	0.070
	33.0	0.430	0.110
	65.0	0.665	0.181
	95.0	0.796	0.299
	150.0	0.931	0.442

For DuFrain et al. to have obtained the observed chromosome aberrations, quite possibly one or both of two events also transpired during the irradiation of lymphocytes: (1) settling of the cells and activity in the solution may have occurred because it was not agitated; and (2) the activity may have been attracted to the cell membrane of the lymphocytes. Either situation leads to higher specific energy densities in the cells and increased probabilities that the cells were irradiated and damaged. Thus, microdose distribution is an important determinant of biological effect.

Average dose to a biological system of cells and body fluids can therefore be a misleading concept unless the microdistribution of activity with respect to sensitive biological sites is adequately defined. Care must be taken in the interpretation and extension of dose response curves, particularly in the case of internally deposited alpha particle emitters. Microdosimetric evaluations are recommended for all cell studies involving alpha-emitting radionuclides.

REFERENCES

DuFrain, R. J., G. Littlefield, E. E. Joiner and E. L. Frome. 1979. "Human Cytogenetic Dosimetry: A Dose Response Relationship for Alpha Particle Radiation from ^{241}Am." Health Phys. 37:279-289.

Purrott, R. J., A. A. Edwards, D. C. Lloyd and J. W. Stather. 1980. "The Induction of Chromosone Aberrations in Human Lymphocytes by In Vitro Irradiation with α-Particles from Plutonium-239." Int. J. Radiat. Biol. 38(3):277-284.

Roesch, W. C. 1977. "Microdosimetry of Internal Sources." Radiat. Res. 70:494-510.

IN-VITRO ALPHA-PARTICLE MICRODOSIMETRY

R. J. Traub, D W. Murphy, D. R. Fisher and R. Harty

We have begun experiments which will allow us to demonstrate the applicability of microdosimetry calculations to radiation protection. Microdosimetry, extended to the dosimetry of internal emitters at this laboratory (Roesch 1977), utilizes the stochastic quantity "specific energy (Z)." The specific energy is the value of the energy actually imparted divided by the mass of the site.

Experiments to verify microdosimetric calculations can be applied to cells either in vivo or in vitro. In our experiments we are utilizing two types of radioactive sources. The first is a zirconium oxide microsphere labeled with plutonium. The second source type is a polystyrene microsphere labeled with ^{244}Cm. The former has been generously supplied by Dr. L. M. Holland of Los Alamos Scientific Laboratory. The latter microspheres are being developed at this laboratory. Polystyrene microspheres have the relative advantages of being smaller, having a density closer to the density of tissue, and causing less attenuation of the alpha particles.

The present experiments utilize the zirconium microspheres dispersed among Chinese hamster ovary (CHO) cells growing on the bottom of plastic flasks. The experiments are designed so that in all cases the average energy deposited in the system remains constant while microscopic energy distributions are varied. This is done by varying the concentration of the microspheres inversely with their activity. That is, microspheres with high activity will be in a lower concentration than that of microspheres having a lower activity. Thus, the total number of alpha particles emitted is nearly the same in all cases, as is the average radiation dose. However, as the activity of individual particulate sources is increased and the number of sources is correspondingly decreased, the probability of a cell being hit decreases; but if hit, the amount of energy deposited in a cell will be greater.

BEST DOCUMENT AVAILABLE

We anticipate that the response of CHO cells to radiation (e.g., cell survival and mutation rate) should correlate better with the specific energy (Z) and the probability of a cell being hit than with the absorbed dose. We hope that these experiments will demonstrate the applicability of microdosimetry to internally deposited radionuclides.

REFERENCE

Roesch, W. C. 1977. "Microdosimetry of Internal Sources." Radiat. Res. 70:494-510.

DEPOSITION OF INHALED ^{239}Pu-NITRATE IN KIDNEYS OF BEAGLE DOGS

R. J. Traub and J. F. Park

The deposition of plutonium in the kidneys of beagles that had inhaled ^{239}Pu-nitrate was studied to determine the extent to which plutonium accumulated in the kidney. Accumulation, if it occurred, would increase the dose to the kidney.

The data were obtained from beagle dogs which had inhaled ^{239}Pu-nitrate aerosol (Cannon et al. 1979). The data were grouped according to the number of days past exposure at the time of sacrifice. Then the percentage of the body burden in the kidney was computed for each group, as shown in Figure 1.

This study indicates that less than one percent of the body burden at sacrifice is deposited in the kidney, and that this organ burden is also present shortly after the inhalation. No trend of increased deposition of plutonium in the kidney was found between three and 1310 days post inhalation. Based on these data, it appears that the fraction of inhaled plutonium nitrate deposited in the kidney is small and remains fairly constant following an exposure.

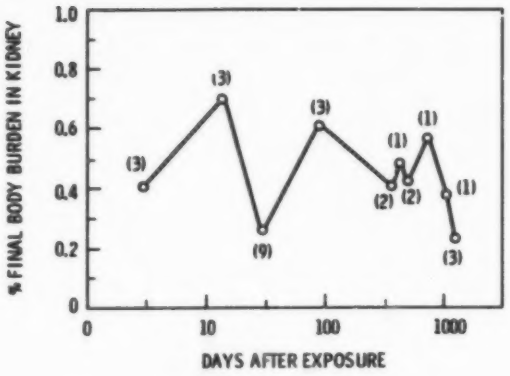

FIGURE 1. Deposition of Plutonium in Dog Kidneys Following Inhalation. Numbers in parentheses indicate number of dogs.

REFERENCES

Cannon, W. C., G. E. Dagle, R. L. Buschbom and E. F. Blanton. 1979. "Initial Deposition and Early Clearance of Inhaled $^{239}Pu(NO_3)_4$ Aerosols in Beagle Dogs." Biomedical Sciences. Part 1 of Pacific Northwest Laboratory Annual Report for 1978 to the DOE Assistant Secretary for Environment. PNL-2850 PT1, Pacific Northwest Labortory, Richland, Washington.

BEST DOCUMENT AVAILABLE

BLANK PAGE

• Radiation Instrumentation—Radiological Chemistry

During the past year, major efforts in this program have concentrated on lowering the background for the measurement of small amounts of radioactivity by beta and gamma counting, on the design of specialized systems, on specific procedures for the measurement of certain radionuclides, on improved computer programs for the analysis of gamma-ray spectral data, and on the development of X-ray fluorescence techniques that permit concentrations to be measured without the weight of the sample being known.

APPLICATIONS TO ENVIRONMENTAL MEASUREMENTS OF A LOW-BACKGROUND HIGH-RESOLUTION INTRINSIC GERMANIUM DETECTOR

N. A. Wogman

Application of a new spectrometer (Wogman 1981a) is allowing environmental measurements at extremely low background levels. Originally the system was used to study the radioactivity present in radioanalytical detector construction materials such as titanium, aluminum, stainless steel, NaI(Tl) crystals, charcoal, MgO, $CaCO_3$, and quartz as well as components such as phototubes (Wogman 1980, 1981b). The data developed indicate that aluminum contains high concentrations of ^{232}Th, ^{238}U, and minimal quantities of ^{40}K. Concentrations are typically on the order of 0.1 disintegrations per minute per gram of sample (dpm/g) ^{232}Th, 0.02 dpm/g ^{238}U, and <0.4 dpm/g ^{40}K. Stainless steels are quite pure with respect to primordial radionuclides, yet they often contain ^{60}Co from use in steel furnace hearths. Molecular sieves contain 4 to 5 dpm/g of ^{232}Th, 4 to 5 dpm/g ^{238}U, and 9 dpm/g ^{40}K.

The new low-background spectrometer is presently being applied to problems in the energy generation and fuel extraction fields. It is being used to measure photons from plutonium, americium, and curium isotopes which are created in the nuclear fuel cycle. Additional radionuclides in the nuclear power industry which are being measured are: ^{22}Na, ^{144}Ce, ^{54}Mn, ^{110m}Ag, ^{152}Eu, ^{154}Eu, ^{155}Eu, ^{60}Co, ^{106}Ru, ^{137}Cs, ^{65}Zn, ^{134}Cs, and ^{125}Sb. It is also being used to determine the radionuclides in soils from low level waste sites. The type of data generated for soils collected at Beatty, Nevada is illustrated in Table 1. Some 24 radioisotopes are being studied at concentration levels of a few dpm/g of soil. Typically, radioisotopes of ^{137}Cs and ^{60}Co, as well as the primordial series, are measured.

The system is also applied to measurement problems associated with the mining and milling of uranium which require the analysis of ^{228}Ac, ^{226}Ra, ^{238}U, ^{230}Th, and ^{210}Pb.

Figure 1 shows the noncoincidence and coincidence spectra of deep ocean sea sediments. This material is being measured for its ^{7}Be, ^{137}Cs, and ^{40}K content to determine the deposition rate of material through the fallout radionuclide ^{137}Cs, the cosmogenically produced radionuclide ^{7}Be and the primordial radionuclide ^{40}K. The spectra show that the ^{137}Cs is completely separated along with ^{40}K and ^{7}Be in the noncoincident spectra. This makes the low level measurement quite simple. The new system is also being applied in studies of trace elements by activation analysis.

As part of an ongoing study of coal-fired power plants, we are engaged in chemical characterization studies to determine the fate of environmentally important trace constituents. To assess the fate of trace elements, we are applying multielement neutron activation analytical techniques to measure a large group of elements in coal, fly ash, bottom ash, and stack-emitted particulates. These data are combined with material flowrates to compute elemental mass balances for coal-fired power plant facilities.

Because of its sensitivity and multielement analysis capability, instrumental neutron activation analysis (INAA) is the preferred analytical technique for several target elements considered in the study. The application of neutron activation and a coincidence-noncoincidence Ge(Li)-NaI(Tl) detector system (Wogman 1981a) greatly enhances the sensitivity for many elements which are measured in the noncoincidence spectrum, such as barium, chromium, cesium, nickel, rubidium, selenium, strontium, titanium, vanadium, uranium, and zinc. Elemental assays for coal and by-product coal ashes as obtained by coincidence-noncoincidence gamma-ray spectroscopy are presented in Table 2.

BEST DOCUMENT AVAILABLE

TABLE 1. Soil Sample Analyses with Ge(Li) Coincidence/Anticoincidence Spectrometer

Beatty, Nevada, November 1979 and February 1980

Sample Location	Date Time Counted	Length of Count Minutes	(Concentrations in dpm/g)									
			^{110}Ag	^{228}Ac	^{241}Am	^{7}Be	^{214}Bi	^{144}Ce	^{57}Co	^{58}Co	^{60}Co	^{137}Cs
BKG No. 4	1534 02/04/80	950	< 0.098	3.68 ± 0.27	< 0.046	< 0.21	3.42 ± 0.32	< 0.14	< 0.014	< 0.023	< 0.039	0.081 ± 0.019
19	1029 02/02/80	1422	< 0.059	4.91 ± 0.19	< 0.065	< 0.22	< ± 0.21	< 0.12	< 0.016	< 0.017	0.791 ± 0.035	5.97 ± 0.06
29	1529 02/05/80	902	< 0.073	4.48 ± 0.24	< 0.0084	< 0.28	3.88 ± 0.28	< 0.15	< 0.019	< 0.020	0.059 ±0.026	3.60 ± 0.55
35	1053 02/03/80	1230	< 0.061	4.82 0.21	< 0.10	< 0.49	3.76 ± 0.23	< 0.20	< 0.027	< 0.019	0.099 ± 0.023	67.8 ± 0.2
37	1538 02/04/80	927	< 0.069	4.48 ± 0.23	< 0.094	< 0.43	3.55 ± 0.27	< 0.18	< 0.024	< 0.020	0.332 ± 0.033	33.7 ± 0.2
39	0749 02/06/80	405	< 0.12	5.59 ± 0.39	< 0.14	< 0.63	5.04 ± 0.51	< 0.27	< 0.035	< 0.036	0.224 ± 0.055	17.2 ± 0.2
43	1449 02/06/80	935	< 0.083	4.84 ± 0.24	< 0.10	< 0.33	4.22 ± 0.28	< 0.16	< 0.022	< 0.020	1.44 ± 0.06	12.2 ± 1.0
50-51	0845 02/04/80	387	< 0.11	4.01 ± 0.36	< 0.16	< 0.76	3.06 ± 0.47	< 0.30	< 0.043	< 0.034	0.422 ± 0.058	43.2 ± 0.3
59	0647 02/07/80	439	< 0.11	3.40 ± 0.31	< 0.12	< 0.42	2.98 ± 0.40	< 0.20	0.051 ± 0.027	< 0.030	< 0.039	0.251 ± 0.027
185E 1st	0745 02/05/80	444	< 0.10	3.88 ± 0.32	< 0.12	< 0.44	3.54 ± 0.41	< 0.20	< 0.027	< 0.030	< 0.041	0.458 ± 0.033
185E 2nd	0653 03/07/80	405	< 0.18	4.99 ± 0.46	< 0.080	< 0.67	4.10 ± 0.56	< 0.25	< 0.027	0.066 ± 0.050	0.234 ± 0.076	1.73 ± 0.08

^{155}Eu	^{40}K	^{54}Mn	^{22}Na	^{95}Nb	^{210}Pb	^{103}Ru	^{106}Ru	^{124}Sb	^{125}Sb	^{46}Sc	^{88}Y	^{65}Zn	^{95}Zr
< 0.050	81.5 ± 1.7	0.043 ± 0.014	< 0.044	0.038 ± 0.026	2.36 ± 0.45	< 0.035	< 0.15	0.29 ± 0.17	< 0.024	< 0.048	< 0.046	< 0.043	< 0.043
0.136 ± 0.057	84.9 ± 1.0	< 0.011	< 0.022	< 0.021	< 1.0	< 0.030	< 0.13	< 0.079	0.029 ±0.022	0.042 ±0.028	< 0.026	< 0.029	< 0.030
< 0.073	87.8 ± 1.3	< 0.014	< 0.029	< 0.027	< 1.3	< 0.040	< 0.17	< 0.12	< 0.026	< 0.033	< 0.033	< 0.039	< 0.040
< 0.10	87.8 ± 1.2	< 0.012	< 0.025	< 0.021	< 1.5	< 0.075	< 0.16	< 0.11	< 0.058	< 0.029	< 0.027	< 0.032	< 0.036
< 0.088	86.4 ± 1.3	0.023 ± 0.014	< 0.029	0.043 ± 0.026	< 1.5	< 0.068	< 0.16	< 0.10	< 0.041	< 0.033	< 0.032	< 0.040	< 0.038
< 0.13	101 ± 2	0.036 ± 0.024	< 0.049	< 0.045	< 2.6	< 0.089	< 0.28	< 0.23	0.074 ± 0.054	< 0.061	< 0.053	< 0.062	< 0.066
< 0.082	81.8 ± 1.2	< 0.016	< 0.28	< 0.024	< 1.7	< 0.048	0.25 ± 0.17	< 0.13	< 0.032	< 0.040	< 0.036	< 0.040	< 0.041
< 0.15	80.0 ± 1.9	< 0.028	< 0.047	< 0.040	< 2.8	< 0.11	< 0.28	< 0.20	< 0.072	< 0.055	< 0.054	< 0.072	< 0.068
< 0.10	80.3 ± 1.8	< 0.019	< 0.041	0.051 ± 0.036	< 2.3	< 0.053	< 0.26	< 0.19	0.075 ± 0.033	0.106 ± 0.053	< 0.044	< 0.061	< 0.061
< 0.10	76.4 ± 1.8	< 0.022	< 0.039	< 0.039	< 2.1	< 0.051	< 0.25	< 0.19	< 0.034	< 0.060	< 0.049	< 0.056	< 0.065
< 0.091	84.0 ± 2.8	< 0.033	< 0.074	< 0.072	1.41 ± 0.80	< 0.11	< 0.27	0.69 ± 0.51	< 0.046	< 0.12	< 0.11	< 0.097	< 0.11

BEST DOCUMENT AVAILABLE

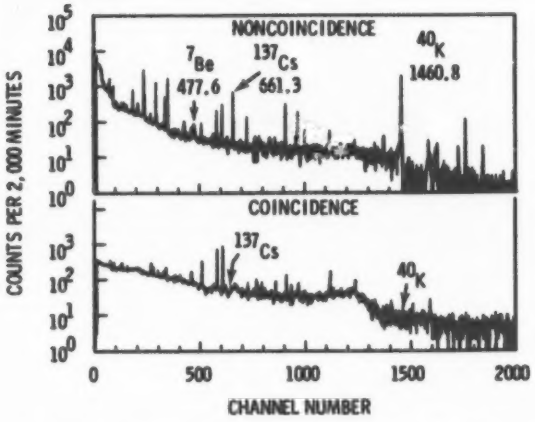

FIGURE 1. Coincidence and Noncoincidence Spectra of 120 Grams of Sea Sediment

REFERENCES

Wogman, N. A. 1981a. "Design and Environmental Applications of an Ultra-Low Background, High Efficiency Intrinsic Ge Gamma-Ray Spectrometer." In Proceedings of International Symposium on Methods of Low-Level Counting and Spectrometry, IAEA-SM-252/25, Berlin, West Germany.

Wogman, N. A. 1981b. "Natural Contamination in Radionuclide Detection Systems." Physical Sciences. Part 4 of Pacific Northwest Laboratory Annual Report for 1980 to the DOE Assistant Secretary of Environment. PNL-3700 PT 4, Pacific Northwest Laboratory, Richland, Washington.

Wogman, N. A. 1980. "Natural Contamination in Radionuclide Detection Systems." In Proceedings of IEEE Meeting. PNL-8989, November 1980, Orlando, Florida.

TABLE 2. Selected Elemental Abundances in Coal and Coal Ashes as Determined by Neutron Activation and Coincidence-Noncoincidence Gamma-Ray Spectroscopy

	(values in μg/g unless noted)			
Element	Sub-Bituminous Feed Coal	Bottom Ash	Fly Ash	Emitted Stack Particulates
Al(%)	1.21 ± 0.02	9.41 ± 0.10	11.36 ± 0.07	—
Ti(%)	0.032 ± 0.007	—	—	—
V	4.1 ± 0.8	33 ± 6	48 ± 7	—
Cr	23.2 ± 0.6	35.2 ± 0.8	34.5 ± 0.7	3610 ± 91
Mn	43 ± 2	340 ± 30	298 ± 28	—
Co	1.03 ± 0.05	4.2 ± 0.1	6.8 ± 0.1	48 ± 3
Ni	<11	—	—	2190 ± 140
Zn	7.6 ± 1.0	12 ± 4	71 ± 5	1650 ± 230
Se	1.1 ± 0.2	3.4 ± 0.6	11.3 ± 0.7	160 ± 14
As	1.28 ± 0.04	3.4 ± 0.4	20 ± 1	83 ± 1.4
Rb	5 ± 1	26 ± 2	26 ± 2	46 ± 14
Sr	390 ± 40	2670 ± 90	3300 ± 100	2900 ± 300
Cs	0.39 ± 0.12	1.5 ± 0.2	1.8 ± 0.1	2.5 ± 0.6
Ba	626 ± 36	4000 ± 300	5800 ± 300	12,800 ± 900
Ge	13.2 ± 0.3	100 ± 2	114 ± 2	101 ± 4.6
Th	2.80 ± 0.06	24 ± 1	28 ± 1	26 ± 1.4
U	0.98 ± 0.06	8.4 ± 0.6	10.8 ± 0.7	9.1 ± 0.9

BEST DOCUMENT AVAILABLE

SENSITIVITY COMPARISON OF NaI(Tl) AND GERMANIUM GAMMA-RAY SPECTROMETERS FOR DETECTING RADIONUCLIDES IN ENVIRONMENTAL SAMPLES

N. A. Wogman

Environmental studies require the measurement of a variety of radioisotopes emitting gamma rays which are emitted singly, in multiples, or in coincidence. These decay characteristics dictate the measurement techniques which must be used for the various research studies. The concentrations of the radionuclides in these samples are generally quite low, requiring the use of low-level radionuclide detection systems. The normal objectives of the analyses are to obtain rapidly, economically, and with minimal effort, accurate measurements of the concentrations of the radionuclides in the samples. These objectives can be realized by using low background, high sensitivity gamma-ray spectrometers which are, in general, anticoincidence-shielded, high-resolution systems.

New designs for gamma-ray spectrometer systems use low background construction materials (Wogman 1981a; Wogman and Laul 1981) and construction designs that achieve maximum coincidence detection of photons and contribute minimal background. Table 1 illustrates the radionuclides that typically are measured by low background spectrometers in environmental samples and their associated analytical sensitivities. The radioisotopes listed were measured with multidimensional gamma-ray spectrometers (Wogman and Brodzinski 1979), anticoincidence shielded germanium spectrometers (Wogman 1981b), and planar germanium spectrometers.

The multidimensional gamma-ray spectrometer system (Wogman and Brodzinski 1979) employs, as principal detectors, two 23-cm diameter by 20-cm thick NaI(Tl) activated crystals. These detectors are housed inside an anticoincidence shield made of NaI(Tl) material. The detector system is coupled to a computer memory and uses the gamma-ray decay characteristics of each radionuclide for its identification and measurement. The anticoincidence shielded germanium spectrometer (Wogman 1981b) incorporates a 25% efficient, high resolution, coaxial diode inside a 30-cm diameter NaI(Tl) shield. The system design provides a peak-to-Compton ratio greater than 1000 to 1 for ^{137}Cs. By use of these systems, sensitivities on the order of a few counts per thousand minutes are obtained. By combining beta proportional counting with the multidimensional gamma-ray spectrometers, lower backgrounds and higher sensitivities can be achieved than

TABLE 1. Radionuclides Measured in Environmental Samples

Radioisotope	Sensitivity[a] MDGRS[b]	GE(A.C.)[c]
^{7}Be		2.7
^{22}Na	0.06	
^{26}Al	0.05	
^{40}K	4.6	
^{46}Sc	0.06	
^{54}Mn		0.4
^{55}Fe		3.1[c]
^{57}Co		0.17
^{58}Co	0.1	
^{60}Co	0.07	
^{65}Zn		0.9
^{88}Y	0.07	
^{95}Zr		0.7
^{95}Nb		0.3
^{94}Mo		0.2
^{103}Ru		0.3
^{106}Ru	0.4	
^{110m}Ag	0.08	
^{124}Sb	0.09	
^{125}Sb		0.8
^{131}I		0.3
^{132}Te	0.1	
^{134}Cs	0.07	
^{136}Cs	0.08	
^{137}Cs		0.4
^{140}Ba	0.09	
^{141}Ce		0.3
^{144}Ce		1.3
^{147}Nd		1.6
^{155}Eu		0.6
^{210}Pb		9.4
^{226}Ra	0.07	
^{239}Np		1.9
^{232}Th	0.2	
^{238}U	0.4	

(a) Sensitivities at the 95% confidence level based on 100 g samples or on the sampling of 10^6 SCF of air, using analysis times of 1000 min.
(b) Multidimensional gamma-ray spectrometer.
(c) An anticoincidence shielded intrinsic germanium [or Ge(Li)] gamma-ray spectrometer.

are available with either system independently. For example, ^{106}Rh (daughter of long-lived ^{106}Ru) is normally analyzed through its coincident 0.51 to 0.62 MeV gamma-ray cascade. The large NaI(Tl) detectors used to measure low-level activities in large samples cannot adequately resolve this peak from that of positron annihilation, 0.51 to 0.51 MeV. The beta-gamma-gamma spectrometer which provides separate beta-gamma-gamma, beta-gamma, gamma-gamma,

BEST DOCUMENT AVAILABLE

and gamma spectra effectively removes many interfering gamma rays from the spectrum, permitting a more sensitive analysis of ^{106}Rh.

The detection sensitivities for radionuclides measured in environmental samples listed in Table 1 illustrate that most radioisotopes can be detected at the subdisintegration per minute per sample level. In general, the anticoincidence shielded germanium systems are superior for radioisotopes emitting single photons, while the multidimensional gamma-ray spectrometer systems are superior for radioisotopes emitting coincident photons.

REFERENCES

Wogman, N. A. 1981a. "Natural Contamination in Radionuclide Detection Systems." IEEE Transactions on Nuclear Science, Vol. NS-28, No. 1.

Wogman, N. A. and J. C. Laul. 1981. "Natural Contamination in Radionuclide Detection Systems." In Proceedings of Second Symposium on Natural Radiation Environment, Bombay, India.

Wogman, N. A. and R. L. Brodzinski. 1979. "The Development and Application of a Beta-Gamma-Gamma Multidimensional Spectrometer." Nuclear Instruments and Methods 109:277-283.

Wogman, N. A. 1981b. "Design and Environmental Applications of an Ultra-Low Background, High Efficiency Intrinsic Germanium Gamma-Ray Spectrometer." In Proceedings of the International Symposium on Methods of Low Level Counting and Spectrometry, IAEA-SM-252/25, Berlin, West Germany.

ALPHA PARTICLE DETECTION USING ALPHA ETCHING TECHNIQUES

C. W. Thomas

A detector was designed using alpha particle track etching techniques on LR-115-type 2 Kodak Pathé cellulose nitrate film. This detector measures radon progeny concentrations in air down to the 0.01 working level and integrates these concentrations over long time periods. Initial track etching tests showed that hole sizes produced from the interaction of alpha particles and the cellulose nitrate film were about the same size for particles with incident angles to the film of ~60° to 90°; also tests showed that alpha particles with energies of 1.5 to 4.0 MeV produced holes of comparable size. Alpha particles with energies less than 1.5 MeV or greater than 4.0 MeV produced holes of very small diameter. It was, therefore, concluded that the film holder design should allow only alpha particles with incident angles to the film greater than ~60°; radon progeny alpha particles with residual energies of 1.5 MeV to 4.0 MeV would thus generate the same hole size. For alpha particle energies from ^{222}Rn (5.5 MeV) and ^{218}Po (6.0 MeV), residual energies of this magnitude would impact the film if the alpha particles pass through an air column of 1.5 to 3.3 cm to reach the film. For the more energetic radium C' (^{218}Po, α = 7.7 MeV), the air absorption path to slow the α to 1.5 to 4.0 MeV would be from 3.0 cm to 5.0 cm.

Figure 1 shows the hole sizes obtained from a 5.50 MeV alpha particle passing through 2.5 cm of air to reach the film surface. Figure 2 shows the newly developed radon progeny exposure detector. LR-115 film is positioned in the mouth of the funnel-shaped detector; the sides are covered with aluminum foil. During exposure, the detector holder entrance is covered with a porous filter. Under these conditions, the ^{222}Rn and daughter products through radium C' (^{218}Po, ^{214}Pb, ^{214}Bi, ^{214}Po) should be near equilibrium over long exposure periods.

FIGURE 1. Holes Produced in LR-115 Film from 5.5 MeV Alpha Particles Passing Through 2.5 cm of Air to Reach the Film Surface

BEST DOCUMENT AVAILABLE

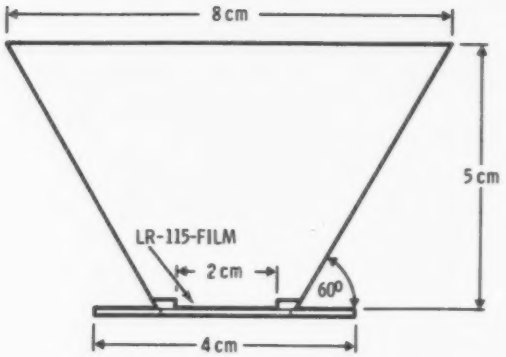

FIGURE 2. Exposure Holder for LR-115 Film Used in Alpha Etching

Etching of the LR-115 cellulose nitrate film with NaOH is the process used to develop holes. When alpha particles penetrate the 12-micron thick cellulose nitrate layer on the LR-115 film, structural damage to the cellulose nitrate occurs. When the film is in contact with a heated sodium hydroxide solution, the film is etched, producing a measurable hole. Varying the sodium hydroxide concentration, the temperature, and the etching time affects the size of the hole. During etching, all surfaces are etched including the microscopic hole produced by the alpha particle damage. If 2 microns of the overall surface are removed, then the hole will etch 2 microns in all directions, resulting in a 4-micron hole. If etching occurs for too long, background holes are produced. Studies have shown that very distinct holes are produced in the film when it is etched with 6.25 molar sodium hydroxide at 55°C for 3.5 to 4.0 hr. Under these conditions, few, if any, background holes are produced.

AN ANALYTICAL METHOD FOR MEASUREMENT OF ^{226}Ra USING ALPHA ENERGY ANALYSIS

C. W. Thomas

An analytical procedure to measure ^{226}Ra has been developed so that it can be used to age-date salt dome core samples. The procedure uses 100-gram sample sizes and traces the ^{226}Ra using both ^{224}Ra and ^{133}Ba. In the procedure, radium and the other alkaline earth metals are carried on a precipitate of calcium ammonium phosphate from a solution of pH = 9. The precipitate is dissolved in nitric acid and the alkaline earth metals are then carried on a fuming nitric acid precipitate. The alkaline earth nitrates are dissolved in water and loaded on a Dowex-50 column (100–200 mesh) that has been equilibrated with 2 molar ammonium hydroxide and washed thoroughly with water. The alkaline earths are sequentially removed, as shown in Figure 1, by eluting with 5×10^{-3} molar (ethylene diamine tetraacetate, sodium form) whose pH has been adjusted to 7.8 by using ammonium hydroxide. The alkaline earths were traced by using ^{45}Ca, ^{85}Sr, ^{133}Ba, and ^{228}Ra. As shown in Figure 1, the calcium elutes immediately, followed by strontium and barium. Radium does not elute under these conditions. The column containing the radium is washed thoroughly with water and then washed with a solution of 60% ethanol and 1 molar HCl to remove large amounts of EDTA that remain. Radium is removed using 8 molar HCl. The radium-containing solution is evaporated to dryness and the radium is dissolved with nitric acid at pH = 2. This solution is set aside while the plating dish using barium sulfate is prepared.

A 100 µg precipitate of barium sulfate is coated onto a stainless steel dish by placing it on a hot ring evaporating plate, directly adding 100 µg of barium carrier and 200 µg of sulfuric acid followed by evaporation to dryness. The solution containing the radium is then piped directly on the barium sulfate coated dish using a contact time of 30 minutes. During this time, radium is absorbed onto the barium sulfate precipitate. The solution is then removed from

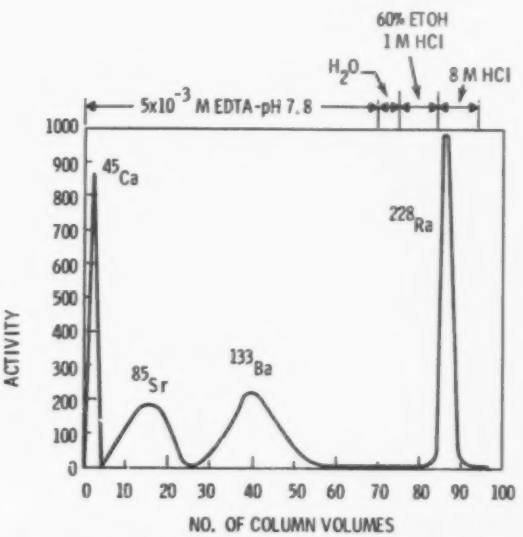

FIGURE 1. Alkaline Earths Elution Using EDTA, H_2O, and Ethanol-HCl Solution

BEST DOCUMENT

the dish, the dish is dried, and the coprecipitated radium measured using alpha energy spectrometry.

Radiochemical yields, determined by measuring the ^{224}Ra, range from 50% to 70% for the salt dome core samples. Eight samples per week can be chemically analyzed. Detection limits for measurements made using the alpha energy spectrometer are 0.08 d/m of ^{226}Ra per sample.

IN-SITU SUBTERRANEAN DETERMINATION OF ACTINIDES BY HIGH-RESOLUTION GAMMA-RAY SPECTROMETRY

R. L. Brodzinski

Actinide elements have been released, either directly or inadvertently, into isolated subterranean environments during waste disposal operations associated with nuclear fuels reprocessing and fabrication of weapons. To make meaningful waste management decisions regarding additional releases, decommissioning of existing facilities, or remedial action if required, the identities, concentrations, distributions, and rates of migration of these isotopes need to be measured.

Normally, determination of actinide isotopes by gamma-ray spectrometry is not considered a viable option due to the ubiquitously low branching fractions for high-energy photon emissions. However, successful application of high-resolution gamma-ray spectrometry to in situ characterization of subterranean fission product concentrations (Nielson, Wogman and Brodzinski 1977), uranium ore explorations (Brodzinski and Wogman 1976), and in situ determination of ^{90}Sr by bremsstrahlung analysis (Brodzinski and Nielson) inspired application of the technique to in situ actinide determinations.

The detector used for these experiments was a 108 cm^3 closed ended coaxial intrinsic germanium diode having a full-width-at-half-maximum resolution of 1.83 keV at 1332 keV. The crystal is housed in a 7.30-cm outside diameter stainless steel canister which also contains the necessary signal processing electronics and a spillproof liquid nitrogen cryostat providing a 12-hr holding time. The canister has a 2.54-cm screw stud at the diode end to which 14-cm ouside diameter lead collimators or shields can be attached for the purpose of selecting quantities of gamma radiation or solid angles of interrogation. Collimators provide resolution of horizontal strata as thin as 1 cm or angular resolution as small as 0.1 steradians. Colored lights are located on the top perimeter of the canister for visual observation of the rotational orientation of the system when used with directional collimators.

The detector was calibrated in a large facility filled with sand having a bulk density of 1.37 and homogeneously spiked with known quantities of plutonium and americium isotopes in two separate sectors approximately a factor of 10 apart in concentration.

This technology is capable of simultaneously measuring the concentration of the six actinide isotopes, ^{235}U, ^{238}U, ^{237}Np, ^{239}Pu, ^{241}Pu, and ^{241}Am, at levels as low as 10 nCi g^{-1} in less than 7 min. In fact, except for ^{241}Pu, the measurement can be made in less than 15 sec. In addition to the above actinide isotopes, characteristic photons from the progeny of primordial thorium and uranium are observed in each spectrum. These isotopes, along with the readily identifiable primordial ^{40}K, are useful for providing a check on the operation and reliability of the equipment as well as identifying changes in sediment configuration or composition, such as void areas, foreign cobble, or lithologic changes. Measurement of a long-term secular equilibrium progeny (e.g., $^{241}Bi/^{238}U$) and a short-term transient equilibrium daughter (e.g., $^{234m}Pa/^{238}U$) allows both the primordial concentration and the introduced concentration of a single isotope to be determined.

Actual detection limits at the 90% confidence level for each actinide, based on field data taken from inside a steel well casing with a 7.1 mm thick wall, are illustrated in Figure 1 as a function of counting time. Even greater sensitivity is possible for measurements made in boreholes or wells cased with thin-wall or plastic pipe.

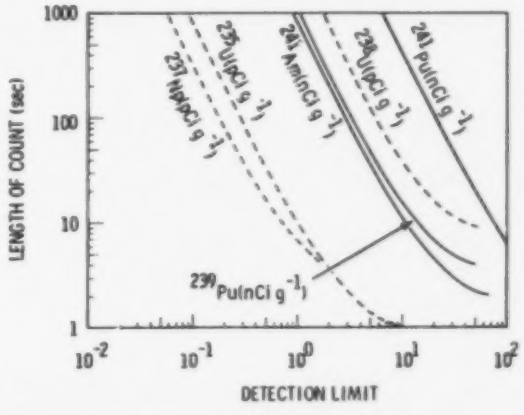

FIGURE 1. Detection Limits for In-Situ Determination of Actinides in Subterranean Environments Using High Resolution Gamma-Ray Spectroscopy

REFERENCES

Brodzinski, R. L. and N. A. Wogman. 1976. "Exploration of Uranium Ore Deposits." In Proceedings of IAEA Symposium, Vienna, p. 757, STI/Pub/434.

Brodzinski, R. L. and H. L. Nielson. 1980. "A Well Logging Technique for the In Situ Determination of ^{90}Sr." Nucl. Instr. and Methods 173:299.

Nielson, H. L., N. A. Wogman and R. L. Brodzinski. 1977. "In-Situ Subterranean Gamma-Ray Spectroscopy. Nucl. Instr. and Methods 143:385.

PROPOSED ULTRASENSITIVE INVESTIGATION OF NEUTRINOLESS AND TWO-NEUTRINO DOUBLE BETA DECAY OF ^{76}Ge*

N. A. Wogman, R. L. Brodzinski and F. T. Avignone, III**

Until recently, neither two-neutrino nor zero-neutrino double beta decay had been observed in a direct experiment. Recently, however, the direct observation of the double beta decay of ^{82}Se was reported by Moe and Lowenthal (1979), and the tota] half-life reported was $(1.0 \pm 0.4) \times 10^{19}$ yr. Previously indirect evidence existed of double beta decay from geological experiments (Hennecke 1978). Neither geological experiments nor poor energy resolution direct measurements give strong evidence concerning neutrinoless double beta decay nor can they place sensitive limits on its half-life.

Most attempts to observe double beta decay have been made using detectors of poor energy resolution; however, one high resolution attempt was reported in 1973 by Fiorini and his coworkers (Fiorini et al. 1973), and was an attempt to observe the full decay-energy peak in the hypothesized double beta decay of ^{76}Ge, which is calculated from the measured mass excess to lie at 2.045 ± 0.003 MeV. The source was the 7.7% abundant ^{76}Ge in a Ge(Li) detector with an active volume of 68.5 cm^3. The detector was placed in a graded shield; distilled mercury, nylon, copper, and lead surrounded the paraffin which was located in a tunnel under Mount Blanc. The result revealed that the half-life for the neutrinoless double beta decay is greater than 5×10^{21} yr, which has a reported value of the lepton-nonconserving parameter $\eta = 10^{-3 \pm 1}$.

Using an existing low-background gamma-ray spectrometer composed of a NaI(Tl) anticoincidence shield, a 28% efficient detector, and no preliminary precautions on radiopurity, we obtained only 102 counts in 40 days in the 11 keV region about 2.045 MeV. This corresponds to a limit $T_{1/2}(0\nu) > 2.3 \times 10^{21}$ yr which is lower than the present limit of 5×10^{21} yr.

Since this first experiment, we have learned that almost all of the background observed in germanium detectors comes from within the cryostat, but that virtually none comes from the diode itself. We have conducted a completely new set of Monte Carlo calculations which account for the coincidence relationships between the observed gamma rays in the background. These data have allowed a new gamma-ray system to be designed. Basically, the new system consists of a large high-resolution intrinsic germanium diode inside of a large NaI(Tl) anticoincidence annulus as shown in Figure 1.

All materials will be precounted in existing high-sensitivity multidimensional gamma-ray

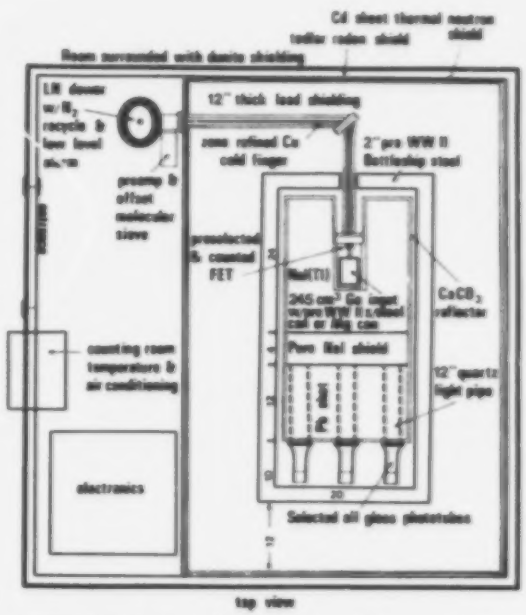

FIGURE 1. Proposed Low Background Gamma-Ray Spectrometer for Investigating Neutrinoless and Two-Neutrino Double Beta Decay of ^{76}Ge

---

* Direct funding of the gamma-ray spectrometer designed for this basic physics experiment has been requested from Basic Energy Sciences, DOE.

** University of South Carolina, Columbia, SC 29209.

BEST DOCUMENT AVAILABLE

spectrometers to insure radiopurity. The preamplifier will be located external to the lead cave because it is a known source of radioactivity. Similarly, the liquid nitrogen cryostat is removed from the line-of-sight of the detector, and the selection and location of molecular sieve material are being chosen to reduce radiation incident on the germanium diode. All connections and wires will be fabricated from 99.9999% pure silver. The NaI(Tl) anticoincidence shield will also be fabricated from precounted "clean" materials. Only four photomultiplier tubes will be used on the annulus since these tubes are the single largest source of radioactivity in the system. Pure NaI, quartz, and lead will be used to shield the system from the phototubes. The internal reflector around the NaI(Tl) crystal will be $CaCO_3$ instead of MgO, because of higher radiopurity. All metals will be preselected pre-World War II battleship steel or stainless steel to avoid the radioactivities ubiquitously present in modern steels. The cave will consist of 12 in. of clean pure virgin lead and 2 in. of battleship steel. A cadmium sheet will surround the lead cave to absorb thermal neutrons generated by the spontaneous fission of natural uranium in the surrounding strata. A Tedlar sheet will seal the entire cave and detector system to prevent the intrusion of radon gas.

It is also necessary to eliminate the cosmic rays with a large earthen overburden. Thus the plan is to locate the system in a mine at depths of 7000 ft. To provide the necessary environment for the electronics, the counting system will be housed in a small room constructed from low background battleship steel and fitted with an air conditioner. The steel room will be further shielded from primordial radioactivities in the mine walls by a barrier of low background dunite. A new technical breakthrough in the growing of large single germanium crystals will make cylindrical detectors of 3 in. diameter by 3 in. long readily available. The new system should place a new lower limit of up to $t_{1/2} = 5 \times 10^{23}$ yr with reasonable probability. The (0ν-$\beta\beta$) decay of ^{76}Ge would then be directly observable.

REFERENCES

Moe, M. K. and D. D. Lowenthal. 1979. "An Experimental Investigation of the Double Beta Decay of ^{82}Se." University of California, Irvine Report UCI-10P19-143.

Hennecke, E. W. 1978. "Additional Evidence of Beta Beta Decay of ^{128}Te." Phys. Rev. C17:1168. (Also see references given in the review by D. Bryman and C. Picciotto, Rev. Mod. Phys. 50:11.)

Fiorini, E., A. Pullia, G. Bertolini, F. Cappellani and G. Restelli. 1973. "Neutrinoless Double Beta Decay of ^{79}Ge." II Nuovo Cimento 13:747.

AN ANTICOINCIDENCE SHIELDED WINDOWLESS GAS-FLOW PROPORTIONAL BETA COUNTER

C. W. Thomas

A windowless, 2 pi counter made from thin-wall plastic material was constructed in 1980 (Thomas and Lepel 1980). This counter was designed to measure radionuclides emitting soft beta particles and/or weak x-rays. The counter showed excellent response for the measurement of ^{63}Ni beta particles and ^{59}Ni and ^{55}Fe x-rays, but had background counting rates of up to 16 counts per minute. To reduce the background, the windowless counter was positioned between two 9 in. diameter by 4 in. thick NaI(Tl) detectors which in turn were surrounded by two 36 in. diameter by 18 in. thick plastic phosphor annuli. The counter and these large anticoincidence shields are shown in Figure 1. A block diagram of the signal routing of the NaI(Tl) shield, the plastic phosphor shield, and the primary detector is shown in Figure 2. To suppress the background counting rate, the signals from the upper and lower NaI(Tl) detectors are coupled, as are the signals from the plastic phosphors. These signals are shaped, delayed, and fed into a universal coincident/anticoincident module. The signal from the beta detector is also delayed and fed into the module. If no signal occurs in either of the shields, the beta detector signal is allowed to scale. If either shield sees a signal, a blocking pulse eliminates scaling of the beta signal and also turns off the timing circuit. Under these conditions, the background counting rates for the gas-flow beta detector were reduced from 16 counts per minute with no shield to 0.4 counts per minute with the full shield. In addition to suppressing the background, the shielding system also allows the beta detector to measure single beta events in the presence of gamma-emitting radioisotopes.

BEST DOCUMENT AVAILABLE

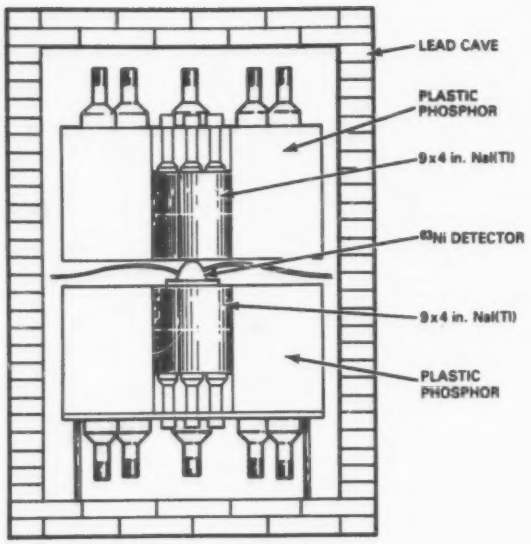

FIGURE 1. An Anticoincidence Shielded ^{63}Ni Windowless Gas-Flow Proportional Beta Detector

REFERENCE

Thomas, C. W. and E. A. Lepel. "A Windowless Gas-Flow Proportional Beta Counter for Measuring ^{63}Ni and ^{59}Ni." Physical Sciences. Part 4 of Pacific Northwest Laboratory Annual Report for 1980 to the DOE Assistant Secretary for Environment. PNL-3700 PT4, Pacific Northwest Laboratory, Richland, Washington.

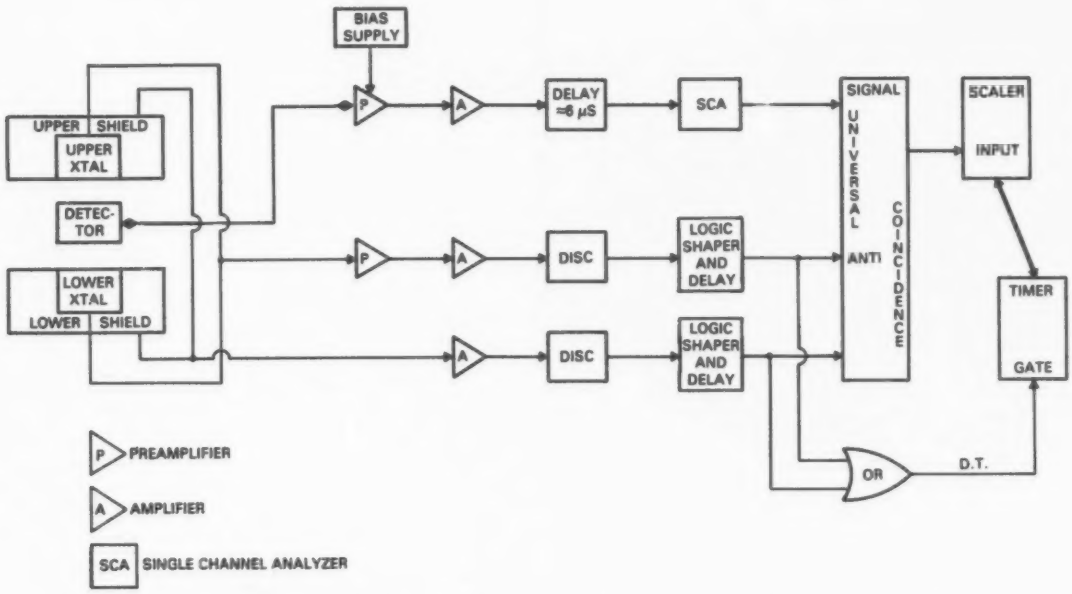

FIGURE 2. A Block Diagram Showing Signal Routing from Beta Detector, NaI(Tl) Shield, and Plastic Phosphor

BEST DOCUMENT AVAILABLE

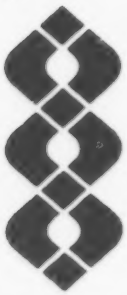

Oil Shale

BLANK PAGE

• Oil Shale and Tar Sands Research

Oil shale and tar sand in the United States represent a potential supply of nearly one trillion barrels of crude oil. The renewed commercial interest in developing these reserves has increased the need for studies that would help developers assure that conversion processes are environmentally acceptable. A vital part of this environmental research program is the physical and chemical characterization of the effluents from the various proposed conversion schemes. Characterization studies are important and should begin at an early stage of development, preferably at the pilot-plant or semiworks stage. The complex nature of the effluents has required the development of new procedures for sampling, analyzing, and chemically separating them. In this section, new and improved techniques for organic, inorganic, and speciation analysis are presented with applications for oil shale research. Also reported is the progress of a program to provide representative and well-characterized fossil-fuel samples for environmental and health effects studies and for interlaboratory comparisons to ensure accuracy of the data.

ORGANIC AND MUTAGENIC PROPERTIES OF OIL SHALE RETORT WATERS

A. P. Toste, R. A. Pelroy, R. B. Myers, and D. L. Stewart

Considerable technological research is currently underway to develop a shale oil industry in the United States. Concern about the potential health and environmental impacts of a shale oil industry has, in turn, prompted considerable biomedical and environmental research, much of it directed at chemically and biologically evaluating the genotoxicity/carcinogenicity of the oils and the associated retort waters which come into contact with the oils. The primary goal of this study was to examine the organic and mutagenic properties of retort waters from various retorting technologies: Paraho, aboveground retort; Occidental, modified in situ retort (vertical); and Vernal, true in situ retort (horizontal).

A second goal of this study was to develop and test a method of extracting and chemically fractionating the organic species of the oil shale retort waters. Three extraction methods were tested: (1) solvent extraction with pH adjustment; (2) XAD-4 partition chromatography; and (3) C_{18}-partition chromatography. Each method was evaluated both chemically and biologically. On the basis of high-performance liquid chromatography (HPLC) and the Ames mutagenesis assay, C_{18}-partition chromatography proved to be the method of choice. The concentration of the C_{18}-extractable organics, or hydrophobic organic fraction, for the various retort waters ranged from 1 to 30 mg/mℓ, corresponding to 31% to 70% of the total organic carbon of the retort water (Table 1).

TABLE 1. Organics in Oil Shale Retort Waters

Retort Water	Organic[a] Fraction (mg/ml)	Total Organic Carbon (mg/ml)	pH
Paraho	29.85 ± 0.08	42.75	8.4
Paraho (Condensate)	1.28 ± 0.13	4.08	8.7
Occidental	1.47 ± 0.01	4.23	8.9
Vernal	1.02 ± 0.15	2.93	8.5

[a]Extractable by C_{18} partition chromatography with MeOH elution.

The hydrophobic organic fraction of each retort water was subsequently fractionated on the basis of polarity by normal phase HPLC using an NH_2-column and a three-solvent linear-gradient mobile phase system: hexane followed by methylene chloride, followed in turn by isopropanol. Organic species in the hydrophobic organic fractions generally chromatographed in three distinct regions: nonpolar, moderately polar, and polar. Standards like polyaromatic hydrocarbons and nonpolar heterocyclics eluted in the nonpolar region; amines and N-heterocyclics eluted in the moderately polar region; and phenol and mixed-function heterocyclics, e.g., aminopyridinol, eluted in the polar region. An important feature of this chromatographic fractionation is that there appears to be an appreciable separation of nonmutagenic phenolic-type compounds from mutagenically active aromatic amines. Phenolic-type compounds are generally major constituents of synfuel samples, whereas

BEST DOCUMENT AVAILABLE

primary aromatic amines are minor constituents. Each HPLC fraction, as well as the waters' hydrophobic organic fraction, was analyzed: (1) chemically, using combined gas chromatography-mass spectrometry (GC-MS); and (2) biologically, using the standard Ames mutagenesis assay with Salmonella typhimurium TA98 and S9 as a metabolic activator.

On the basis of the HPLC fractionation, most of the species in the hydrophobic organic fraction of each retort water chromatographed in the polar HPLC region but some species chromatographed in the moderately polar HPLC region (Figure 1). The organic content of the various samples appeared to be quite heterogeneous. Gas chromatographic-mass spectrometric analyses of the HPLC fractions of the oil shale retort waters revealed that the moderately polar HPLC region contained mainly nitrogenous compounds; e.g., alkylated pyrroles and pyridines. The polar HPLC region mainly contained oxygenated and mixed-function compounds, e.g., carboxylic acids.

The mutagenic activity of each retort water was confined to its hydrophobic organic fraction. The activities ranged from 0.02 to 1.29 rev/μg. No mutagenic activity was detected in the complementary hydrophilic, or aqueous, fraction. After HPLC fractionation of the hydrophobic organic fraction, virtually all of the mutagenic activity was concentrated in the polar HPLC region. The mutagens of a Paraho retort water appeared to be more heterogeneous than those of a Paraho condensate water; the mutagens of Occidental and Vernal retort waters appeared to be less heterogeneous.

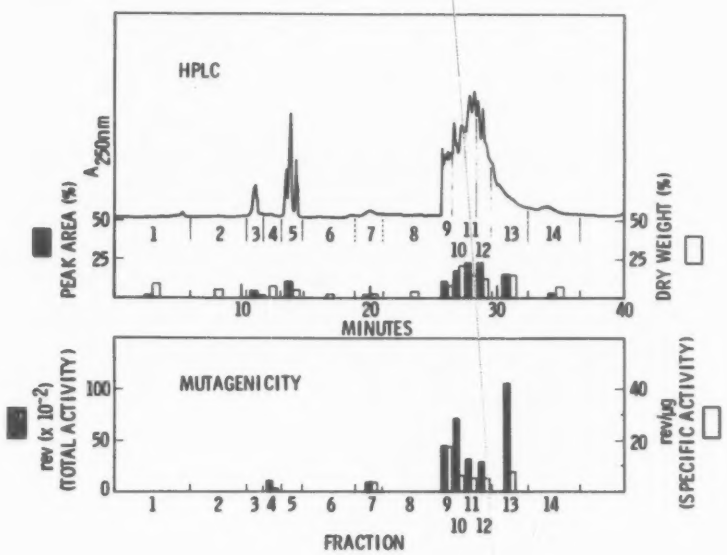

FIGURE 1. HPLC of Hydrophobic Organic Fraction from Paraho Storage Retort Water

BEST DOCUMENT AVAILABLE

POLAR ORGANICS IN SHALE OILS

D. S. Sklarew, R. A. Pelroy, A. P. Toste,
D. M. Schoengold, R. Pahl, S. P. Downey

The basic objective of this program is to identify potential environmental pollutants resulting from production of shale oils. Emphasis has been placed on the polar components of a shale oil for two reasons: (1) the polar components have been shown to be most mutagenic in the standard Ames mutagenicity assay (Pelroy, Sklarew and Downey 1981) and (2) the polar components are most likely to be leached by groundwater or runoff in the event of a spill.

The polar components of the Paraho shale oil have been isolated by a two-stage fractionation procedure. In the first stage, partition chromatography on Sephadex LH-20 was used to separate the crude oils into nonpolar hexane, moderately polar 10% toluene/hexane, and polar methanol fractions. The methanol fraction comprises ~3 wt% of the whole shale oil material but shows 90 to 100% of the mutagenic activity in the Ames assay with Salmonella typhimurium TA98.

In the second stage the polar methanol fraction was further fractionated on a semipreparative amine high-performance liquid chromatography (HPLC) column and an elution gradient with hexane, methylene chloride, and isopropanol. The activity of the Paraho methanol fraction appears to be attributable to several types of components as seen by the wide distribution of mutagens in both moderately polar (Fractions 3 and 4) and strongly polar (Fractions 7 and 8) HPLC subfractions (Figure 1).

Chemical characterization of a number of these fractions has been undertaken. Fractions 3 through 6 have been analyzed by gas chromatography-mass spectrometry (GC-MS) using a fused silica capillary SE-52 column in splitless mode. Fraction 3 contains indole, C_{-1} to C_{-5} alkylindoles, carbazole, C_{-1} to C_{-4} alkylcarbazoles, alkylpyridines, minor alkylquinolines, naphthol, and minor phenols.

Fraction 3 has also been analyzed by the more sensitive technique of single ion monitoring GC-MS. Using this method, the aminonaphthalenes have been detected. However, primary aromatic amines of higher molecular weight are below our detection limits. In Fraction 5, phenols and naphthols predominate. Series of C_1- through C_7-alkylphenols and C_1- to C_2-alkylnaphthols are present.

The highly polar fraction (equivalent to Fraction 7), which contains a large proportion of the total activity, has been analyzed by selective detector GC as well as GC-MS. Two closely matched 30 m fused

Figure 1

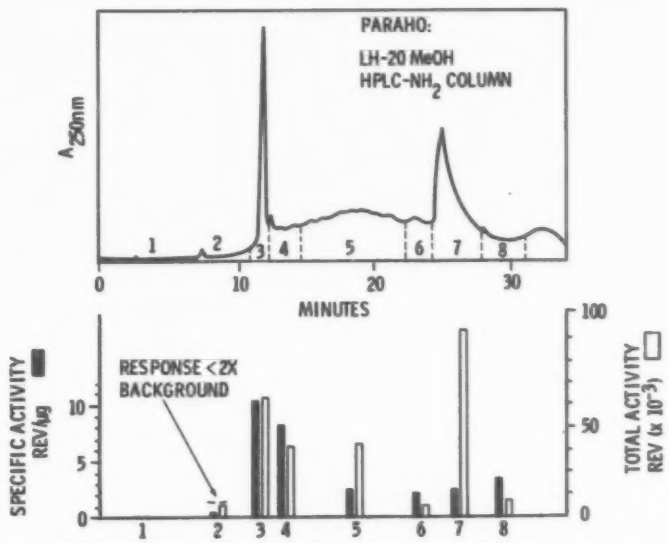

FIGURE 1. Specific and Total Mutagenic Activity of HPLC Fractions from Paraho LH-20 Methanol Against *Salmonella typhimurium* TA 98

BEST DOCUMENT AVAILABLE

silica Carbowax columns were inserted into the same injection port; one was connected to a flame ionization detector (FID), the other to a nitrogen-phosphorus detector (NPD). A large number of nitrogen-containing peaks were present (Figure 2). GC-MS analysis in electron impact and methane chemical ionization modes further substantiated the presence of a large number of nitrogen-containing components. Tentative identifications have been made on the basis of the mass spectral data; in some cases identifications were confirmed by GC retention data. In addition, methylated or silylated derivatives of this sample have been used to aid in identification. Compounds present in this fraction include C_2- through C_{24}-carboxylic acids, C_1- through C_7-alkylphenols, and C_3- through C_7-singly unsaturated alkylphenols. In addition, there appears to be a series of amides ranging from at least C_6- through C_{12}-alkylamides. The other nitrogenous components appear to include two or three homologous series starting with 109, 125, and 133. Isotopic abundances, which may not be very reliable in this complex mixture, suggest the presence of oxygen in addition to the nitrogen. Some of the spectra are consistent with those of pyridines and pyridinols. There appears to be evidence to hypothesize the presence of a series of pyridines and pyridinols as well as the analogous pyrrole and possibly indole series. Some of these components or their higher homologs may begin to explain the mutagenicity of the highly polar shale oil fraction. To determine the degree of potential contamination of surface or groundwater in the event of a shale oil spill, three shale oils were extracted with water at different pH (6.5 and 8.5) and different salinities. The different salt solutions are shown in Table 1. As expected, >70% of the extracted material eluted in the polar methanol fraction from the Sephadex LH-20 separation and in the highly polar fraction (equivalent to Fraction 7, Figure 1) in the HPLC separation. The organics in the water extracts of the shale oils were concentrated on a C_{18}-reverse phase column. Mutagenic activity was measured in the original oil, the extracted oil, the total water extract, and the organic concentrate of the water extract (Table 2). The salinity did not seem to have much effect on the extractable activity; therefore, the data are not shown. The weighted specific activity was calculated by multiplying the specific activity for a given fraction by the percentage of that fraction in the crude material. The percentage of mutagenic activity recovered relative to the original oil was also calculated. The water extract of the most mutagenic oil, Paraho, was itself most mutagenic, though small amounts of activity could be extracted from all three oils. Approximately 2% of the mutagenic activity of the Paraho shale oil could be extracted during a relatively brief contact with water. This could be a significant amount in the event of a large shale oil spill.

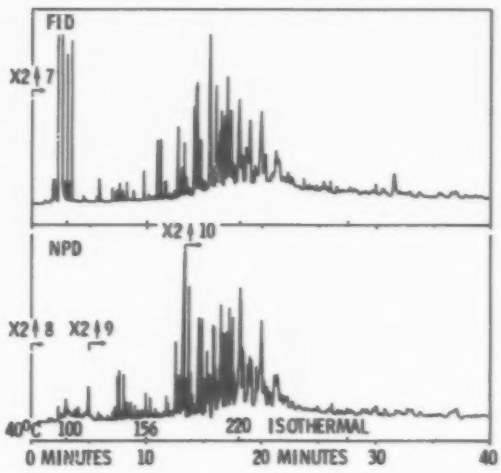

FIGURE 2. FID/NPD Dual Trace Gas Chromatograms of the Highly Polar HPLC Fraction (Equivalent to Fraction 7, Figure 1) from Paraho LH-20 Methanol Fraction. GC: Carbowax, 3 m fused silica capillaries

TABLE 1. Salt Solutions Used for Water Extraction of Shale Oils

Salt solution #1[a]		Salt solution #2[b]	
Ca^{++}	120 ppm	Na^{+}	3900 ppm
Mg^{++}	140	NH_4^{+}	3400
Na^{+}	200	$CO_3^{=}$	600
HCO_3^{-}	550	HCO_3^{-}	15700
$SO_4^{=}$	860	$SO_4^{=}$	1900
pH	7.5	$S_2O_3^{=}$	2200

(a) To approximate general groundwater concentrations in the Piceance Basin, Colorado.
(b) To approximate oil shale retort water concentrations (Fox, Farrier, and Poulson 1978).

BEST DOCUMENT AVAILABLE

TABLE 2. Water Extraction of Shale Oils

Sample		Specific Activity (rev/μg fraction)	Wt. (%)	Weighted Specific Activity (rev/μg crude)	Recovery (%)
Paraho Oil					
pH 6.5	Oil	0.32	100.0	0.32	100
	Water Extract	0.37	2.0	0.0074	2.3
	Organic Concentrate	0.93	0.5	0.0047	1.5
	Extracted Oil	0.33	98.0	0.32	100.0
pH 8.5	Water Extract	0.35	1.8	0.0063	2.0
	Organic Concentrate	0.75	0.6	0.0045	1.4
	Extracted Oil	0.30	98.2	0.29	90.6
Geokinetics Oil					
pH 6.5	Oil	0.16	100.0	0.16	100.0
	Water Extract	0.10	0.19	1.9×10^{-4}	0.1
	Organic Concentrate	0.14	0.12	1.7×10^{-4}	0.1
	Extracted Oil	0.11	99.81	0.11	68.6
Occidental Oil					
pH 6.5	Oil	0.11	100.0	0.11	100.0
	Water Extract	0.22	0.17	3.7×10^{-4}	0.3
	Organic Concentrate	0.46	0.13	6.0×10^{-4}	0.5
	Extracted Oil	0.12	99.83	0.12	109.1

REFERENCES

Pelroy, R. A., D. S. Sklarew and S. P. Downey. 1981. "Comparison of the Mutagenicities of Fossil Fuels." Mutation Res. 90:233-245.

Fox, P. D., S. Farrier and R. E. Poulson. 1978. "Chemical Characterization and Analytical Considerations for an In-Situ Oil Shale Process Water." LETC/RI-78/7.

BEST DOCUMENT AVAILABLE

ISOLATION OF METALLIC COMPLEXES IN SHALE OIL

K. B. Olsen, C. L. Wilkerson, A. P. Toste and D. J. Hayes

Considerable interest presently is being placed upon the quantity and speciation of trace metal contaminants in crude shale oils produced from various oil shale retorting technologies. The significance of this interest is related to: (1) the potential for the trace metals to act as catalytic poisons during upgrading and refining; and (2) the direct impact of metals on equipment and the environment if shale oil is used as a boiler fuel; and (3) the potential and environmental effects of these compounds.

As a method to isolate and identify metallic complexes, two shale oils produced by an aboveground and a vertical modified in-situ retorting technology were fractionated on silica gel. A 19-mm ID x 450-mm column was loaded with activated silica gel (heated four hours at 120°C) in hexane. One gram of filtered shale oil was dissolved in a minimal amount of hexane and loaded onto the column. The elution scheme started with nonpolar hexane, proceeded through increasingly polar solvents (hexane/toluene, toluene/ethylacetate) and ended with methanol. Twenty-nine 75 mℓ fractions were collected. Each fraction was evaporated to dryness, weighed, and then redissolved in 10 mℓ of methylene chloride for determination of nickel, chromium, iron, and molybdenum by direct current plasma emission spectroscopy (DCP). A small aliquot of the CH_2Cl_2 solution was also analyzed for arsenic by instrumental neutron activation analysis. The metallogram for the in-situ shale oil is shown in Figure 1.

A preliminary scan of each of the twenty-nine fractions by UV-VIS spectroscopy showed evidence that fraction #9 of the in-situ shale oil contained a metalloporphyrin-type compound. Subsequently, fraction #9 was further purified using alumina chromatography and a fraction enriched in the observed metalloporpnyrin was obtained. Analysis by UV-VIS spectroscopy and DCP confirmed the distinct presence of a metalloporphyrin containing the metal nickel. Further analysis by direct-probe mass spectrometry yielded a spectrum (Figure 2) showing three or four possible porphyrin species with parent peaks located at 518, 490, and 475 m/e. The ion cluster m/e 503 is probably due to the M-15 (loss of CH_3) of the m/e 518 cluster. This 518/503 relationship compares well with the mass spectrum of abelsonite (Figure 3), a nickel-containing metalloporphyrin recently identified in Green River oil shale. With the evidence supplied by the UV-visible spectrum, the DCP metal analysis and the mass spectrum of the porphyrin-rich fraction, we tentatively identified the presence of abelsonite-type nickel-porphyrin in the shale oil produced by in-situ retorting.

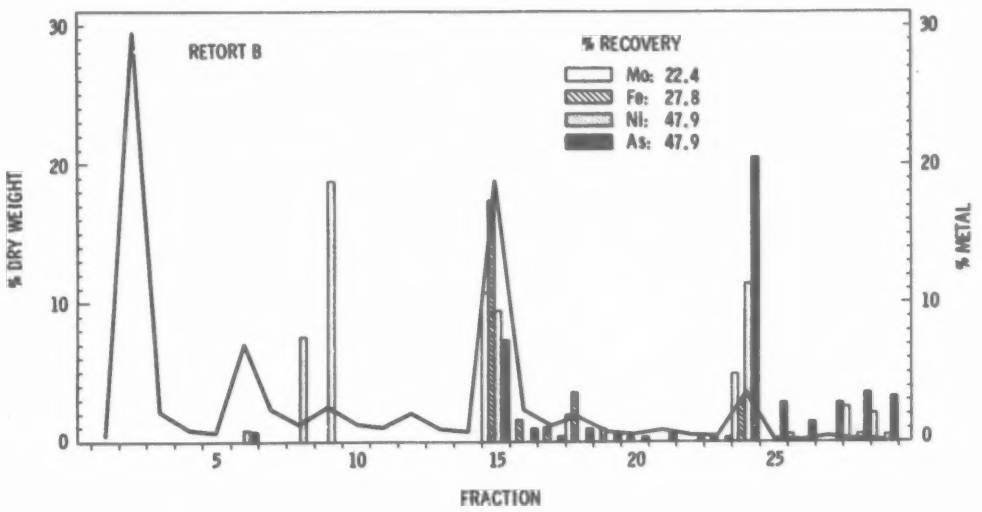

FIGURE 1. Silica Gel Fractionation of Shale Oil Metals

BEST DOCUMENT AVAILABLE

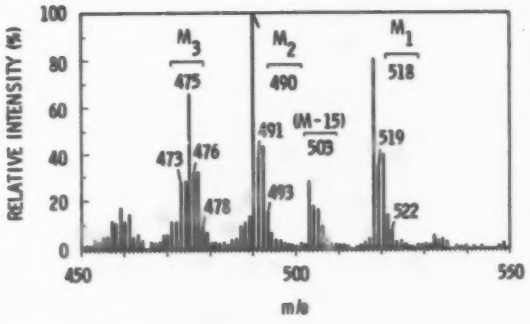

FIGURE 2. Mass Spectrum of Species in Nickel-Aromatic Fraction after Alumina Separation

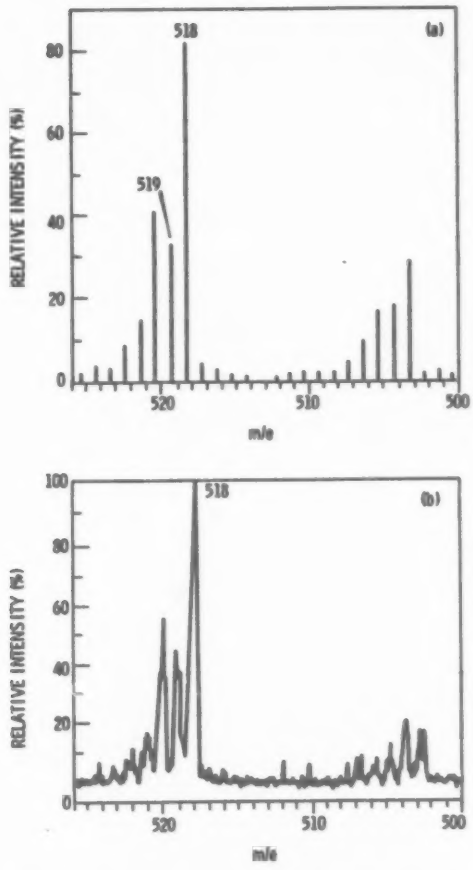

FIGURE 3. Comparison of Nickel Shale Oil Porphyrin and Abelsonite: a) Partial Mass Spectrum of Nickel Porphyrin Isolated from Shale Oil; b) Partial Mass Spectrum of Abelsonite from Green River Formation, Utah (Milton et al. 1978).

With further development and application of silica gel/aluminum chromatography, specific element detection, and mass spectrometry, we hope now to investigate the nature of other metal-containing complexes in shale oil. Specific interest will be on molybdenum and arsenic speciation and structural determinations of these complexes.

SPECIATION OF SULFUR COMPOUNDS IN OIL SHALE BY-PRODUCT WATERS

K. H. Abel

Numerous sulfur species could be present in the by-product waters of an oil shale retort. These species include sulfite, sulfate, thiosulfate, thiocyanate, polysulfate, and organo-sulfur. A characterization of those actually present is important in order to establish first the degree of waste control necessary to prevent groundwater contamination, and second, the appropriate technology used to remove sulfur.

Ion chromatography was utilized to examine water soluble sulfur species present in Rio Blanco Retort 0 waters. A "fast-run" anion column and strong eluent (0.08M Na_2CO_3, 0.06M $NaHCO_3$) were utilized on a Dionex Model 16 chromatograph to provide more rapid analysis of the complex sulfur species. These conditions shortened analysis time to approximately 35 minutes, from injection to thiocyanate elution.

Sour water samples were examined with sulfate concentrations in parts per million (Table 1). Thiosulfate, fluorine, and chlo- rine were determined. Thiocyanate was also present in the solutions, but has not been quantified to date.

TABLE 1. Oil Shale Sour Water Samples. Sulfate concentrations shown in ppm.

Samples	SO_4	S_2O_3	F	Cl
RB-0-SW-60	740	840	6.1	9.0
RB-0-SW-64	1450	205	5.9	9.8

BEST DOCUMENT AVAILABLE

SULFUR AND NITROGEN GAS ANALYSIS AT RIO BLANCO RETORTS

D. S. Sklarew, D. J. Hayes and K. B. Olsen

Nonhydrocarbon constituents in potentially valuable hydrocarbon-rich oil shale retort gases pose technical and environmental problems. To minimize these potential problems, the industry requires knowledge of the nature of the sulfur and nitrogen species present in the retort gases. Such characterization studies at Rio Blanco Retorts 0 and 1 have identified seven sulfur species and established the presence of numerous nitrogen components.

Two series of analyses were conducted at the Rio Blanco retorts using gas chromatography. On-site measurement proved necessary because of the instability of the retort gases. Grab samples were also taken to confirm species identification. Sampling information is summarized in Table 1.

Stainless steel and Teflon® tubing were used to connect the sampling ports to the gas chromatograph. Equilibration of the tubing with the sample was probable due to continuous contact. Also, loss of condensable gases in the unheated tubing seems unlikely since significant quantities of relatively high molecular weight species were observed in the retort gases.

Sulfur, nitrogen, and hydrocarbon species were analyzed by gas chromatography using the columns and detectors shown in Table 2.

A Teflon-lined gas sampling valve allowed quantitative introduction of the gas samples. The GC program rate was slow enough to enable separation of the hydrocarbons from the sulfur species; separation is essential since hydrocarbon species have a

®Registered Trademark of E. I. du Pont de Nemours and Co.

TABLE 1. Sampling Information at Rio Blanco

Sample	Time of Sampling Relative to Start of Burn	Retort Zone During Sampling	Sampling Location[a]
Retort 0	~1 week after	major pyrite zone	after the knockout drum ~100 yds from GC
Retort 1	~1 month after	low pyrite zone	before knockout drum ~30 ft from GC

(a)Note that the samples were taken before the retort gas passed to the incinerator/scrubber which was used to convert the sulfur and nitrogen species to SO_x and NO_x, respectively; flue gas was then scrubbed prior to release to the atmosphere.

TABLE 2. Gas Chromatographic Methods

Species	GC Column (6' x 1/8" glass)	Detector
CH_3SH, H_2S, COS, CS_2, thiophene, methylthiophene	Porapak QS	Flame photometric (FPD), Meloy SO_2 analyzer[a]
SO_2, H_2S, COS, CS_2, thiophene, methylthiophene	Chrom 107	FPD, Meloy SO_2 analyzer
Nitrogen species	Chrom 103, Porapak QS	Nitrogen-phosphorus (NPD)
Hydrocarbons	Porapak QS, Chrom 107	Flame ionization (FID)

(a) Meloy SO_2 analyzer, which is an FPD, was used in place of the FPD on the GC at Retort 1.

BEST DOCUMENT AVAILABLE

pronounced quenching effect on the flame photometric detector (FPD). Four types of standards were used to identify and quantitate the samples: permeation tubes, gas cylinder, liquid solutions in hexane, and neat liquids (used for qualitative analysis only).

Dilutions were necessary to (1) bring the sample gas within the dynamic range of the detectors, and (2) approximately match the sample and standard responses since the FPD response is nonlinear. For Retort 0, the dilution apparatus consisted of two rotameters and a glass mixing chamber. For Retort 1, a vacuum pump was used to evacuate the gas sampling loop and the gas sample was introduced into the GC at a known reduced pressure to effect a dilution.

Hydrocarbon gases from C_1 through C_7 were detected at Rio Blanco Retorts 0 and 1 by GC and GC-MS. Included were saturated, singly unsaturated, and doubly unsaturated hydrocarbons, as well as benzene and toluene.

Several nitrogen species are present in the offgas (Figures 1 and 2). The Chromosorb® 103 column is useful for the higher boiling components and is considered a good packing material for aliphatic amines. Some of the peaks appear to correspond to nitriles; however, identifications thus far are very tentative.

®Registered Trademark of Johns Manville

Four sulfur gases were identified at Rio Blanco by comparing retention times with standards on two GC columns: H_2S, COS, CS_2, and thiophene. CH_3SH was identified on the Porapak® QS GC column (Figure 3) and a small SO_2 peak was also tentatively identified on the Chromosorb 107 column. Gas chromatographic-mass spectrometric analysis of a grab sample confirmed the presence of COS, CS_2, thiophene, and methylthiophene (unknown peak 1).

Numerous H_2S measurements were available from on-site monitors. The results for the sulfur gases are summarized in Table 3; H_2S values are taken from Rio Blanco process monitors. The differences in values within Retort 1 are due in part to differences in retort conditions; i.e., low values were obtained during routine air injection and higher values were obtained when air injection was reduced. The cause of the differences in values between the two retorts is not known. However, some of the differences may be explained by differences in the mineralogy of the retorted zones: Retort 0 included a high pyrite zone whereas Retort 1, at the time of sampling, was in a low pyrite zone. Studies are continuing with emphasis on sulfur quantitation and nitrogen species identification during the end of the burn at Retort 1.

®Registered Trademark of Waters Associates, Inc.

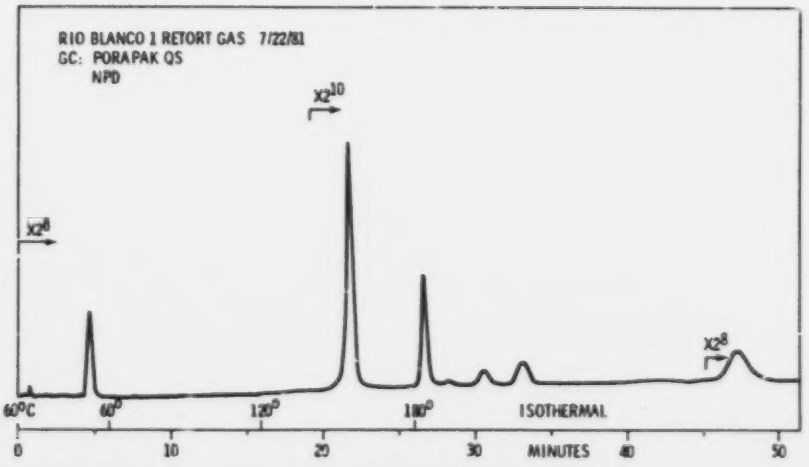

FIGURE 1. Gas Chromatogram of Nitrogen Gases from a Rio Blanco Offgas—Porapak QS, 6 feet x 1/8 inch, Glass; Nitrogen-Phosphorus Detector

BEST DOCUMENT AVAILABLE

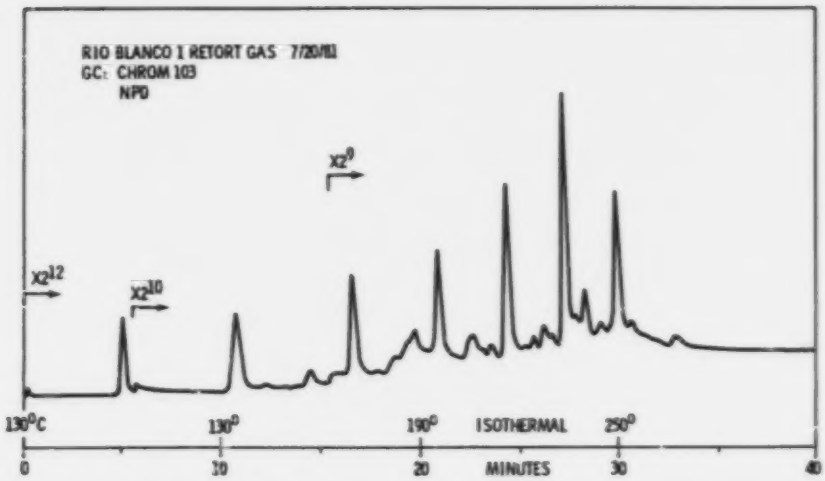

FIGURE 2. Gas Chromatogram of Nitrogen Gases from a Rio Blanco Offgas—Chromosorb 103, 6 feet x 1/8 inch, Glass; Nitrogen-Phosphorus Detector

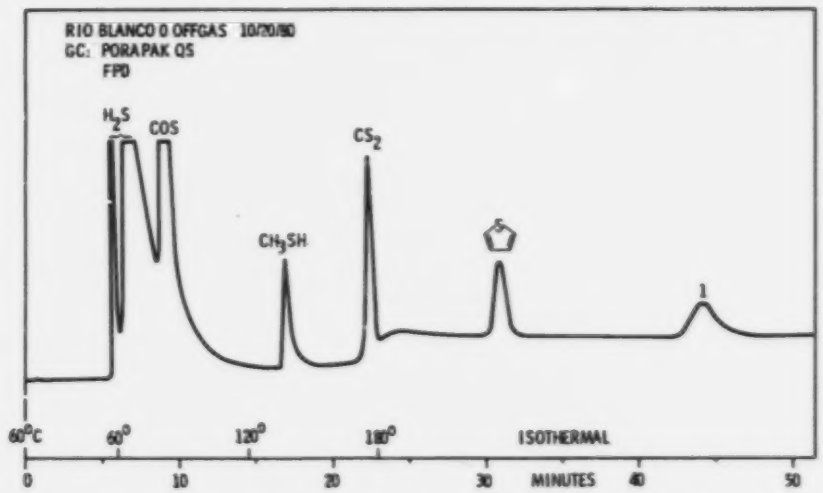

FIGURE 3. Gas Chromatogram of Sulfur Gases from a Rio Blanco Offgas—Porapak QS 6 feet x 1/8 inch, Glass; Flame Photometric Detector

BEST DOCUMENT AVAILABLE

TABLE 3. Sulfur Gases in Rio Blanco Retorts 0 and 1[a]

Sulfur Gases	Retort 0 10/20/80 (08:30) -10/21/80 (11:30)	Retort 1[b] 7/14/81 (18:00)* -7/15/81 (10:50)	7/15/81 (11:50)** -7/16/81 (14:00)	7/16/81 (19:00)*** -7/17/81 (21:00)
H_2S[c] (%)	2.0	1.5	0.5	0.6
COS (ppm)	500	—[d]	105	72
CH_3SH (ppm)	85	120	39	48
CS_2 (ppm)	25	37	8	9
Thiophene (ppm)	115	37	32	14
Methylthiophene (ppm)	110	60	67	24
SO_2 (ppm)	7	—[e]	—[e]	<10

(a) Values are ±20%
(b) Retort conditions based on Rio Blanco Oil Shale Co. (RBOSC) data are:
(*) low air input
(**) increased air input
(***) changed flows
(c) Based on RBOSC data
(d) Not determined due to overlap with H_2S
(e) Not determined on Porapak QS column

PRODUCT AND EFFLUENT CHARACTERIZATION STUDIES AT RIO BLANCO'S RETORT 0

C. L. Wilkerson, D. S. Sklarew, K. B. Olsen, K. H. Abel, J. S. Fruchter and C. L. Nelson

Chemical characterization studies of oil shale pilot plants provide information for assessing environmental implications and for identifying effluent contaminants which may require or affect control technology. During FY 1981 a PNL field sampling and characterization program was conducted at the Colorado C-a Federal Lease Tract where Rio Blanco Oil Shale Company (RBOSC) retorted two pilot-scale modified in-situ retorts. Personnel from PNL collected representative samples of product shale oil, retort water, gas condensate, and boiler blowdown. These liquid samples were subsequently returned to PNL for laboratory analysis. On-site gas phase characterization was conducted to measure several trace constituents in the raw and treated offgas. The measured constituents included vapor mercury, arsenic, and other trace elements, trace sulfur species, and trace nitrogen species.

The Rio Blanco in-situ retort produced considerably higher concentrations of H_2S in the low-Btu retort offgas as compared to similar retorts operated by Occidental Oil Shale, Inc., at Logan Wash, Colorado. The observed level of H_2S in Rio Blanco (Retorts 0 and 1) and Occidental (Retort 6) in-situ retort offgas was between 0.5 to 4 and 0.1 to 0.2 mole percent, respectively. The reason for the observed differences is unclear; however, the richer shales and higher sulfur content of the central Piceance Creek Basin, site of the C-a Lease Tract, are assumed to be a factor. Levels of vapor mercury in Retort 0 offgas showed a variable behavior with greater concentrations (10 to 25 $\mu g/m^3$) detected in the offgas near the end of the retort burn. This trend has been predicted from carefully monitored laboratory studies. Radon levels in Retort 0 offgas were observed to be relatively constant in the 6 to 7 pCi/ℓ range which is typical of ambient air in the Rocky Mountain region. Concentrations of NO in Retort 0 treated offgas ranged from 63 to 176 ppm. Measurements for trace sulfur showed that from 1 to about 5% of the total sulfur in the gas phase was present as non-H_2S compounds. The most abundant non-H_2S compound was observed to be COS. Other compounds detected included CS_2, SO_2, CH_3SH, thiophene, and methylthiophene.

Retort water from Retort 0 contained significantly less dissolved solids than retort water from other retorting technologies studied to date. The observed low concentrations of dissolved constituents are believed due to a dilution effect of groundwater in-flow and/or steam condensation. The major anions present were sulfate, thiosulfate, and carbonate-bicarbonate. The major cations were ammonium, sodium, magnesium, and calcium. Toxic trace metals were generally present in low concentrations. For example, arsenic levels ranged

BEST DOCUMENT AVAILABLE

from less than 0.01 to 0.72 ppm. In spite of apparent dilution, a few retort water parameters were observed to increase systematically with time. These include pH, alkalinity, ammonia, organic carbon, conductivity, arsenic, potassium, molbydenum, and antimony.

Analysis of the product shale oil from Retort 0 showed some significant differences from previously analyzed Green River shale oils. The concentration of sulfur was observed to be 1.9 wt%, a value almost three times that generally reported for Green River shale oil. The total nitrogen, arsenic, nickel, and molybdenum were observed to be 1.5 wt% and 7.6, 19, and 13 ppm, respectively. The nickel and molybdenum values exceed previously measured values for these trace metals in other shale oils, whereas arsenic is relatively low.

FOSSIL FUEL RESEARCH MATERIALS

C. L. Wilkerson and J. S. Fruchter

The purpose of the fossil fuel research materials program is to obtain, store, prepare and distribute representative samples of new synthetic fuels and associated byproduct materials for subsequent DOE research studies. Representative samples of feedstocks, synfuels and associated byproduct materials are homogenized, chemically characterized, and then used in DOE studies of analytical procedure development, environmental pollution, health effects, and effluent treatment research and development.

A number of samples from oil shale retorts and coal conversion processes that are available in our refrigerated repository were listed in the 1980 Pacific Northwest Laboratory (PNL) Annual Report to the DOE Assistant Secretary for Environment (PNL-3700 PT4). These materials, plus those added in this year's work, are listed in Table 1. The major new oil shale research materials added to the repository in FY 1981 were obtained from operations of the Rio Blanco Oil Shale Company (RBOSC) on the C-a Federal Lease Tract in Colorado. Samples of crude shale oil, retort water, gas condensate and scrubber blowdown were obtained from the retorting of Retort 0 and Retort 1. These two modified in situ retorts were retorted by RBOSC during the periods October 13-December 26, 1981 and June 21 to date, respectively. Other C-a Tract samples were obtained in FY 1981. These include retorted C-a shale from RBOSC-sponsored tests of the Lurgi surface retorting technology and raw C-a shale oil core samples (core CE-709) received from the Los Alamos Scientific Laboratory (LASL). Chemical characterization and health effects studies are in progress on these new oil shale research materials.

During FY 1981 new samples were also obtained from coal conversion processes, including special experimental process distillates from the SRC-I and SRC-II processes. The experimental distillates represent specific "boiling range" distillate cuts being tested for health effects and analyzed for mutagenic constituents. This information is being incorporated in plant design decisions for product boiling range endpoints.

Other research materials that were added in FY 1981 include new materials derived from native petroleum, including a commercial creosote, #2 diesel fuel, #6 heavy fuel oil, a road tar, and a coal-derived asphalt. Petroleum-based materials are being tested to provide comparative analyses relative to synfuel counterparts.

BEST DOCUMENT AVAILABLE

TABLE 1. Currently Available Fossil Fuel Reference Materials

1. Solvent-Refined Coal Process-I
   a. Solvent-refined coal
   b. Mineral residue
   c. Light oil (naphtha)
   d. Recycle solvent
   e. Wash solvent
   f. Experimental process distillates
2. Lawrence Livermore 125-kg Retort
   a. Mohagany Zone raw shale (24 gal/ton)
   b. Spent shale (Run S-11)
3. Lawrence Livermore 7-T Retort
   a. Spent shale (Run L-1)
   b. Crude shale oil (Run L-1)
   c. Process water (Run L-1)
4. Vernal, Utah In Situ
   a. Process water
   b. Crude shale oil
5. Crude Petroleums
   a. Wilmington (high N)
   b. Gato Ridge (high metals, high N, high S)
   c. Prudhoe Bay
6. Paraho Semiworks Retort[a]
   a. Raw shale
   b. Retorted shale
   c. Crude shale
   d. Product water
   e. Raw shale crushing fines from filter baghouse
   f. Retorted shale fines from filter baghouse
7. CO_2 Acceptor
   a. Ash
   b. Spent acceptor
8. Solvent-Refined Coal Process-II
   a. Light distillate
   b. Middle distillate
   c. Heavy distillate
   d. Vacuum bottoms
   e. Experimental process distillates
9. Paraho Refined Fuels
   a. Hydrotreated shale oil
   b. JP-5 (jet)
   c. JP-8 (jet)
   d. DFM (diesel)
   e. Acid sludge
10. Conventional Petroleum Fuels
    a. JP-5 (jet)
    b. JP-8 (jet)
    c. DFM (diesel)
11. Occidental In Situ Retort[b]
    a. Crude shale oil
    b. Retort water (Room 6)
    c. Boiler blowdown
12. Rio Blanco In Situ Retorts 0 & 1[b]
    a. Crude shale oil
    b. Sour water (underground separator)
    c. Offgas condensate
    d. Scrubber blowdown
13. Comparative Non-Synfuel Materials
    a. Commercial creosote
    b. #2 diesel fuel
    c. #6 heavy fuel oil
    d. Road tar
    e. Coal-derived asphalt
14. C-a Tract Samples
    a. Raw shale (core CE-709)
    b. Retorted shale (Lurgi process)[c]

(a) Use of any materials from Paraho requires approval from Development Engineering, Incorporated (operators of Paraho retort) on a case-by-case basis.
(b) Use of any materials from Occidental requires coordination through the DOE-ASEV Modified In Situ Task Force—W. Chappel, University of Colorado, Chairman.
(c) Use of this material requires approval from Rio Blanco Oil Shale Company.

BEST DOCUMENT AVAILABLE

BLANK PAGE

Multitechnology

BLANK PAGE

• Environmental Pollutant Characterization by Direct-Inlet Mass Spectrometry

The utility of direct-inlet mass spectrometry (DIMS) for the detection, characterization and monitoring of toxic airborne particulate pollutants is being experimentally determined. The dependence of the particle detection efficiency of the DIMS system on particle size was determined.

CHARACTERIZATION OF ENVIRONMENTAL POLLUTANTS BY DIRECT-INLET MASS SPECTROMETRY

C. R. Lagergren and J. J. Stoffels

The purpose of this task is to experimentally determine the utility of direct-inlet mass spectrometry (DIMS) as an analytical technique for the detection, characterization and monitoring of specific toxic particulate airborne pollutants that enter the environment as by-products of energy generation or other industrial activities.

The DIMS technique is essentially a method by which particles in air are transported directly to the hot ionizing filament of a surface ionization mass spectrometer without the need for any collection, manipulation or processing procedures. Individual particles striking the hot filament form bursts of ions which are then mass analyzed and measured. Burst rates are related to particle concentration in sampled air while the total charge per burst is a measure of particle size. Mass analysis of the ions provides a means of selectivity for a specific particle material and potentially the identification of its chemical composition. Ionization efficiencies by surface ionization for a wide range of elements are sufficiently high so that submicrometer-size particles of such elements and their compounds can be detected and measured.

Our previous investigations have shown that the DIMS method can provide information about the size of individual particles. For a pure material, cesium nitrate, and a filament temperature of 960°C, the number of ions in a burst is proportional to the square rather than the cube of the particle size. The ion yield (ions/atom) from an individual particle, therefore, is inversely proportional to size. With appropriate calibration the complete size distribution of airborne particles of homogeneous material is determinable in real time from mass spectrometric measurements. However, the efficiency with which the direct-inlet system transmits particles to the mass spectrometer filament varies with particle size and must first be determined in order to derive the actual size distribution from the distribution of integrated ion-burst measurements. Therefore, the transmission efficiency of the inlet system was measured for monodisperse cesium nitrate aerosols of different sizes.

Monodisperse aerosols were obtained by passing a polydisperse aerosol through an electrostatic classifier* which separated a narrow size range of particles from the parent distribution. A steady concentration of monodisperse particles was maintained in the dilution plenum of the aerosol generator. The concentration and size distribution of particles in the plenum were measured using a laser aerosol spectrometer.** The aerosol in the plenum was simultaneously measured by the direct-inlet mass spectrometer. To equalize any particle losses in the sampling lines from the dilution chamber, the lines were sized to give equal transit times to the laser spectrometer and the mass spectrometer.

The particle detection efficiency of the direct-inlet mass spectrometer was measured for cesium nitrate particles of diameters from 0.15 to 1.6 μm. The particle detection efficiency is the number of ion bursts per cm^3 of inlet air divided by the particle concentration measured by the laser aerosol spectrometer. The detection efficiency is equal to the particle transmission efficiency of the inlet if all particles striking the filament result in a detectable ion burst. This is a reasonable assumption for cesium nitrate which ionizes readily.

The results of these measurements are shown in Figure 1 and reflect the dependence of aerosol beam divergence on particle size. The particle transmission efficiency--that is, detection efficiency--varies as the 1.47 power of the particle size. An efficiency of 58% was measured for transmitting cesium nitrate particles 1.6 μm in diameter to the flat ribbon filament 0.75 mm wide located 90 mm from the capillary nozzle outlet. This high transmission efficiency indicates a very small divergence of the particle beam

---

* Model 3071, Thermo-Systems Inc., St. Paul, MN 55164, U.S.A.

** Model He-Cd LAS-X, Particle Measuring Systems, Boulder, CO 80301, U.S.A.

BEST DOCUMENT AVAILABLE

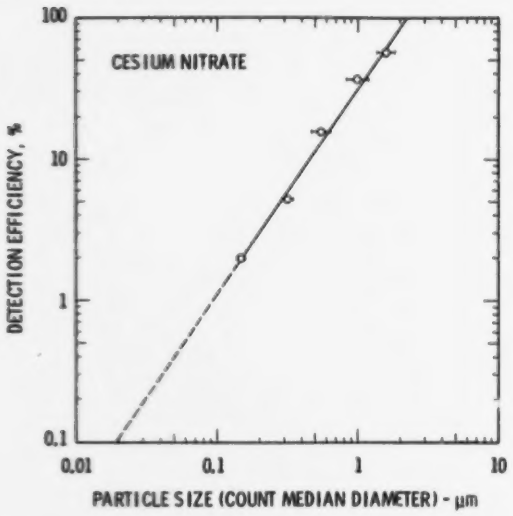

FIGURE 1. Detection Efficiency of the Direc.-Inlet Mass Spectrometer for Cesium Nitrate Particles of Different Sizes. Detection efficiency equals particle transmission efficiency if all particles striking the filament are detected. Bars on the data points indicate the width of the particle size distribution.

from the capillary axis. Assuming that the particles are uniformly distributed throughout a cone originating at the nozzle outlet, an angle of divergence from the axis of about 3° accounts for the 5.2% detection efficiency of the 0.32 µm particles.

BEST DOCUMENT AVAILABLE

• Trace Analysis by Laser Excitation

Analyses of ultratrace levels of both inorganic and organic species are critical in the estimation of potential environmental and health effects. In the trace analysis by laser excitation program, laser techniques are developed and evaluated for laboratory and field use. During the past year, a resonance ionization technique was developed which should be extremely sensitive to all metallic elements. The application of this technique to a selected set of elements is described in the following report.

DOUBLE RESONANCE IONIZATION SPECTROSCOPY DETECTION OF HEAVY METALS

B. A. Bushaw

Double resonance ionization spectroscopy (DRIS), a laser-based method of ultratrace analysis developed in this laboratory, is applicable to most of the metallic elements. The primary species of interest for application of this technique include toxic heavy metals and several long-lived radioisotopes generated in the nuclear fuel cycle. DRIS is complementary to flameless atomic absorption methods for trace metal analysis, exhibiting limits of detection typically three to six orders of magnitude lower than flameless atomic absorption, while the upper limit for linear detection response inherently overlaps the lower range accessible by flameless atomic absorption.

The DRIS technique uses a two-color pulsed dye laser system to excite the atomic species of interest to a state just below the ionization limit. The atom may then be detected by several different ionization processes. The laser system used for the double resonance excitation is depicted in Figure 1. The first dye laser is tuned to a wavelength corresponding to a transition from the ground state to a low lying excited state where absorption of a photon from the laser beam promotes the atom to the selected excited state. The second dye laser is tuned to a wavelength which will sequentially raise the low lying excited state to a high lying Rydberg state. Once the atom has been placed in the Rydberg state in this manner, it may be ionized either by collisions within a buffer gas or by absorption of a third photon from either of the two lasers. The absorption of a third photon may often be significantly enhanced by carefully selecting the Rydberg state to produce a coincidental third resonance between the Rydberg state and an autoionizing level with either of the two laser wavelengths. Once the atom is ionized, it may be detected by conventional ion counting techniques.

Several features of DRIS, derived from the utilization of two resonant transitions between bound atomic states, make it promising as an analytical instrument for routine use:

1. Since two distinct atomic transitions are used, extremely high selectivity may be achieved. Dye lasers of relatively modest bandwidth (1 cm^{-1}) allow an overall spectral selection of greater than 10^8, essentially eliminating the possibility of coincidental resonances from interfering species.

2. The lasers may be operated at relatively low power levels since the bound-bound transitions have much higher cross sections than direct excitation into the ionization continuum. This minimizes the off resonance ionization of other species that may be present. Also, the relatively low power lasers offer long-term reliability, high-repetition rate, and low dye and electrical power consumption.

Thus far, DRIS has been applied to the detection of four different metallic species. Using collisional ionization, the detection of rubidium at near the single atom limit has been demonstrated (reported in FY 1980). Mercury has been measured in discrete air samples with a demonstrated sensitivity of 50 femtograms. This means that mercury may be determined in "unpolluted" air by taking samples as small as 50 mℓ, a significant improvement over atomic absorption techniques where several cubic meters of air must be sampled for reliable measurements. The extreme sensitivity for mercury suggests that the method could be used for real time on-line monitoring in moderately polluted environments (down to approximately 1 ng/liter air). Cadmium has been detected in a real-time mode where the cadmium vapor was introduced into a stream of helium carrier gas. At the lowest value measured, cadmium was present at less than 1 part in 10^{13}, yet the signal-to-noise ratio for the measurement was approximately 100. DRIS has also been used to investigate the doublet P Rydberg

BEST DOCUMENT AVAILABLE

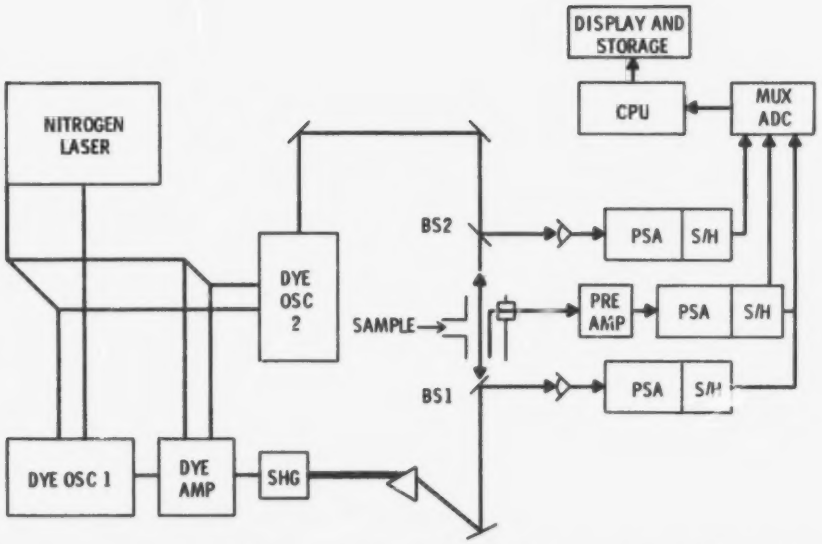

FIGURE 1. Double Resonance Ionization Spectroscopy Apparatus. The first dye laser (dye OSC 1 and dye amp) can be frequency doubled (SHG) and is used to pump the resonance line transmission. The second dye laser (dye OSC 2) is used to pump the resonance level to Rydberg level transition. The intensity of both lasers is sampled with 5% beam splitters (BS 1 and BS 2) and detected with photodiodes. The ionization signal is detected with an ion counting wire which is capacitatively coupled to a charge-sensitive preamplifier. The laser intensity and ionization signals are processed through pulse shaping amplifiers (PSA) and sample and hold modules (S/H). They are then fed into a minicomputer with a multiplexed analog-to-digital converter for data storage and analysis.

series of thallium. The two-photon nature of the process allows the investigation of states with the same parity as the ground state, which is normally forbidden to one-photon spectroscopy. Figure 2 shows a spectrum of these series in thallium obtained by scanning the second laser wavelength. More than 60 previously unobserved states with principal quantum up to n = 65 have been identified. While absolute detection limits have not yet been determined for thallium, the spectra shown in Figure 2 were taken of the vapor above solid thallium metal at 115°C, where the vapor pressure is estimated to be less than 10^{-8} torr.

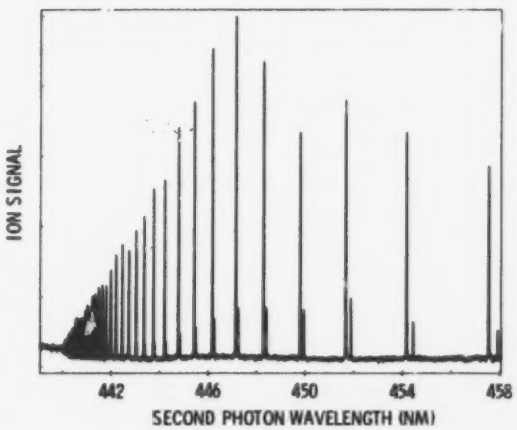

FIGURE 2. Double Resonance Ionization Spectrum of the Doublet P Rydberg Series of Thallium. The first excitation step is from the ground state to the $7^2S_{1/2}$ level at 377.68 nm. Rydberg levels from n = 15 (at right end of spectra) up to n = 65 are observed by scanning the second dye laser wavelength. In the observed doublet structure, the intense lines are for the J = 3/2 fine levels while the weak ones are J = 1/2.

BEST DOCUMENT AVAILABLE

Publications and Presentations

BLANK PAGE

PUBLICATIONS

Braby, J. A. and W. C. Roesch. 1980. "Microdosimetry of 0.5 to 2.0 MeV Electron Beams." In Proceedings of the Seventh Symposium on Microdosimetry, Vol. I, pp. 665-676, September 8-12, 1980, Oxford, England, eds. J. Booz, H. G. Ebert and H. D. Hartfiel. Harwood Academic Publishers Ltd., New York, EUR-7147 Commission of the European Communities.

Bushaw, B. A. and T. J. Whitaker. 1981. "Doppler-Cancelled, Two Photon Resonant Ionization Spectroscopy." J. Chem. Phys. 74(11):6519.

Cocke, C. L., R. DuBois, T. J. Gray, E. Justiniano and C. Can. 1981. "Coincidence Measurements of Direct and Transfer Ionization in Low Energy Ar^{+q} + (He, Ne, Ar, Xe) Collisions." Phys. Rev. Lett. 46:1671.

DuBois, R. D., L. Mortensen and M. Rodbro. 1981. "Collisionally Induced Alignment Produced by Electron and Light-Ion Impact: Auger Electron Emission Following 2p Ionization and Excitation." J. Phys. B: Atom Molec. Phys. 14:1613-1624.

Felix, W. D., D. D. Mahlum, W. C. Weimer, R. A. Pelroy and B. W. Wilson. "Chemical and Biological Characteristics of SRC-II Products and By-Products." In Proceedings of the Fuel Conversion Symposium, September 15, 1980, St. Louis, Missouri. U.S. Environmental Protection Agency, Washington, D.C. (in press).

Felix, W. D., D. D. Mahlum, B. W. Wilson, W. C. Weimer and R. A. Pelroy. 1981. "Chemical Characterization and Bioassay of SRC Process Materials." In Proceedings of Environmental Aspects of Fuel Conversion Technologies, VI, October 26-30, 1981. Denver, Colorado (in press).

Fisher, D. R. and W. C. Roesch. 1981. "The Microdosimetry of Plutonium in Beagle Dog Lung." In Proceedings of the Seventh Symposium on Microdosimetry, September 8-12, 1980, Oxford England, Vol. II, pp. 1399-1408, ed. J. Booz, H. E. Ebert and H. D. Hartfiel. Harwood Academic Publishers Ltd., New York, EUR-7147, Commission of the European Communities.

Fruchter, J. S. and C. L. Wilkerson. 1981. "Characterization of Oil Shale Retort Effluents." In Oil Shale: The Environmental Challenges, Chapter 3. K. Petersen, ed., Colorado School of Mines Press, Golden, Colorado.

Later, D. W., M. L. Lee and B. W. Wilson. 1981. "Selective Detection of Amino Polycyclic Aromatic Hydrocarbons in Solvent Refined Coal." Submitted to Anal. Chem.

Later, D. W., M. L. Lee, K. D. Bartle, R. C. Kong and D. L. Vassilaros. 1981. "Chemical Class Separation and Characterization of Organic Compounds in Synthetic Fuels." Anal. Chem. 53:1612-1620.

Mahlum, D. D., W. D. Felix and R. H. Gray (eds.). 1981. Coal Conversion and the Environment: Chemical, Biomedical and Ecological Considerations. NTIS, Springfield, Virginia (in press).

Manson, S. T. and L. H. Toburen. 1981. "Energy and Angular Distributions of Electrons from Fast He^{+} + He Collisions." Phys. Rev. Lett. 46:8:529-531.

Miller, J. H. and R. H. Heflich. 1980. "Modeling the Dose-Response Relationship for Cytotoxicity of Human Cells Exposed to Chemical Carcinogens." PNL-SA-8679. To appear in Proceedings of the 20th Hanford Life Sciences Symposium, Richland, Washington, October 19-23, 1980.

Miller, J. H. "A Model for the Effect of Excision Repair on the Cytotoxicity of Chemical Carcinogens." PNL-SA-9180. Paper submitted to Chemical-Biological Interactions (in press).

Miller, J. H. and M. L. West. 1981. "Inhomogeneous Kinetics in the Quenching of Prompt Radioluminescence: Analysis of Alpha Particle and Proton Induced Fluorescence Decay Curves." J. Chem. Phys. 74:728-731.

Miller, J. H. "Stochastic Model of Radiation Quality Effects in the Quenching of Prompt Radioluminescence." PNL-SA-8893. Radiation Research (in press).

BEST DOCUMENT AVAILABLE

Nelson, J. M., L. A. Braby and W. C. Roesch. 1980. "Rapid Repair of Sublethal Damage in Irradiated Cells." In Proceedings of the Seventh Symposium on Microdosimetry, Vol. II, pp. 1319-1329, eds. J. Booz, H. G. Ebert and H. D. Hartfiel. Harwood Academic Publishers Ltd. New York, ERU-7147 Commission of the European Communities.

Newman, C. N. and H. E. Kubitschek. 1980. "Evidence for RecA-mediated Asymmetric Strand Repair of 5-Iodo-[^{125}I]-2'-Deoxyuridine-Induced Lethal Lesions in Escherichia Coli. J. Mol. Biol. 141:335-340.

Pelroy, R. A., D. A. Sklarew, A. P. Toste and B. W. Wilson. 1981. "The Mutagenic and Chemical Properties of SRC-I Materials: A Status Report." PNL-3604. Pacific Northwest Laboratory, Richland, Washington.

Pelroy, R. A., D. S. Sklarew and S. P. Downey. 1981. "A Comparison of the Ames Mutagenicities of Fossil Fuels." Mutation Res. (in press).

Pelroy, R. A. and M. R. Petersen. "Mutagenic Characterization of Synthetic Fuel Materials by the Ames/Salmonella Assay System." Mutat Res. (in press).

Pelroy, R. A., D. S. Sklarew and S. P. Downey. "Comparison of the Mutagenicity of Fossil Fuels." Mutat. Res. (in press).

Pelroy, R. A. and B. W. Wilson (eds.). 1981. Fractional Distillation as a Strategy for Reducing the Genotoxic Potential of SRC-II Coal Liquids: A Status Report. PNL-3787. NTIS, Springfield, Virginia.

Pelroy, R. A. and B. W. Wilson. "Relative Concentrations of Polyaromatic Primary Amines and Azaarenes in Mutagenically Active Nitrogen Fractions from a Coal Liquid." Mutat. Res. (in press).

Ratcliffe, C. A. 1980. "Deflector System for 2 MeV Electron Beam." PNL-SA-9028. In Proceedings of the 1980 Conference of the Society of Northeastern Accelerator Personnel, Madison, Wisconsin, October 13-15, 1980.

Roesch, W. C., L. A. Braby and J. M. Nelson. 1980. "Microdosimetry and the Reproductive Survival of Cells." In Proceedings of the Seventh Symposium on Microdosimetry, Vol. II, pp. 1501-1511, September 8-12, 1980, Oxford, England, eds. J. Booz, H. E. Ebert and H. D. Hartfiel. Harwood Academic Publishers Ltd., New York, EUR-7147 Commission of the European Communities.

Sklarew, D. S. and B. Nagy. 1981. "Pyrolysis of Transvaal Kerogens. I. Diagenesis of Kerogen in a Stromatolite Near Zeerust, South Africa: One Possible Chemical Evolution Process." Precam. Res. 15:97-111.

Sklarew, D. S., J. S. Fruchter, D. M. Schoengold, M. R. Tompkins and C. L. Morris. 1981. "Measurement of Sulfur Species in Offgas from Rio Blanco's Retort O, Tract C-a, Colorado." PNL-SA-9235.

Sklarew, D. S., R. A. Pelroy, A. P. Toste, D. M. Schoengold and S. P. Downey. 1981. "Polar Mutagens in Shale Oils and Coal Products." In Proceedings of the 182nd National Meeting of the American Chemical Society, Division of Environmental Chemistry, 21(2):216.

Smith, R. D. and A. L. Johnson. 1981. "Ribbon Storage Techniques for Liquid Chromatography-Mass Spectrometry." Anal. Chem. 53:1120-1122.

Smith, R. D. and A. L. Johnson. 1981. "Deposition Method for Moving Ribbon Liquid Chromatograph-Mass Spectrometer Interfaces." Anal. Chem. 53:739.

Smith, R. D., J. E. Burger and A. L. Johnson. 1981. "Liquid Chromatography-Mass Spectrometry with Electron Impact and Secondary Ion Mass Spectrometry with a Ribbon Storage Interface." Anal. Chem. 53:1603.

Smith, R. D. 1981. Evaluation of Flyash Surface Phenomena and the Application of Surface Analysis Technology. PNL-3842. Pacific Northwest Laboratory, Richland, Washington.

Smith, R. D., J. A. Campbell and W. D. Felix. 1980. "Atmospheric Trace Element Pollutants from Coal Combustion." Mining Engineering, 1603.

Smith, R. D. and A. L. Johnson. 1981. "High Temperature Chemistry of Benzene: 2. Bimolecular Reactions During Pyrolysis." Submitted to Physical Chem.

Smith, R. D. and A. L. Johnson. 1981. "High Temperature Chemistry of Benzene: I. Pyrolysis Kinetics and Carbon Formation Mechanisms." Submitted to Physical Chem.

Stoffels, J. J. 1981. "A Direct-Inlet Mass Spectrometer for Real-Time Analysis of Airborne Particles." International Journal of Mass Spectrometry and Ion Physics 40:217-222.

BEST DOCUMENT AVAILABLE

Stoffels, J. J. 1981. "A Direct Inlet for Surface Ionization Mass Spectrometry of Airborne Particles." International Journal of Mass Spectrometry and Ion Physics 40:223-234.

Stoffels, J. J. and C. R. Lagergren. 1981. "On the Real-Time Measurement of Particles in Air by Direct-Inlet Surface Ionization Mass Spectrometry." International Journal of Mass Spectrometry and Ion Physics 40:243-254.

Toburen, L. H., N. Stolterfoht, P. Ziem and D. Schneider. "Electronic Screening in Heavy-Ion-Atom Collisions." PNL-SA-8892. Submitted to Physical Review (in press).

Toburen, L. H., W. E. Wilson, and H. G. Paretzke. "K-Auger Emission from Carbon Foils for 1 MeV Proton Impact." PNL-SA-8892. Submitted to Physical Review A (in press).

Toburen, L. H., P. Ziem, N. Stolterfoht, D. Schnieder and M. Prost. 1980. "Dynamic Screening by Projectile Electrons in Heavy Ion Collisions." In Proceedings of the 1980 Small Accelerator Conference, Denton, Texas, November 1-3, 1980. Abstract published in Bul. Am. Phys. Soc. 25:757.

Toburen, L. H., P. Ziem, N. Stolterfoht, D. Schneider and M. Prost. 1981. "Dynamic Screening by Projectile Electrons in Heavy Ion Collisions." IEEE Trans. Nucl. Sci. Vol. NS-28, 2:1131-1134.

Toste, A. P., R. A. Pelroy, R. B. Myers and D. L. Stewart. 1981. "Organic and Mutagenic Properties of Oil Shale Retort Waters." In Proceedings of the 182nd National Meeting of the American Chemical Society, Division of Environmental Chemistry 21(2):216.

Toste, A. P., R. A. Pelroy, B. W. Wilson, D. S. Sklarew and W. C. Weimer. 1981. "The Role of HPLC in the Organic Analysis and Biotesting of Synthetic Fuels." To be published in Proceedings of the Western Chromatography Symposium, Oct. 15-16, 1981, Newport Beach, California.

Whitaker, T. J. and B. A. Bushaw. 1981. "Laser-Induced Fluorescence Analysis of Vapor-Phase Pyrene." J. Phys. Chem. 85(15):2180.

Whitaker, T. J. and B. A. Bushaw. 1981. "Doppler-Cancelled, Two Photon Resonant Ionization Spectroscopy." In: Laser Spectroscopy for Sensitive Detection, Proc. Soc. Photo-Opt. Instr. Eng. 286:40-47.

Whitaker, T. J. and B. A. Bushaw. 1981. "Collisional Ionization of Rubidium Atoms in Rydberg States." Chem. Phys. Lett. 79:506.

Willey, C., R. A. Pelroy, D. S. Sklarew and B. W. Wilson. "Chemical Analysis and In-Vitro Mutagenicity Testing of Water Soluble Constituents from an SRC Solid Product." In Abstracts of the American Chemical Society Meeting, August 24-28, 1981. American Chemical Society, Washington, D.C. (in press).

Wilson, W. E. and H. G. Paretzke. 1980. "Spatial Dependence of Frequency Distributions in Ionization and Energy Imparted in Nanometer Volumes by 0.25 to 3 MeV Protons." In Proceedings of the Seventh Symposium on Microdosimetry, Vol. I, pp. 423-434, September 8-12, 1980, Oxford, England, (eds. J. Booz, H. G. Ebert and H. D. Hartfiel). Harwood Academic Publishers Ltd. New York, ERU-7147 Commission of the European Communities.

Wilson, W. E. and L. H. Toburen. 1980. "Delta-Ray Production in Ion-Atom Collisions." In Proceedings of the Seventh Symposium on Microdosimetry, Vol. I, pp. 435-448, September 8-12, 1980, Oxford, England, (eds. J. Booz, H. G. Ebert and H. D. Hartfiel). Harwood Academic Publishers Ltd. New York, EUR-7147 Commission of the European Communities.

Wilson, W. E. and H. G. Paretzke. 1981. "Calculation of Distributions for Energy Imparted and Ionization by Fast Protons in Nanometer Sites." Radiat. Res. 87:521-537.

Wilson, B. W., R. A. Pelroy and R. A. Renne. 1981. Estimating Potential Genotoxicity for Direct Coal Liquefaction Materials. PNL-SA-9596. Pacific Northwest Laboratory, Richland, Washington, 20 p.

Wilson, B. W., C. Willey, D. W. Later and M. L. Lee. "The Effect of Process Distillation on the Distribution of Amino Polycyclic Aromatic Hydrocarbons in Refined Coal Liquids." Submitted to Fuel (in press).

Wilson, B. W. and R. A. Pelroy. 1981. "Effects of Catalytic Hydrogenation on Coal Liquids Which Exhibit Microbial Mutagenic Activity," pp. 87-100. In Current Topics in Environmental and Toxicological Chemistry, Vol. 3, Mutagenicity Testing and Related Analytical Techniques, R. W. Frei and V. A. Th. Brinkman (eds.). Current Topics in Environmental and Toxicological Chemistry, Gordon and Breach Science Publishers, New York, New York.

BEST DOCUMENT AVAILABLE

Wilson, B. W., R. A. Pelroy, M. Lee and D. Later. 1981. "Strategies for the Identification of Genotoxic Constituents in Heavy-End Coal Liquids." In Proceedings of the American Society for Mass Spectrometry Meeting, June 1981, Minneapolis, Minnesota. American Society for Mass Spectrometry, Bethesda, Maryland (in press).

Wilson, B. W., M. R. Petersen, R. A. Pelroy and J. T. Cresto. 1981. "In-Vitro Assay for Mutagenic Activity and Gas Chromatographic-Mass Spectral Analysis of Coal-Liquefication Material and the Products Resulting from Its Hydorgenation." Fuel 60:289-294.

Wilson, B. W., W. C. Weimer, W. D. Felix, R. A. Pelroy and D. D. Mahlum. "Solvent Refined Coal." In Proceedings of Workshop on Chemical Characterization of Hazardous Substances in Synfuels, Nov. 4-6, 1981. Seattle, Washington.

BEST DOCUMENT AVAILABLE

PRESENTATIONS

Braby, L. A. and W. C. Roesch. 1981. "Microdosimetry for Cells Irradiated by Electron Beams." Presented at the Radiation Research Society 29th Annual Meeting, May 31-June 4, 1981. Radiat. Res. 87:489.

Braby, L. A. and W. C. Roesch. 1980. "Radiation Quality of Different Electron Beams," Presented as an abstract at the Twenty-Fifth Annual Meeting of the Health Physics Society, July 21-25, 1980. Published as an abstract in the Health Physics 39:6, page 1022.

Bushaw, B. A. 1981. "Doppler-Free Multiphoton Ionization Spectroscopy of the Noble Gases." Presented at the First International Symposium on Resonance Ionization Spectroscopy, June, 1981, Gatlinburg, Tennessee.

Bushaw, B. A. 1981. "Double Resonance Ionization Detection of Heavy Metals." Presented at Workshop on Advanced Laser Technology for Chemical Measurements, October, 1981, Ames, Iowa.

Bushaw, B. A. and T. J. Whitaker. 1981. "Doppler-Cancelled, Two Photon Resonant Ionization Spectroscopy." Laser Spectroscopy for Sensitive Detection, Washington, D.C. Published Proceedings: Proc. Soc. Photo-Opt. Instr. Eng. 286:40-47, 1981.

Bushaw, B. A. and T. J. Whitaker. 1981. "Collisionally Induced Ionization of Rubidium Atoms in Rydberg States." International Quantum Electronics Conference, Boston, Massachusetts.

Drucker, H., R. A. Pelroy, R. A. Renne and B. W. Wilson. 1981. "A Comparison of In Vitro and In Vivo Assays for Mutagenicity/Carcinogenicity of SRC Materials." Presented at the 1981 Annual Summer Toxicological Forum. July 20-24, 1981, Aspen, Colorado.

DuBois, R. D., L. H. Toburen and L. L. Nichols. 1981. "Ionization Cross Sections for Ne^{+} and Ne^{2+} by Proton Impact." PNL-SA-9868. Presented at the American Physical Society DEAP Meeting in New York on December 3-5, 1981.

Felix, W. D. 1981. "Implications of Chemical and Biological Testing on Assessment Activities." Presented at the EPA/DOE Workshop on Risk Assessment. July 20-21, 1981, Washington, D.C.

Felix, W. D., D. D. Mahlum, B. W. Wilson, W. C. Weimer and R. A. Pelroy. 1981. "Chemical Characterization and Bioassay of SRC Process Materials." Presented at Environmental Aspects of Fuel Conversion Technologies, VI. October 26-30, 1981, Denver, Colorado.

Fisher, D. R. 1981. "Principles and Applications of Internal Microdosimetry." Presented at the Joint Meeting on Internal Dosimetry of the Columbia and Northern California Chapters of the Health Physics Society, March 22-24, 1980, South Lake Tahoe, California.

Fisher, D. R. and R. T. Hadley. 1981. "A Statistical Lung Model for Microdosimetry." PNL-SA-9277. Presented at the Health Physics Society 26th Annual Meeting, June 21-26, 1981, Louisville, Kentucky.

Fisher, D. R. and R. Harty. 1981. "The Microdosimetry of Lymphocytes Irradiated by Alpha Particles." PNL-SA-9315. Presented at the Radiation Research Society Annual Meeting, May 31-June 4, 1981, Minneapolis, Minnesota.

Fruchter, J. S., D. S. Sklarew and A. P. Toste. 1981. "Health Effects Studies on Oil Shale Materials at PNL." Presented at the DOE Oil Shale Peer Review Meeting on Health Effects Research, Los Alamos, New Mexico, March 31-April 1, 1981.

Fruchter, J. S., C. L. Wilkerson, A. P. Toste, D. S. Sklarew, K. B. Olsen and K. H. Abel. 1981. "Characterization of Oil Shale Waste Water Effluents." Presented at the DOE Oil Shale Peer Review Meeting on Oil Shale Wastewater Management, November 17-18, 1981, Laramie, Wyoming.

Fruchter, J. S., C. L. Wilkerson, J. C. Evans and R. W. Sanders. 1980. "Analysis of Oil Shale Products Using a Multitechnique Approach." (PNL-SA-3506) ANS/ACS Symposium on Nuclear Methods in Fossil Fuel Research, December 1-4, 1980, Mayaquez, P. R.

Johnson, A. L. and R. D. Smith. 1981. "The Pyrolysis of Benzene at 600° to 1800°C." Presented at the 36th Northwest Regional Meeting, American Chemical Society, June 17-19, 1981, Bozeman, Montana.

BEST DOCUMENT AVAILABLE

Johnson, A. L. and R. D. Smith. 1981. "An Overview of the High Temperature Behavior of Simple Aromatic Hydrocarbons." Presented at the Ninth Midwest High Temperature Chemistry Conference, June 9-11, 1981, Los Alamos, New Mexico.

Johnson, A. L. and R. D. Smith. 1981. "The High Temperature Pyrolysis of Benzene." Presented at the 182nd National Meeting, American Chemical Society, August 23-28, 1981, New York, New York.

Justiniano, E., C. L. Cocke, T. J. Gray, R. D. DuBois and C. Can. 1981. "A Systematic Study of Charge Transfer in Collisions of Highly-Charged Low-Velocity Recoil Ions Incident on He." Presented at the XII International Conference on the Physics of Electronic and Atomic Collisions (ICPEAC) July 14-22, 1981, Gatlinburg, Tennessee.

Laul, J. C., E. A. Lepel, W. C. Weimer and N. A. Wogman. 1981. "Precise Trace Rare Earth Analysis by Radiochemical Neutron Activation." PNL-SA-9143. Presented at the Modern Trends in Activation Analysis International Conference, June 15-19, 1981, Toronto, Canada.

Laul, J. C. and W. C. Weimer. 1981. "Behavior of REE in Geological and Biological Systems." PNL-SA-8161. Presented at the Fifteenth Rare Earth Research Conference June 15-18, 1981, Rolla, Missouri.

Laul, J. C. and N. A. Wogman. 1981. "Application of Neutron Activation Analysis to Geological Materials." PNL-SA-9130. Presented at the International Symposium on Trace Analysis and Technological Development, February 16-19, 1981, Bombay, India.

Manson, S. T. and L. H. Toburen. 1981. "Theoretical and Experimental Study of the Energy and Angular Distribution of Electrons Ejected in He^{+} + He Collisions." PNL-SA-9504A. Presented at the International Conference on the Physics of Electronic and Atomic Collisions (ICPEAC), July 14-22, 1981, Gatlinburg, Tennessee.

Miller, J. H. 1981. "A Stochastic Approach to Diffusion Kinetics." PNL-SA-9027A. Presented at the 28th IUPAC Congress, August 16-21, 1981, Vancouver, B.C.

Miller, J. H. 1981. "Modeling the Effect of Excision Repair on the Cytotoxicity of Chemical Carcinogens in Human Cells." PNL-SA-9181A. Abstract presented at the Organ and Species Specificity in Chemical Carcinogenesis Symposium, March 2-4, 1981, Raleigh, North Carolina.

Miller, J. H. 1981. "Modeling Effects of Excision Repair in the Survival of Human Cells Exposed to Coal-Related Chemical Carcinogens." Presented at Argonne National Laboratory, April 23, 1981.

Miller, J. H. 1981. "Monte Carlo Technique for Including Track Structure Effects in Diffusion Kinetic Calculations." Presented at Argonne National Laboratory, April 24, 1981.

Miller, J. H., L. H. Toburen and S. T. Manson. 1980. "Bethe-Born Approximation for the Energy Distribution of Electrons Ejected from Neon by Proton Impact." Presented as an abstract at the DEAP Meeting, December 1980, Los Angeles, California. Published in the Bul. Am. Phys. Soc. 25:1116.

Miller, J. H. 1981. "Stochastic Approach to Diffusion Kinetics in Aqueous Systems." Abstract presented at the Radiation Research Society 29th Annual Scientific Meeting, May 31-June 4, 1981. Radiat. Res. 87:467.

Nelson, J. M., L. A. Braby and W. D. Roesch. 1981. "Multiple Sub-Lethal Damage Repair Mechanisms in Eukaryotes, Demonstrated by Reproductive Survival." Presented to the Radiation Biology Section (C. A. Tobias), Donner Laboratory, March 6, 1981, Berkeley, California.

Nelson, J. M. 1981. "Stationary Cell Kinetics: Age Distributions in Agenic Populations." Presented to the Department of Biological Structure, School of Medicine, University of Washington, May 19, 1981 Seattle, Washington.

Nelson, J. M., L. A. Braby and W. D. Roesch. 1981. "Sub-Lethal Damage Repair Processes and Age Distributions of Stationary Phase Cells." Presented to the Radiobiology Department (Paul Todd), Pennsylvania State University, June 9, 1981, State College, Pennsylvania.

Nelson, J. M., W. C. Roesch and L. A. Braby. 1981. "Investigations of Fast and Slow Repair of Split-Dose Irradiation Damage in Eukaryotic Cells." Presented to the Radiobiology Section, Harvard University School of Public Health, June 10, 1981, Boston, Massachusetts.

Nelson, J. M., L. A. Braby and W. C. Roesch. 1981. "Dose Dependence of Multiple Event Damage in Chlamydomonas reinhardi." Presented at the Radiation Research Society 29th Annual Scientific Meeting, May 31- June 4, 1981. Radiat. Res. 87:406.

BEST DOCUMENT AVAILABLE

Nelson, J. M. 1981. "Age Distribution of Stationary Phase Mammalian Cells." PNL-SA-9107A. Presented at the Cell Kinetics Society Fifth Annual Meeting, March 1-4, 1981, Pacific Grove, California.

Olsen, K. B., C. L. Wilkerson, A. P. Toste and D. J. Hayes. 1981. "Isolation of Metallic Complexes in Shale Oil and Oil Shale Retort Water." DOE/NBS Workshop on Environmental Speciation and Monitoring Needs, May 18, 1981, Gaithersburg, Maryland.

Olsen, K. B., A. P. Toste, C. L. Wilkerson and D. J. Hayes. 1981. "Isolation of Metallic Complexes from Shale Oils." Presented at the 182nd National Meeting of the American Chemical Society, August 23-28, 1981, New York, New York.

Olsen, K. B. 1981. "Analysis of Selected Trace Metals in Nonaqueous Media by D. C. Plasma Emission Spectroscopy." Presented at the 6th National Conference on Spectrochemical Excitation and Analysis, September 9-11, 1981, Edgartown, Massachusetts.

Roesch, W. C., L. A. Braby and J. M. Nelson. 1981. "Double Two-Event Models for the Response of Chlamydomonas reinhardi to Radiation." Presented at the Radiation Research Society 29th Annual Scientific Meeting, May 31-June 4, 1981. Radiat. Res. 87:406.

Roesch, W. C., L. A. Braby and J. M. Nelson. 1980. "Allowing for Protraction-Fractionation and LET Effects in Interpreting Radiobiological Data." Presented at the 25th Annual Meeting of the Health Physics Society, July 21-25, 1980, Seattle, Washington. Published as an abstract in Health Physics, 39:6, page 1022.

Rudd, M. E., R. D. DuBois, L. H. Toburen and C. A. Ratcliffe. 1981. "Ion and Electron Production Cross Sections for H^+, H_2, $^3He^+$, and $^4He^+$ on Ar." PNL-SA-9403A. Presented at the XII International Conference on the Physics of Electronic and Atomic Collisions (ICPEAC) July 14-22, 1981, Galinburg, Tennessee.

Sklarew, D. S., R. A. Pelroy, A. P. Toste, D. M. Schoengold, S. P. Downey and R. Pahl. 1981. "Polar Mutagens in Shale Oils and Coal Products." Presented at the 182nd National Meeting of the American Chemical Society, August 23-28, 1981, New York, New York.

Smith, R. D. 1981. "Liquid Chromatograph-Mass Spectrometry Using Ribbon Storage Techniques and SIMS Analysis." Presented at the Pittsburgh Conference on Analytical Chemistry and Applied Spectroscopy, March 9-13, 1981, Atlantic City, New Jersey.

Smith, R. D. 1981. "Design and Development of a New LC-MS Using SIMS and Collision-Induced Dissociation." Presented at the Twenty-ninth Annual Conference on Mass Spectrometry and Allied Topics, May 24-29, 1981, Minneapolis, Minnesota.

Smith, R. D. and A. L. Johnson. 1981. "Analysis of Biomass Samples Using an LC-MS Incorporating SIMS, Ribbon Storage Techniques, and a Triple Quadrupole Mass Spectrometer." Presented at the Twenty-ninth Annual Conference on Mass Spectrometry and Allied Topics, May 24-29, 1981, Minneapolis, Minnesota.

Smith, R. D. 1981. "New Approaches to Liquid Chromatography/Mass Spectrometry." Invited paper. Presented at the 34th Annual Summer Symposium on Analytical Chemistry, June 30-July 2, 1981, Pittsburgh, Pennsylvania.

Smith, R. D. and A. L. Johnson. 1981. "The Application of Collision-Induced Dissociation Techniques in a New Liquid Chromatograph-Mass Spectrometer Using Both Electron Impact and Ion Bombardment Ionization." Presented at the 182nd National Meeting of the American Chemical Society, August 23-28, 1981, New York, New York.

Smith, R. D. 1981. "New Approaches to Combining Chromatography and Mass Spectrometry for Synfuels Analysis." Presented at DOE/OHER Workshop on "Chemical Characterization of Hazardous Substances in Synfuels," November 4-6, Seattle, Washington.

Toburen, L. H. 1981. "Continuum Electron Emission in Heavy Ion-Atom Collisions." PNL-SA-9306. Invited Talk. Presented at the Seminar on High Energy Ion-Atom Collision Processes, March 17-19, 1981, Debrecen, Hungary.

Toburen, L. H. 1981. "Secondary Electron Emission in H^+ - Ne Collisions." PNL-SA-9873. Presented at the DEAP Meeting of the American Physical Society in New York on December 3-5, 1981.

Toburen, L. H., J. H. Miller and W. E. Wilson. 1981. "Energy Distribution of Electrons Ejected by High Velocity Ions." Presented at the Radiation Research Society 29th Annual Scientific Meeting, May 31-June 4, 1981. Radiat. Res. 87:469.

BEST DOCUMENT AVAILABLE

Toste, A. P., D. S. Sklarew, R. A. Pelroy, D. M. Schoengoid, S. P. Downey and W. C. Weimer. 1980. "Comparison of Chemical and Mutagenic Properties of a Coal Liquid and a Shale Oil." Presented at the 20th Hanford Life Sciences Symposium, October 20, 1980, Richland, Washington.

Toste, A. P., R. A. Pelroy, R. B. Myers and D. L. Stewart. 1981. "Organic and Mutagenic Properties of Oil Shale Retort Waters." Presented at the 182nd National Meeting of the American Chemical Society, August 27, 1981, New York, New York.

Toste, A. P., R. A. Pelroy, B. W. Wilson, D. S. Sklarew and W. C. Weimer. 1981. "The Role of HPLC in the Organic Analysis and Biotesting of Synthetic Fuels." Presented at the Western Chromatography Symposium, October 15-16, 1981, Newport Beach, California.

West, M. L. and J. H. Miller. 1981. "Quenching of Fluorescence in Pulsed Proton Irradiation: Dependence on Solute Concentration." Presented at the Radiation Research Society 29th Annual Scientific Meeting, May 31-June 4, 1981. Radiat. Res. 87:467.

Wilkerson, C. L., J. C. Evans, J. S. Fruchter, R. W. Sanders, R. D. Giaugue, J. P. Fox, F. Asaro, D. L. Anderson, W. H. Zoller and R. E. Heff. 1981. "Interlaboratory Analysis of Major and Trace Elements in a Colorado Oil Shale Reference Material." Presented at the 6th International Conference on Modern Trends in Activation Analysis, June 15-19, 1981, Toronto, Canada.

Willey, C., R. A. Pelroy and D. L. Stewart. 1981. "Comparative Analysis of Sulfur Heterocycles Isolated from Four Shale Oils." Presented at the Sixth International Symposium on Polynuclear Aromatic Hydrocarbons, October 27-29, 1981, Columbus, Ohio.

Willey, C. R., R. A. Pelroy, D. S. Sklarew and B. W. Wilson. 1981. "Chemical Analysis and In Vitro Mutagenicity Testing of Water Soluble Constituents from a SRC Solid Product." Presented at the American Chemical Society Meeting, August 24-28, 1981, New York, New York.

Wilson, B. W., R. A. Pelroy and R. A. Renne. 1981. "Estimating Potential Genotoxicity for Direct Coal Liquefaction Materials." Presented at the American Institute of Chemical Engineers Meeting, August 16-19, 1981, Detroit, Michigan.

Wilson, W. E. and J. H. Miller. 1981. "Analytical Model for Electron Ejection by High Velocity Ions." Presented at the Radiation Research Society 29th Annual Scientific Meeting, May 31-June 4, 1981. Radiat. Res. 87:468.

Wilson, B. W., R. A. Pelroy, M. Lee and D. Later. 1981. "Strategies for the Identification of Genotoxic Constituents in Heavy-End Coal Liquids." Presented at the American Society of Mass Spectrometry Meeting, June, 1981, Minneapolis, Minnesota.

Wilson, B. W., W. C. Weimer, W. D. Felix and R. A. Pelroy. 1981. "Solvent Refined Coal. Presented at the Workshop on Chemical Characterization of Hazardous Substances in Synfuels." November 4-6, 1981, Seattle, Washington.

Wogman, N. A. 1980. "Natural Contamination in Radionuclide Detection Systems." Presented at the IEEE Nuclear Science Symposium, November 5-7, 1980, Orlando, Florida.

Wogman, N. A. 1981. "Design and Environmental Applications of an Ultralow Background, High Efficiency Intrinsic Germanium Gamma-Ray Spectrometer." Presented at the IAEA Symposium on Methods of Low-Level Counting and Spectrometry, April 6-10, 1981, West Berlin, Germany.

Wogman, N. A. and J. C. Laul. 1981. "Natural Contamination in Radionuclide Detection Systems." Presented at the Symposium on Natural Radiation Environment, Janu- ary, 1981, Bombay, India.

Wogman, N. A. 1981. "Low Level Radionuclide Measurement of Extraterrestrial and Environmental Samples." Presented at the Special ANS Session on Environmental Monitoring, Terrestrial and Extraterrestrial, December 1981, San Francisco, California.

Wogman, N. A. and J. C. Laul. 1981. "Natural Contamination in Radionuclide Detection Systems." PNL-SA-8416. Presented at the Symposium for Radiation Protection, Association for Radiation Protection, January 19-23, 1981, Bombay, India.

BEST DOCUMENT AVAILABLE

Author Index

BLANK PAGE

AUTHOR INDEX

Abel, K. H.; 83, 87
Avigonne, F. T., III; 72

Baer, D. R.; 3
Braby, L. A.; 41, 42, 44, 46, 49, 51, 53
Brodzinski, R. L.; 71, 72
Bushaw, B. A.; 95

Cocke, C. L.; 27

Downey, S. P.; 79
DuBois, R.D.; 24, 26, 27

Fisher, D. R.; 55, 57, 61, 62
Fruchter, J. S.; 87, 88

Hadley, R. T.; 57
Harty, R.; 55, 61, 62
Hayes, D. J.; 82, 84
Heflich, R. H.; 11

Johnson, A. L.; 1, 5

Kalkwarf, D. R.; 15

Lagergren, C. R.; 93

Manson, S. T.; 21, 23, 27
Metting, N. F.; 46
Miller, J. H.; 11, 27, 31, 35, 37
Murphy, D. W.; 62
Myers, R. B.; 77

Nelson, J. M.; 41, 42, 44, 46, 49
Nelson, C. L.; 87
Newman, C. N.; 12
Nichols, L. L.; 24, 26

Olsen, K. B.; 82, 84, 87

Pahl, R.; 79
Paretzke, H. G.; 31, 53
Park, J. F.; 63
Pelroy, R. A.; 77, 79
Prost, M.; 23

Ratcliffe, C. A.; 24
Roesch, W. C.; 41, 42, 44, 49, 51, 55, 57
Rudd, M. E.; 24

Schneider, D.; 23
Schoengold, D. M.; 79
Sklarew, D. S.; 79, 84, 87
Smith, R. D.; 1, 3, 4, 5
Stewart, D. L.; 77
Stoffels, J. J.; 93
Stolterfoht, N.; 23

Thomas, C. W.; 69, 70, 73
Toburen, L. H.; 21, 23, 24, 26, 27, 31
Toste, A. P.; 77, 79, 82
Traub, R. J.; 62, 63

Weimer, W. C.; 6
West, M. L.; 35, 37, 38
Wilkerson, C. L.; 82, 87, 88
Wilson, B. W.; 6
Wilson, W. E.; 21, 27, 31, 52, 53
Wogman, N. A.; 65, 68, 72

Ziem, P.; 23

BLANK PAGE

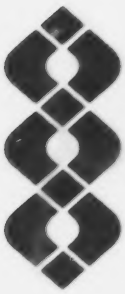

Organization Charts Distribution

BLANK PAGE

BEST DOCUMENT AVAILABLE

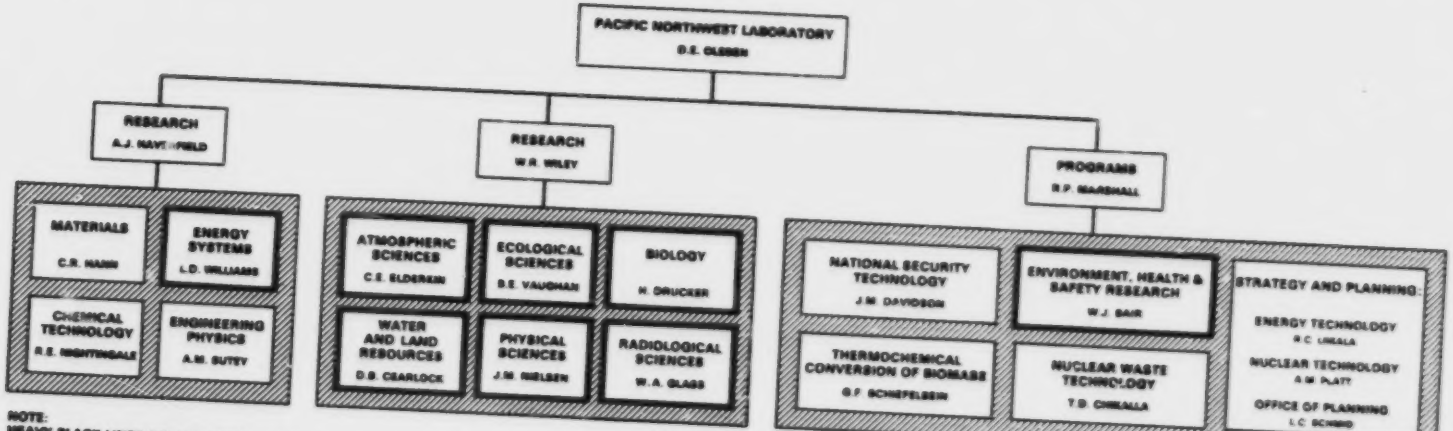

NOTE:
HEAVY BLACK LINES DENOTE ORGANIZATIONAL COMPONENTS IN WHICH ENVIRONMENT, HEALTH AND SAFETY RESEARCH IS BEING CONDUCTED AS OF DECEMBER 1, 1991.

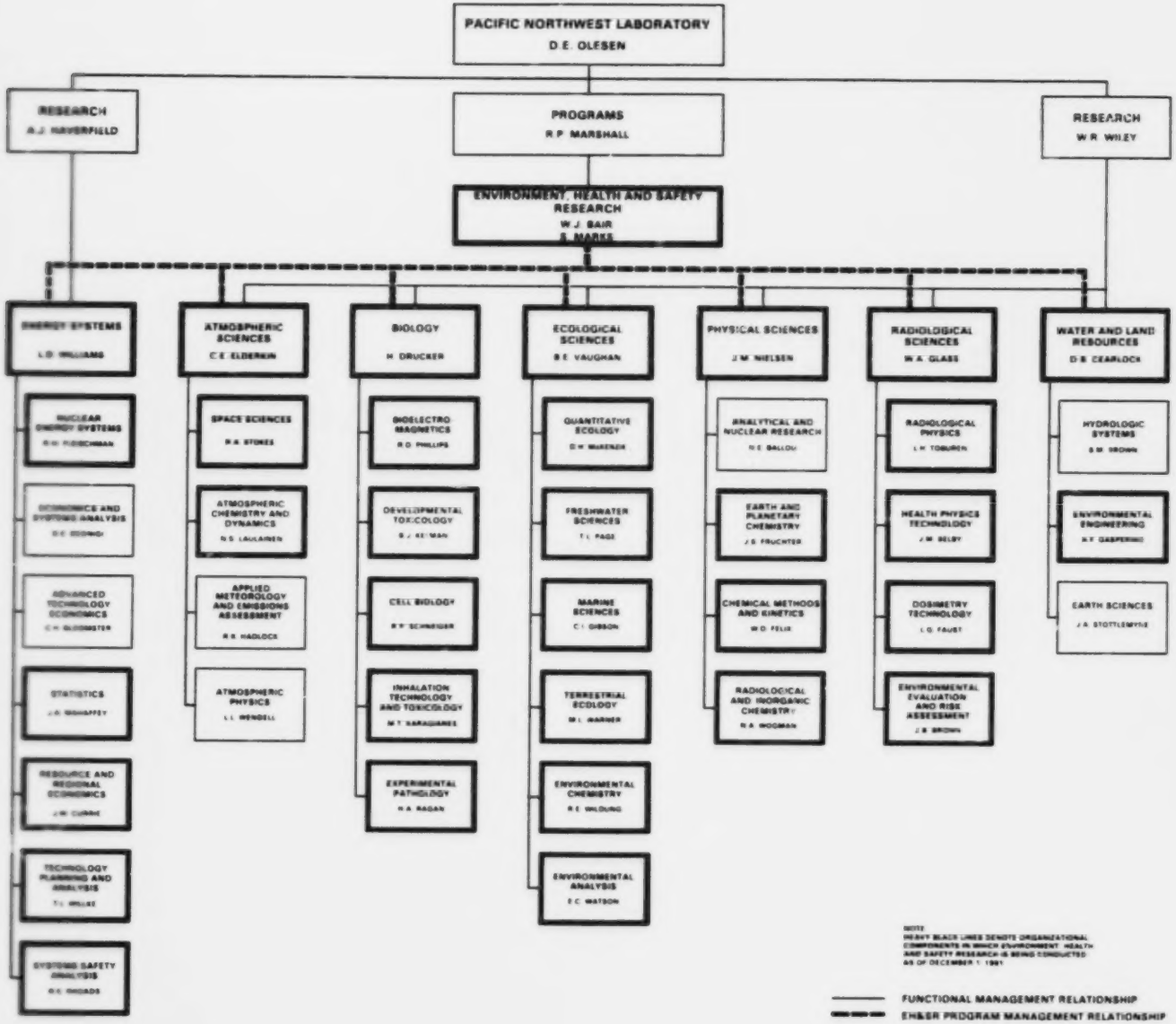

BEST DOCUMENT AVAILABLE

DISTRIBUTION

No. of Copies

OFFSITE

A. A. Churm, Director
Patent Division
DOE - Chicago Operations
9800 S. Cass Avenue
Argonne, IL 60439

27 DOE Technical Information Center

W. R. Albers
Environmental Protection, Safety and Emergency Preparedness
Department of Energy
Washington, DC 20545

R. Barber
Environmental Protection, Safety and Emergency Preparedness
Department of Energy
Washington, DC 20545

N. F. Barr
Office of Energy Research
Department of Energy
Washington, DC 20545

J. R. Blair
Office of Energy Research
Department of Energy
Washington, DC 20545

J. Coleman
Office of Energy Research
Department of Energy
Washington, DC 20545

R. W. Davies
Environmental Protection, Safety and Emergency Preparedness
Department of Energy
Washington, DC 20545

A. P. Duhamel
Office of Energy Research
Department of Energy
Washington, DC 20545

No. of Copies

C. W. Edington
Office of Energy Research
Department of Energy
Washington, DC 20545

G. Goldstein
Office of Energy Research
Department of Energy
Washington, DC 20545

S. H. Greenleigh
Environmental Protection, Safety and Emergency Preparedness
Department of Energy
Washington, DC 20545

E. Harvey
Office of Energy Research
Department of Energy
Washington, DC 20545

H. L. Hollister
Environmental Protection, Safety and Emergency Preparedness
Department of Energy
Washington, DC 20545

B. House
Environmental Protection, Safety and Emergency Preparedness
Department of Energy
Washington, DC 20545

F. Hudson
Office of Energy Research
Department of Energy
Washington, DC 20545

J. Kane
Office of Energy Research
Department of Energy
Washington, DC 20545

W. J. Little, Jr.
Environmental Protection, Safety and Emergency Preparedness
Department of Energy
Washington, DC 20545

No. of Copies

W. Lowder
Office of Energy Research
Department of Energy
Washington, D.C. 20545

J. N. Maddox
Office of Energy Research
Department of Energy
Washington, DC 20545

D. D. Mayhew
Office of Energy Research
Department of Energy
Washington, DC 20545

H. McCammon
Office of Energy Research
Department of Energy
Washington, DC 20545

T. F. McCraw
Environmental Protection, Safety and Emergency Preparedness
Department of Energy
Washington, DC 20545

M. L. Minthorn, Jr.
Office of Energy Research
Department of Energy
Washington, DC 20545

W. A. Neustadt
Environmental Protection, Safety and Emergency Preparedness
Department of Energy
Washington, DC 20545

D. E. Patterson
Environmental Protection, Safety and Emergency Preparedness
Department of Energy
Washington, DC 20545

M. Schulman
Office of Energy Research
Department of Energy
Washington, DC 20545

No. of Copies

D. H. Slade
Office of Energy Research
Department of Energy
Washington, DC 20545

J. Swinebroad
Environmental Protection, Safety and Emergency Preparedness
Department of Energy
Washington, DC 20545

J. W. Thiessen
Office of Energy Research
Department of Energy
Washington, DC 20545

A. Trivelpiece
Office of Energy Research
Department of Energy
Washington, DC 20545

W. Vaughan
Environmental Protection, Safety and Emergency Preparedness
Department of Energy
Washington, DC 20545

B. W. Wachholz
Environmental Protection, Safety and Emergency Preparedness
Department of Energy
Washington, DC 20545

6 R. W. Wood
Office of Energy Research
Department of Energy
Washington, DC 20545

J. R. Roeder
DOE - Albuquerque Operations Office
P.O. Box 5400
Albuquerque, NM 87115

J. F. Stevens
Dayton Area Office
DOE - Albuquerque Operations Office
P.O. Box 66
Miamisburg, OH 45342

E. W. Bean
Rocky Flats Area Office
DOE - Albuquerque Operations Office
P.O. Box 928
Golden, CO 80401

No. of Copies

D. M. Gardiner
DOE - Chicago Operations Office
9800 South Cass Avenue
Argonne, IL 60439

J. H. Spickard
DOE - Idaho Operations Commission
550 Second Street
Idaho Falls, ID 83401

M. M. Williamson
DOE - Idaho Operations Commission
550 Second Street
Idaho Falls, ID 83401

P. B. Dunnaway
DOE - Nevada Operations Office
P.O. Box 14100
Las Vegas, NV 89114

M. E. Gates
DOE - Nevada Operations Office
P.O. Box 14100
Las Vegas, NV 89114

R. Ray
DOE - Nevada Operations Office
P.O. Box 14100
Las Vegas, NV 89114

J. A. Lenhard
DOE-Oak Ridge Operations Office
P.O. Box 14100
Las Vegas, NV 89114

C. Jackson
DOE - San Francisco Operations Office
133 Broadway
Wells Fargo Building
Oakland, CA 94616

B. Morgan
DOE - Savannah River Operations Office
P.O. Box A
Aiken, SC 29801

W. Reese
DOE - Savannah River Operations Office
P.O. Box A
Aiken, SC 29801

No. of Copies

J. S. Ball
Bartlesville Energy Research Center
Department of Energy
P.O. Box 1398
Bartlesville, OK 74003

G. H. Gronhovd
Grand Forks Energy Research Center
Department of Energy
Box 8213
University Station
Grand Forks, ND 58202

A. W. Decora
Laramie Energy Research Center
Department of Energy
P.O. Box 3395
University Station
Laramie, WY 83071

A. A. Pitrolo
Morgantown Energy Research Center
Department of Energy
P.O. Box 880
Morgantown, WV 26505

I. Wender
Pittsburgh Energy Research Center
4800 Forbes Avenue
Pittsburgh, PA 15213

B. M. Erickson
DOE - Schenectady Naval Reactors Office
P.O. Box 1069
Schenectady, NY 12301

NRC Advisory Committee on Reactor Safeguards
Washington, DC 20555

R. Alexander
Nuclear Regulatory Commission
Washington, DC 20545

W. Cool
Nuclear Regulatory Commission
Washington, DC 20545

F. Swanberg
Nuclear Regulatory Commission
Washington, DC 20545

No. of Copies

J. J. Davis
Asst. Director of Research
Nuclear Regulatory Commission
Washington, DC 20545

R. A. Scarano
Nuclear Regulatory Commission
Mill Licensing Section
Washington, DC 20545

W. R. Ney
Executive Director
National Council on Radiation Protection and Measurement
7910 Woodmont Avenue
Suite 1061
Washington, DC 20014

H. L. Volchok
Department of Energy
Environmental Measurements Laboratory
376 Hudson St.
New York, NY 10014

H. Ellett
Environmental Protection Agency
Washington, DC 20460

P. F. Gustafson
Argonne National Laboratory
9800 S. Cass Avenue
Argonne, IL 60439

M. Inokuti
Argonne National Laboratory
9800 S. Cass Avenue
Argonne, IL 60439

R. Roland
Argonne National Laboratory
9700 South Cass Avenue
Argonne, IL 60439

V. P. Bond
Brookhaven National Laboratory
Upton, Long Island, NY 11973

No. of Copies

Librarian
Research Library, Reference
Brookhaven National Laboratory
Upton, Long Island, NY 11973

C. B. Meinhold
Brookhaven National Laboratory
Upton, Long Island, NY 11973

S. I. Auerbach
Oak Ridge National Laboratory
P.O. Box X
Oak Ridge, TN 37830

J. A. Auxier
Oak Ridge National Laboratory
P.O. Box X
Oak Ridge, TN 37830

W. R. Garrett
Oak Ridge National Laboratory
P.O. Box X
Oak Ridge, TN 37830

C. R. Richmond
Oak Ridge National Laboratory
P.O. Box X
Oak Ridge, TN 37830

R. M. Jefferson
Sandia Laboratories
P.O. Box 5800
Albuquerque, NM 87187

K. A. Smith
Sandia Laboratories
P.O. Box 5800
Albuquerque, NM 87187

Technical Information Service
Room 773A
Savannah River Laboratory
E. I. du Pont de Nemours and Company
Aiken, SC 29801

No. of Copies

E. L. Alpen
Lawrence Berkeley Laboratory
University of California
Building 90, Room 2056
No. 1 Cyclotron Road
Berkeley, CA 94720

J. L. Magee
Lawrence Berkeley Laboratory
Bldg. 29, Rm 206
Berkeley, CA 94720

Librarian
Lawrence Radiation Laboratory
University of California
Technical Information Department, L-3
P.O. Box 808
Livermore, CA 94500

M. L. Mendelsohn
University of California
Lawrence Livermore Laboratory
P.O. Box 808
Livermore, CA 94550

R. Lunt
University of California
Center of Life Sciences
900 Veteran Avenue
West Los Angeles, CA 90024

J. W. Healy
Los Alamos Scientific Laboratory
University of California
P.O. Box 1663
Los Alamos, NM 87545

Librarian
Los Alamos Scientific Laboratory
P.O. Box 1663
Los Alamos, NM 87545

D. F. Petersen
University of California
Los Alamos Scientific Laboratory
P.O. Box 1663
Los Alamos, NM 87545

No. of Copies

G. L. Voelz
University of California
Los Alamos Scientific Laboratory
P.O. Box 1663
Los Alamos, NM 87545

R. O. McClellan
Inhalation Toxicology Research Institute
Lovelace Foundation for Medical Education and Research
P.O. Box 5890
Albuquerque, NM 87115

D. Rall, Director
NIEHS
P.O. Box 12233
Research Triangle Park, NC 27709

W. Weyzen
Electric Power Research Institute
3412 Hillview Avenue
Palo Alto, CA 94304

D. Beirman
Chief, Document Service Branch
Central Intelligence Agency
Attn: CRS/DPSD/DSB/IAS/409779/DB
Washington, DC 20505

Council of Environmental Quality
72 Jackson Place, N.W.
Washington, DC 20006

J. W. McCaslin
INEL, Aerojet Nuclear
550 Second Street
Idaho Falls, ID 83401

Y. E. Yoder
Rockwell International
P.O. Box 464
Golden, CO 80401

J. F. Johnson
Kenworth Trucking
P.O. Box 1000
Kirkland, WA 98033

No. of Copies

H. Rossi
Radiological Research Laboratory
Columbia University
630 West 168th Street
New York, NY 10032

P. W. Todd
793 Westerly Parkway
State College, PA 16801

Leo Bustad, Dean
College of Veterinary Medicine
Washington State University
Pullman, WA 99163

Librarian
Joint Center for Graduate Study
100 Sprout Road
Richland, WA 99352

FOREIGN

Librarian
Australian AEC
Riverina Laboratory
P.O. Box 226
Deniliquin
New South Wales
AUSTRALIA 2710

Librarian
Commonwealth Scientific and Industrial Research Organization
314 Albert Street
P.O. Box 89
East Melbourne, Victoria
AUSTRALIA

H. Daw
Director, Division of Health, Safety and Waste Management
International Atomic Energy Agency
Vienna 1, Kaerentnerring 11,
AUSTRIA

No. of Copies

A. M. Marko
Director Atomic Energy of Canada Ltd.
Biology and Health Physics Division
Chalk River Nuclear Laboratories
Chalk River
Ontario K0J 1J0
CANADA

M. Anderson
Library
Department of National Health and Welfare
Ottawa, Ontario
CANADA

J. Dunster
National Radiological Protection Board
Harwell, Didcot
Oxfordshire OXII ORQ
ENGLAND

Librarian, Building 465
Atomic Energy Research Establishment
Harwell, Didcot
OXON OXII ORD
ENGLAND

D. H. Perison
Atomic Energy Research Establishment
Health Physics and Medical Division
B. 364
Harwell, Didcot, Berkshire
ENGLAND

H. Smith
Biology Department
National Radiological Protection Board
Building 565T
Harwell, Didcot
Oxfordshire, OXII ORQ
ENGLAND

F. D. Sowby
International Commission on Radiological Protection
Clifton Avenue
Sutton, Surrey
ENGLAND

No. of Copies

Director
Commissariat a l'Energie Atomique
Centre d'Etudes Nucleaires de Fontenay-aux-Roses (Seine)
FRANCE

Librarian
Centre d'Etudes Nucleaires de Saclay
P.O. Box 2, Saclay
Fig-sur-Yvette (S&O)
FRANCE

J. C. Nenot
Comite de Radioprotection
69, rue de Micromesnil
75008 Paris,
FRANCE

M. Rzekiecki
Commissariat a l'Energie Atomique
Centre d'Etudes Nucleaires de Cadarache
BP n 13-St. Paul
Les Durance
FRANCE

J. P. Olivier
ENEA (OECD) Health and Safety Office
38, Blvd, Suchet
Paris,
FRANCE

J. K. Miettinen
University of Helsinki
Department of Radiochemistry
Unionkatu 35, Helsinki
FINLAND

A. R. Gopal-Ayengar
c/o P. K. Dayanidhi
15-D Gulmarg
Anushaktinagar
Bombay-400 094
INDIA

W. Jacobi
Institut fur Strahlenschutz
D-8042 Neuherberg
Ingolstaddter Landstrasse 1
FEDERAL REPUBLIC OF GERMANY

No. of Copies

L. Feinendegen
Director of Institute of Medicine
Institut fur Medizin
Kernforschung sanlage Julich
Postfach 1913
517, Julich
FEDERAL REPUBLIC OF GERMANY

Dr. Vittorio Prodi
Comitato Nazionale per L-Energia Nucleare
Laboratorio Fisica Sanitaria
Posiz.
Prot.n. 306/LFS
Via Miazzini, 2
40238 Bologna
ITALY

T. Kumatori
Director
National Institute of Radiological Sciences
4-9-1, Anagawa
Chiba-shi, Chiba 260
JAPAN

J. K. Basson
Vice-President
Raad Op Atomic
Atoomkrag Energy Board
Privaatsk X 256
Pretoria 0001
REPUBLIC OF SOUTH AFRICA

Z. M. Beekman
President of IRPA
Rooseveltlaan 197
1079 AP Amsterdam
THE NETHERLANDS

A. Brink
Sasol-One Limited
P.O. Box 1
Sasolburg 9570
REPUBLIC OF SOUTH AFRICA

B. C. Winkler
Director, Licensing (Standards)
Raad Op Atoomkrag/Atomic Energy Board
Privaatsak X 256/
Private Bag X 256
Pretoria 001
REPUBLIC OF SOUTH AFRICA

No. of Copies

E. Komarov
Environmental Health Division
World Health Organization
Avenue Appia 1211
Geneva 27, SWITZERLAND

K. E. Lennart Johansson
National Defense Research Institute
FOA 45 1
S-901-82
Umea, SWEDEN

M. J. Suess
Regional Officer for Environmental Hazards
World Health Organization
8, Scherfigsvej
DK-2100
Copenhagen, DENMARK

D. Djuric
Institute of Occupational & Radiological Health
11000 Beograd
Deligradska 29,
YUGOSLAVIA

ONSITE

DOE Richland Operations Office

R. E. Austin
P. F. Dunigan
D. R. Elle
R. W. Newlin
H. E. Ransom/P. K. Clark
F. R. Standerfer
M. W. Tiernan

Rockwell Hanford Operations

P. G. Lorenzini

UNC Nuclear Industries

T. E. Dabrowski

Westinghouse Hanford Company

R. O. Budd
D. E. Simpson

Hanford Environmental Health Foundation

D. B. Breitenstein
B. D. Reinert

No. of Copies

Battelle-Seattle

S. M. Nealey
E. B. Perrin
J. E. Rasmussen
A. H. Schilling
C. R. Schuller
R. Shikiar
M. E. Walsh
M. T. Wood

Battelle Memorial Institute

N. E. Carter
L. L. German
R. S. Paul
D. B. Shipler
C. R. Vest
Librarian

Battelle Columbus

A. H. Adelman
A. D. Barker
F. J. Milford
R. H. Poirier
L. A. Rancitelli

Battelle-Washington DC Office

G. Johnson
S. Stryker
C. Vest

No. of Copies

162 Pacific Northwest Laboratory

R. W. Baalman (5)
W. J. Bair (15)
N. E. Ballou (5)
L. A. Braby
D. B. Cearlock
T. P. Chikalla
J. M. Davidson
H. Drucker
R. D. DuBois
C. E. Elderkin
S. J. Farmer
W. D. Felix (10)
D. R. Fisher
J. S. Fruchter (10)
J. J. Fuquay
W. A. Glass (10)
P. Goodenough
R. H. Gray
R. T. Hadley
C. R. Hann
R. Harty
A. J. Haverfield
I. D. Hays
A. F. Johnston
R. C. Liikala
S. Marks
R. P. Marshall
J. E. Mendel
N. F. Metting
J. H. Miller

No. of Copies

J. E. Minor
D. W. Murphy
J. M. Nelson
C. N. Newman
L. L. Nichols
J. M. Nielsen (10)
R. E. Nightingale
D. E. Olesen
J. F. Park
R. W. Perkins (10)
A. M. Platt
C. A. Ratcliffe
W. D. Richmond
W. C. Roesch
M. E. Rudd
G. F. Schiefelbein
L. C. Schmid
J. B. Schuette
C. L. Simpson
M. E. Stifter
A. M. Sutey
L. H. Toburen
R. J. Traub
B. E. Vaughan
M. L. West
W. R. Wiley
L. D. Williams
W. E. Wilson
N. A. Wogman (10)
Technical Information (5)
Publishing Coordination sm (2)